science for a changing world

Prepared in cooperation with the U.S. Army Corps of Engineers, Fort Worth District

Precipitation, Temperature, Groundwater-Level Elevation, Streamflow, and Potential Flood Storage Trends Within the Brazos, Colorado, Big Cypress, Guadalupe, Neches, Sulphur, and Trinity River Basins in Texas Through 2017

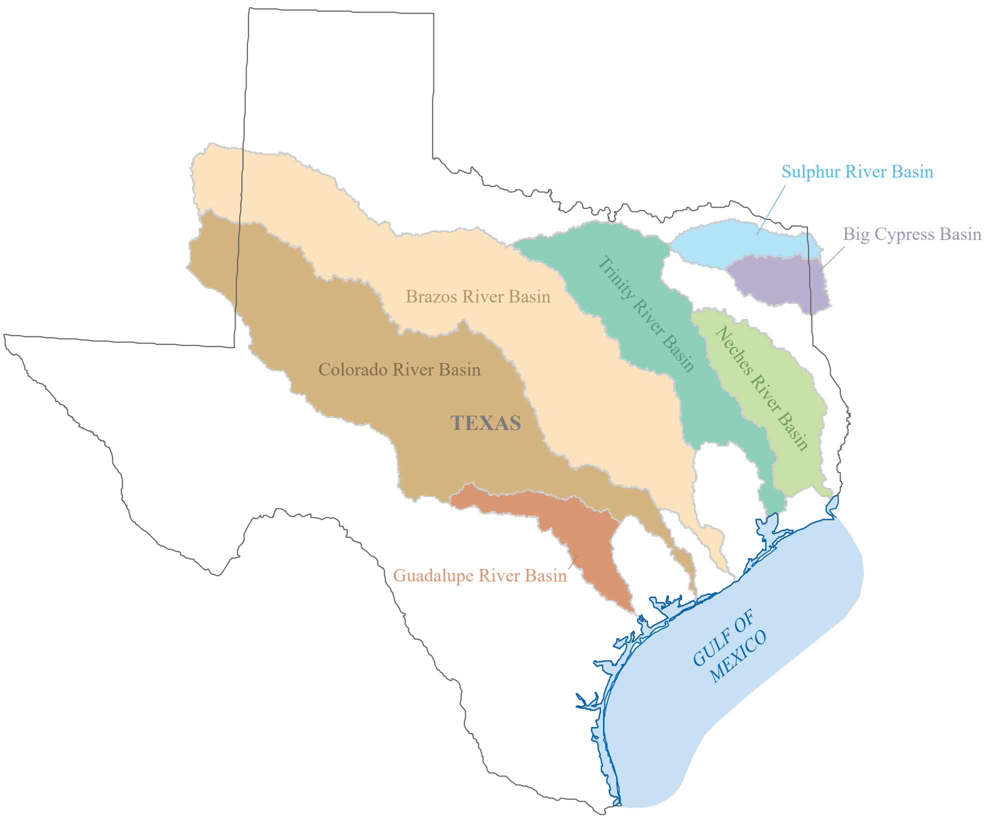

Scientific Investigations Report 2019–5137
Version 1.1, April 2020

U.S. Department of the Interior
U.S. Geological Survey

Precipitation, Temperature, Groundwater-Level Elevation, Streamflow, and Potential Flood Storage Trends Within the Brazos, Colorado, Big Cypress, Guadalupe, Neches, Sulphur, and Trinity River Basins in Texas Through 2017

By Glenn R. Harwell, Jeremy S. McDowell, Cathina L. Gunn, and Brett S. Garrett

Prepared in cooperation with the U.S. Army Corps of Engineers,
Fort Worth District

Scientific Investigations Report 2019–5137
Version 1.1, April 2020

U.S. Department of the Interior
U.S. Geological Survey

U.S. Department of the Interior
DAVID BERNHARDT, Secretary

U.S. Geological Survey
James F. Reilly II, Director

U.S. Geological Survey, Reston, Virginia
First release: 2020
Revised: April 2020 (ver. 1.1)

Suggested citation:
Harwell, G.R., McDowell, J.S., Gunn, C.L., and Garrett, B.S., 2020, Precipitation, temperature, groundwater-level elevation, streamflow, and potential flood storage trends within the Brazos, Colorado, Big Cypress, Guadalupe, Neches, Sulphur, and Trinity River Basins in Texas through 2017 (ver. 1.1, April 2020): U.S. Geological Survey Scientific Investigations Report 2019–5137, 94 p., https://doi.org/10.3133/sir20195137.

Associated data for this publication:
McDowell, J.S., Garrett, B.S., and Harwell, G.R., 2020, Data used to assess precipitation, temperature, groundwater-level elevation, streamflow, and potential flood storage trends within the Brazos, Colorado, Big Cypress, Guadalupe, Neches, Sulphur, and Trinity River Basins in Texas through 2017: U.S. Geological Survey data release, https://doi.org/10.5066/P9L1F7PT.

ISSN 2328-0328 (online)

Acknowledgments

This report was funded by and prepared in cooperation with the U.S. Army Corps of Engineers, Fort Worth District. The authors thank the U.S. Army Corps of Engineers for the opportunity to work with them and for their continued support of long-term streamflow trend analysis and assessment of streamflow-related variables within the Brazos, Colorado, Big Cypress, Guadalupe, Neches, Sulphur, and Trinity River Basins. The authors recognize the professional and technical assistance of U.S. Army Corps of Engineers, Fort Worth District staff, and specifically acknowledge Jerry L. Cotter, P.E., Darlene G. Prochaska, P.E., Helena P. Mosser, P.E., Stephen F. Pilney, P.E., and Michael F. Schwind for their contributions.

Contents

Figures

Tables

Conversion Factors

U.S. customary units to International System of Units

Multiply	By	To obtain
	Length	
inch (in.)	2.54	centimeter (cm)
inch (in.)	25.4	millimeter (mm)
foot (ft)	0.3048	meter (m)
mile (mi)	1.609	kilometer (km)
	Area	
acre	4,047	square meter (m^2)
acre	0.4047	hectare (ha)
acre	0.4047	square hectometer (hm^2)
acre	0.004047	square kilometer (km^2)
square mile (mi^2)	259.0	hectare (ha)
square mile (mi^2)	2.590	square kilometer (km^2)
	Volume	
acre-foot (acre-ft)	1,233	cubic meter (m^3)
acre-foot (acre-ft)	0.001233	cubic hectometer (hm^3)

Temperature in degrees Celsius (°C) may be converted to degrees Fahrenheit (°F) as
°F = (1.8 × °C) + 32.

Temperature in degrees Fahrenheit (°F) may be converted to degrees Celsius (°C) as
°C = (°F – 32) / 1.8.

Datum

Vertical coordinate information is referenced to the North American Vertical Datum of 1988 (NAVD 88).

Horizontal coordinate information is referenced to the North American Datum of 1983 (NAD 83).

Elevation, as used in this report, refers to distance above the vertical datum.

Abbreviations

NID	National Inventory of Dams
NOAA	National Oceanic and Atmospheric Administration
PDSI	Palmer Drought Severity Index
TWDB	Texas Water Development Board
USACE	U.S. Army Corps of Engineers
USGS	U.S. Geological Survey

Precipitation, Temperature, Groundwater-Level Elevation, Streamflow, and Potential Flood Storage Trends Within the Brazos, Colorado, Big Cypress, Guadalupe, Neches, Sulphur, and Trinity River Basins in Texas Through 2017

By Glenn R. Harwell, Jeremy S. McDowell, Cathina L. Gunn, and Brett S. Garrett

Abstract

The U.S. Geological Survey (USGS), in cooperation with the U.S. Army Corps of Engineers (USACE), analyzed streamflow trends and streamflow-related variables through 2017 in seven important water-supply basins to provide information that can help water managers with the USACE and river authorities make future water management decisions. The primary purpose of this report is to document trends in long-term streamflow data at 114 selected USGS streamflow-gaging stations and 36 simulated reservoir-inflow stations in 7 river basins primarily in Texas: Brazos, Colorado, Big Cypress, Guadalupe, Neches, Sulphur, and Trinity. In this report, trends were considered statistically significant if their *p*-values were less than or equal to 0.05 (*p*-value ≤0.05). Streamflow data selected for temporal trend analyses included annual minimum streamflow, annual peak streamflow, and streamflow volume. Precipitation, air temperature, and groundwater-level-elevation data were analyzed for trends that may help to explain changes observed in the streamflow statistics. Basins were divided into sections along county lines for precipitation analyses. Streamflow volumes were analyzed for associations with potential flood storage. The potential flood storage, defined as the difference between maximum storage and normal storage, was computed for each dam from the National Inventory of Dams database and accumulated over time based on the completion date of the dam.

Precipitation and air temperature trends were analyzed for each of the eight climate divisions (High Plains, Trans-Pecos, Low Rolling Hills, Edwards Plateau, North Central Texas, South Central Texas, East Texas, and Upper Coast). Results of precipitation trend analyses indicated moderate upward trends in the Upper Coast and East Texas Climate Divisions analyzed on an annual time step from 1900 through 2017. These two climate divisions are in the eastern and southeastern parts of the State, and they receive more mean annual precipitation (45.88 and 46.09 inches, respectively) than the other climate divisions. The results of air temperature analyses indicated upward trends in annual mean air temperature within all climate divisions, with a mean slope of 0.02 degree Fahrenheit per year, or 1 degree every 50 years.

Within the Brazos River Basin, results of precipitation trend analyses on an annual time step indicated that precipitation amounts are most likely increasing in the lower and middle sections of the basin. Downward trends in annual streamflow and in the ratio of streamflow volume to precipitation volume were indicated at 7 of the 15 stations in the upper sections of the basin. The lower sections of the basin had mostly downward trends in annual minimum streamflow, whereas upward trends in annual minimum streamflow were indicated in the upper sections of the basin. Downward trends in annual peak streamflow were indicated at many of the stations in the upper sections of the basin. At the same seven stations in the upper sections of the basin where there were downward trends in annual streamflow, there were also downward trends in the ratio of streamflow volume to precipitation volume. The data from the same seven stations indicated negative associations between potential flood storage volume and annual streamflow volume and downward trends in the ratio of annual streamflow volume to potential flood storage volume. With the known addition of 13,006,394 acre-feet of potential flood storage between 1900 and 2010 in the subbasins analyzed, streamflow volumes have decreased in the upper sections of the Brazos River Basin.

Within the Colorado River Basin, results of precipitation trend analyses on an annual time step indicated no trends in the basin. Downward trends in annual streamflow were indicated at 16 stations in the upper sections of the basin, whereas no trends in annual streamflow were indicated in the lower section of the basin. In the lower section of the basin, one station that was operated as a continuous streamflow-gaging station through 2017 had a downward trend in annual minimum streamflow, and another station (operated through 2007) had an upward trend in annual minimum streamflow. In the upper sections of the basin, data from seven stations indicated upward trends in annual minimum streamflow, and data from six stations indicated downward trends. Data from 18 stations in the upper sections of the basin indicated

downward trends in annual peak streamflow. Thirteen of the 16 stations in the upper sections of the basin with data that indicated downward trends in annual streamflow also have data that indicated downward trends in the ratio of streamflow volume to precipitation volume. Data from the same 13 stations indicated negative associations between potential flood storage volume and annual streamflow volume and downward trends in the ratio of annual streamflow volume to potential flood storage volume. With the known addition of 7,193,147 acre-feet of potential flood storage between 1891 and 2014 in the subbasins analyzed, streamflow volumes have decreased in the upper sections of the Colorado River Basin.

Within the Big Cypress Basin, results of precipitation trend analyses on annual, seasonal, and monthly time steps indicated almost no trends in the basin as defined in this report. However, the annual precipitation *p*-value only slightly exceeded the *p*-value threshold for a statistically significant trend. Given the upward trend in precipitation in the East Texas Climate Division, which includes the Big Cypress Basin, and the low *p*-value for annual precipitation within the basin, precipitation in the basin may be increasing over time. Two annual streamflow trends, one upward and one downward, were in the upper parts of the basin. Data from USGS streamflow-gaging station 07346000 Big Cypress Bayou near Jefferson, Texas, indicated an upward trend in annual minimum streamflow and a downward trend in annual peak streamflow. The station is immediately downstream from Lake O' the Pines; presumably, minimums have increased because of regulated releases, and annual peaks have decreased because of storage from the lake for flood control. Despite the known addition of 2,737,154 acre-feet of potential flood storage between 1898 and 2011 in the subbasins analyzed, there have not been widespread reductions in streamflow volumes in the Big Cypress Basin, except for within the drainage area for the farthest upstream station on the main stem downstream from Mount Pleasant, Texas.

Within the Guadalupe River Basin, results of precipitation trend analyses on an annual time step indicated an upward trend in the lower section of the basin, but no trends in annual streamflow were indicated in the lower section of the basin. In the upper section of the basin, data from 1 of the 13 stations indicated an upward trend in annual streamflow. Data from 6 of the 13 stations in the upper section of the basin indicated a trend in annual minimum streamflow with 4 upward and 2 downward trends. Data from 2 of the 13 stations in the upper section of the basin indicated downward trends in annual peak streamflow. Despite the known addition of 2,016,534 acre-feet of potential flood storage between 1849 and 2013 in the subbasins analyzed, streamflow volumes have not decreased in the Guadalupe River Basin.

Within the Neches River Basin, results of precipitation trend analyses on an annual time step indicated upward trends in the basin. None of the data from stations analyzed in the Neches River Basin indicated annual trends in streamflow despite upward trends in annual precipitation within the basin. Data from 9 of the 19 stations analyzed in the basin indicated upward trends in annual minimum streamflow. Data from one of the simulated-inflow stations indicated a downward trend in annual minimum streamflow into Sam Rayburn Reservoir. Data from two stations indicated downward trends in annual peak streamflow, and data from one small subbasin indicated an upward trend in annual peak streamflow. Despite the known addition of 4,839,609 acre-feet of potential flood storage between 1888 and 2008 in the subbasins analyzed, there have not been widespread reductions in streamflow volumes in the Neches River Basin.

Within the Sulphur River Basin, results of precipitation trend analyses on an annual time step indicated a moderate upward trend within the basin. Data from only one of the stations, the simulated inflow to Jim Chapman Lake, indicated an annual upward trend in streamflow despite an upward trend in annual precipitation throughout the basin. Data from three of the six stations in the Sulphur River Basin indicated upward trends in annual minimum streamflow, and data from one of the six stations indicated a downward trend in annual peak streamflow. Despite the known addition of 6,933,361 acre-feet of potential flood storage between 1904 and 2006 in the subbasins analyzed, streamflow volumes have not decreased in the Sulphur River Basin.

Within the Trinity River Basin, results of precipitation trend analyses on an annual time step indicated upward trends in most sections of the basin. Data from 8 of the 36 stations analyzed for trends in annual streamflow indicated upward trends, and all 8 stations are in the upper sections of the basin. None of the data from stations in the lower sections of the basin indicated trends in annual streamflow. Data from 16 of the 36 stations indicated upward trends in annual minimum streamflow. Upward trends in annual minimum streamflow could be the result of managed reservoir releases in combination with wastewater treatment plant releases in the large Dallas-Fort Worth metroplex in the upper sections of the basin. All the trends in annual peak streamflow were in the sections of the basin that include the Dallas-Fort Worth metroplex. Data from two stations, one USGS streamflow-gaging station and one simulated-inflow station, indicated upward trends in annual peak streamflow, and data from one streamflow-gaging station indicated a downward trend in annual peak streamflow. Of the basins included in this study, the Trinity River Basin has the second largest amount of potential flood storage of 8,947,349 acre-feet from dams added between 1890 and 2013. Eleven stations in the Trinity River Basin had positive associations between potential flood storage volume and annual streamflow volume, indicating that annual streamflow increases as potential flood storage increases. Data from 7 of the 11 stations also indicated upward trends in annual streamflow. The positive associations may be the result of increases in minimum streamflow, which could be the result of any combination of managed reservoir releases, wastewater treatment plant releases, or increased runoff from urbanized areas, particularly in the urbanized area of the Dallas-Fort Worth metroplex.

Introduction

In Texas, surface water in rivers is managed by different river authorities across the State. For the basins included in this study, the river authorities and management entities include the Brazos River Authority, Upper Colorado River Authority, Lower Colorado River Authority, Guadalupe-Blanco River Authority, Upper Guadalupe River Authority, Lower Neches Valley Authority, Angelina-Neches River Authority, Sulphur River Basin Authority, Trinity River Authority, San Angelo Parks and Recreation Department, Tarrant Regional Water District, and the City of Dallas. These river authorities and entities along with the U.S. Army Corps of Engineers (USACE) Fort Worth District operate and maintain reservoirs for water conservation, water supply, and recreation.

Water management strategies are based, in part, on period-of-record simulations of streamflow and reservoir storage and release. Temporal changes in streamflow from land-use changes, changes in climatic patterns, or other changes, may result in over- or under-estimation of streamflow in simulations, thus providing an inaccurate analysis on which to base water management strategies. Documenting trends in streamflow over time could better inform water managers of the appropriateness of period-of-record streamflow simulations for making water management decisions.

Summary statistics and trend analyses were completed for 712 streamflow-gaging stations in Texas that included data through 2003 (Asquith and others, 2007a, b) and for 620 streamflow-gaging stations in Texas that included data through 2007 (Asquith and Heitmuller, 2008). Results indicated statistically significant downward trends in streamflow for the period of record at many of the stations included in this study in the Brazos and Colorado River Basins, the second and third largest basins in Texas by area (Texas Water Development Board [TWDB], 2019a). Water managers recognized the need for an up-to-date assessment of statistical trends in streamflow and other hydrologic variables in the Brazos and Colorado River Basins and for similar assessments in five other major river basins (the Big Cypress, Guadalupe, Neches, Sulphur, and Trinity River Basins) in Texas where the USACE, Fort Worth District, along with other entities, operates and maintains reservoirs (fig. 1). Therefore, the U.S. Geological Survey (USGS), in cooperation with the USACE, analyzed streamflow trends and streamflow-related variables through 2017 in these seven basins to provide information that can help water managers with the USACE and river authorities make future water management decisions.

Purpose and Scope

Long-term records of precipitation, temperature, groundwater-level elevations, streamflow, and potential flood storage within seven river basins primarily in Texas (the Brazos, Colorado, Big Cypress, Guadalupe, Neches, Sulphur, and Trinity River Basins) were evaluated through 2017 for statistically significant changes over time (trends). Streamflow statistics selected for temporal trend analyses included annual minimum streamflow, annual peak streamflow, and streamflow volume. Streamflow volumes were analyzed for associations with precipitation volumes and potential flood storage. Precipitation, air temperature, and groundwater-level elevations were analyzed for trends that may help to explain changes observed in the streamflow statistics. The primary purpose of this report is to document trends in long-term streamflow data at 114 selected USGS streamflow-gaging stations and 36 simulated reservoir-inflow stations (hereinafter referred to as “simulated-inflow stations”) in the seven river basins. Except for one streamflow-gaging station in Louisiana, all the stations are in Texas.

Trends over time and the associations among the different types of time-series data were determined for three different time steps (annual, seasonal, and monthly). Definitively determining the causes for any observed changes in the different types of time-series data that were assessed was beyond the scope of this report.

Description of Study Area

The study area consists of seven major river basins in Texas and the small parts of four of these basins that extend into Arkansas, New Mexico, and Louisiana (fig. 1). The seven river basins (Brazos, Colorado, Big Cypress, Guadalupe, Neches, Sulphur, and Trinity) that are the subject of this report include 122,600 square miles (mi^2) of drainage area in Texas, encompassing about 46 percent of the total 268,600 mi^2 of Texas (USGS, 2019a). The selected basins include all or parts of 188 counties in Texas and overlie seven major aquifers: the Carrizo-Wilcox, Edwards (Balcones Fault Zone), Edwards-Trinity (Plateau), Gulf Coast, Ogallala, Seymour, and Trinity (TWDB, 2019b). Mean annual precipitation ranges from about 9 inches (in.) in the semi-arid western part of the State near New Mexico to more than 50 in. in the subhumid southeastern part of the State near Louisiana (fig. 2*A* in Winters, 2013; National Weather Service, 2019). Data collected from the National Inventory of Dams (NID) includes 4,861 storage structures throughout the 7 river basins in the study, totaling nearly 44 million acre-feet (acre-ft) of potential flood storage (USACE, 2019a).

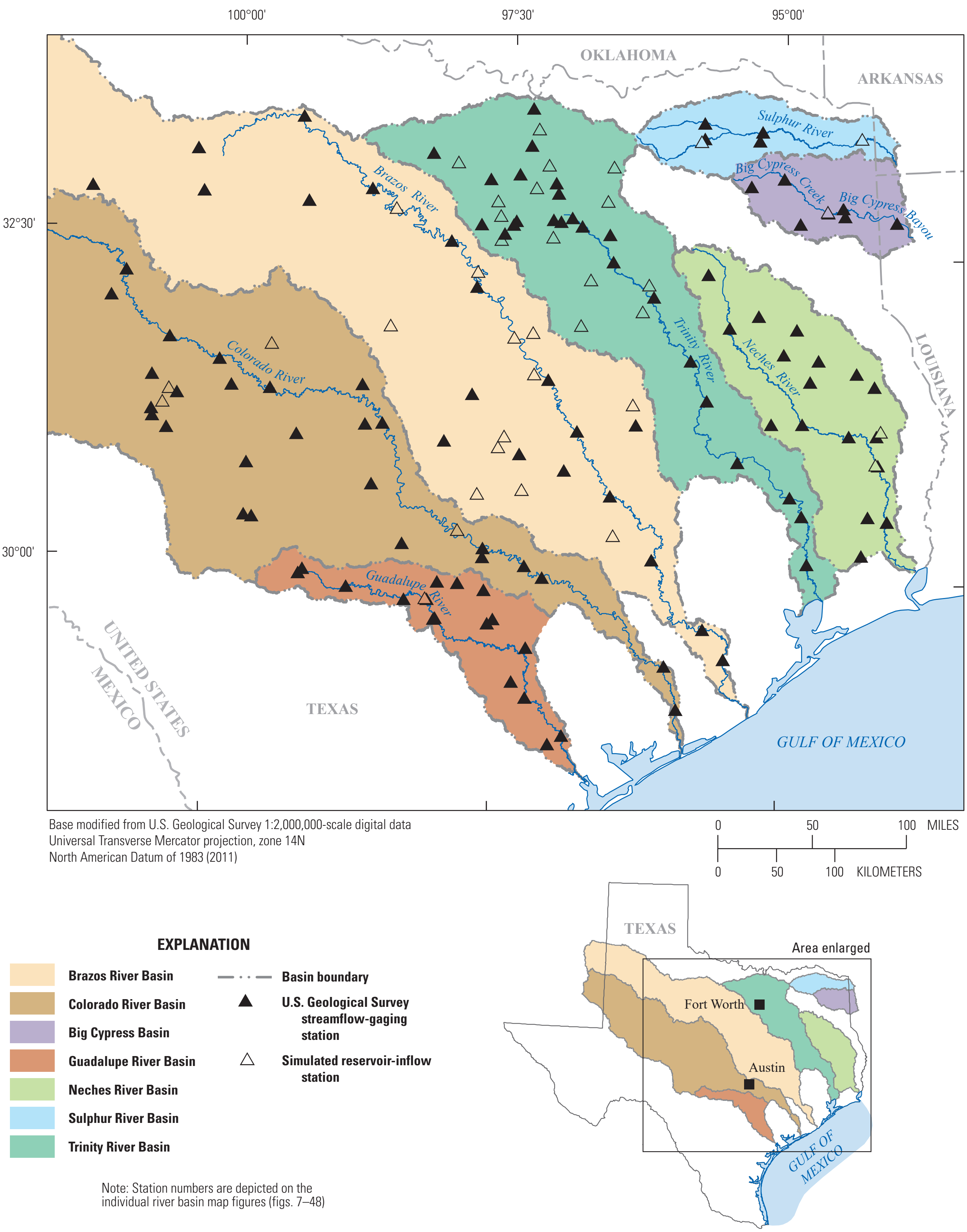

Figure 1. Locations of 114 U.S. Geological Survey streamflow-gaging stations and 36 simulated reservoir-inflow stations that were used to analyze for trends within the Brazos, Colorado, Big Cypress, Guadalupe, Neches, Sulphur, and Trinity River Basins.

Methods

Kendall's *tau*, a rank-based correlation coefficient that measures the monotonic relation between two variables, is commonly used for detecting trends in hydrologic time-series data (Helsel and Hirsch, 2002). In this report, Kendall's *tau* was used to detect upward or downward trends in precipitation and temperature for eight climate divisions representing seven river basins in the study area, streamflow in these seven river basins, and groundwater-level elevations in the seven major aquifers that underlie these river basins. Assessing trends in streamflow was the primary purpose. Because changes in precipitation, temperature and groundwater-level elevations can appreciably affect streamflow, understanding changes in streamflow requires taking these "forcing variables" into account. Annual, seasonal, and monthly trends in precipitation and streamflow were assessed. Three seasons were defined for the seasonal trend assessments: season 1 (November, December, January, and February), season 2 (March, April, May, and June), and season 3 (July, August, September, and October). The purpose of defining three seasons was to analyze for trends at a time step longer than 1 month but shorter than an entire year. If precipitation were to fall within a basin at the end of a month, the streamflow volume associated with that precipitation event would be measured during the following month, thereby influencing the ratio of streamflow volume to precipitation volume in a way that would not be ideal. Grouping months together for seasonal trend analyses reduces the effects of such situations.

Kendall's *tau* measures the strength of the monotonic relation between two variables and is ideal for measuring temporal trends for different time steps (Helsel and Hirsch, 2002). Kendall's *tau* is nonparametric; that is, this test statistic is based on the ranks of the data and not the actual data values. The null hypothesis is that the *tau* values will not differ significantly from zero. The *p*-value is a measure of the strength or the statistical significance of the association between the two variables. Small *p*-values (defined as less than or equal to 0.05 in this report [*p*-value ≤0.05]) indicate a significant association at a 95-percent confidence level (Helsel and Hirsch, 2002). A trend (upward or downward) is indicated when the null hypothesis is rejected; *p*-values >0.05 indicate the absence of a statistically significant trend. Because Kendall's *tau* is a rank-based procedure, it is resistant to the effects of unusual values (outliers). A positive Kendall's *tau* value that differs significantly from zero indicates an upward trend, and a negative Kendall's *tau* value that differs significantly from zero indicates a downward trend. Perfect monotonic relations result in Kendall's *tau* values of either –1 or 1, with –1 indicating a perfectly downward relation and 1 indicating a perfectly upward relation. A statistically significant strong trend is defined in this report as having a *p*-value ≤0.05 and a Kendall's *tau* value that is either greater than or equal to 0.25 (Kendall's *tau* ≥0.25) (strong upward trend) or less than or equal to –0.25 (Kendall's *tau* ≤–0.25) (strong downward trend). A statistically significant moderate downward trend is defined as having a *p*-value ≤0.05 and a Kendall's *tau* that is ≤–0.10 and >–0.25. A statistically significant moderate upward trend is defined as having a *p*-value ≤0.05 and a Kendall's *tau* that is ≥0.10 and <0.25.

Precipitation Trend Analysis

Temporal trends in precipitation (upward or downward) were evaluated because they can help to explain trends in streamflow (Groisman and others, 2004). Monthly precipitation data from 1900 through 2017 were downloaded from the National Oceanic and Atmospheric Administration (NOAA) website for the eight climate divisions representing the river basins in the study area (NOAA, 2019a; U.S. Department of Agriculture, 2019). Annual, seasonal, and monthly precipitation trends were analyzed for each of the eight climate divisions (High Plains, Trans-Pecos, Low Rolling Hills, Edwards Plateau, North Central Texas, South Central Texas, East Texas, and Upper Coast). Palmer Drought Severity Index (PDSI) values were downloaded for the climate divisions along with the precipitation data to analyze for trends in annual precipitation during different moisture conditions. The PDSI measures the duration and the intensity of long-term drought, where an annual mean PDSI >2.00 indicates moist conditions, an annual mean PDSI <–2.00 indicates drought conditions, and an annual mean PDSI between –1.99 and 1.99 indicates mean conditions (Palmer, 1965). Analyzing for trends during the extreme of wet and dry periods may indicate if dry periods or wet periods are becoming more frequent.

Daily precipitation data from 1900 through 2017 were downloaded from the NOAA National Centers for Environmental Information website by using a mapping tool available on the website (NOAA, 2019b). Downloads included daily totals for precipitation stations within polygons on a map. These polygons represented all the counties containing any part of each basin analyzed. The county names associated with each precipitation station, polygons, and the section number to which the station was assigned are provided in McDowell and others (2020). The precipitation stations from which data were retrieved are part of the Global Historical Climatology Network (Menne and others, 2012).

Basins were divided into sections along county lines for precipitation analyses. Sections were defined within each basin by creating roughly equal vertical and horizontal divisions of the aggregated counties overlapping each basin. In this way, possible latitudinal and longitudinal climate differences across the basin were accounted for with respect to precipitation trends. From the daily precipitation data, an area-weighted daily mean precipitation total was computed for each section of the basin. The locations of the precipitation stations used to compute the area-weighted daily mean precipitation for each section in the different basins are shown in figure 2, and the stations are listed in McDowell and others (2020). The area-weighted daily mean precipitation totals were analyzed for temporal trends in precipitation over annual, seasonal, and monthly time steps (McDowell and others, 2020). Annual precipitation data were analyzed with respect to calendar years. Lastly, precipitation data were analyzed during events producing annual peak streamflows to determine if there has been a change over time in the amount of precipitation producing large events (peak streamflow-related precipitation) within the basins. The area-weighted daily mean precipitation totals were summed for each section of each basin at different time steps around the annual peak streamflow and analyzed for trends. Streamflow-gaging stations were assigned the precipitation totals from the section of the basin in which they are located. The different time steps associated with peak streamflow-related precipitation included precipitation on the day of the annual peak; sum of precipitation 5 days before, the day of, and the day after the annual peak; and the sum of precipitation 30, 60, 90, 180, and 365 days before the annual peak. Defining the amount of precipitation that represents the annual peak streamflow is not straightforward. Sometimes smaller precipitation amounts can cause large annual peaks if preceded by wet conditions, in which case there are usually two peaks, with the first peak defining an antecedent wetting event and a second peak defining the annual peak streamflow. If the amount of precipitation producing the annual peaks is changing over time, then a consistent pattern may exist in the trends at the different time steps.

Temperature Trend Analysis

Monthly mean air temperature data from 1900 through 2017 were downloaded from the NOAA website for the same eight climate divisions as those used for precipitation analyses in this study (NOAA, 2019a; U.S. Department of Agriculture, 2019). From the monthly mean air temperature data, the annual mean air temperature was computed as the mean of the 12 area-weighted monthly mean values. Annual mean air temperature data were analyzed with respect to calendar years.

To analyze for temporal trends of annual mean air temperature, multiple regression equations with periodic functions were developed (Helsel and Hirsch, 2002). The sine and cosine functions were used to account for temporal oscillations apparent in scatterplots of time and annual mean air temperature data over the period of record for the climate divisions. The dependent variable was annual mean air temperature, and the independent variables were cos (θ), sin (θ), and time (t), where θ equals 2π multiplied by the fraction of the period (in years) that was analyzed, as described in detail by Helsel and Hirsch (2002, p. 341). For example, if the period of record for a climate division was 100 years, then at year 50 from the beginning of record, 2π would be multiplied by 0.5 (50 divided by 100), the fraction of the time period analyzed. Transforming the time variable by multiplying the fractional portion of the time period analyzed by 2π was done so that 1 year would represent one complete cycle of the sine and cosine functions. Independent variables were considered statistically significant if their p-value was ≤ 0.05. If at least one of the periodic functions was statistically significant, the other periodic function was left in the regression equation because the absence of one affects the phase shift of the function. An upward or downward temporal trend in annual mean air temperature was determined if the coefficient on the time variable was statistically significant and by its sign (positive for upward and negative for downward). A detailed explanation of multiple regression with periodic functions is provided in Helsel and Hirsch (2002, p. 341).

Groundwater-Level Elevation Trend Analysis

Groundwater-level elevation data were downloaded from the TWDB Groundwater Database website (TWDB, 2019c) and analyzed for trends in groundwater-level elevations in the major aquifers of Texas that underlie the seven river basins in the study area (fig. 3). All available groundwater-level elevation measurements coded as publishable according to the TWDB for an aquifer in a given year were used to compute an annual mean groundwater-level elevation for a given aquifer. When the number of measurements used to compute the mean groundwater-level elevation for a given year was ≥ 20, the mean groundwater-level elevation for that year was used in the trend analysis; trends in mean groundwater-level elevations over time were analyzed by using Kendall's *tau*. Groundwater-level elevations obtained from 11,806 wells were compiled and analyzed for this report. Through groundwater/surface-water interactions, groundwater inflows can contribute appreciably to streamflow. The amount of groundwater inflow in a given reach of a river is often positively correlated with groundwater-level elevation; relatively larger groundwater inflows occur when groundwater elevations are higher, and relatively smaller groundwater inflows occur when groundwater elevations are lower (Barlow and Leake, 2012). The purpose of including trends in groundwater-level elevation data in the seven major aquifers of Texas is to identify possible causes for temporal trends identified in streamflow at the stations selected in this study. A detailed analysis of streamflow changes and groundwater and surface-water interactions is beyond the scope of this report.

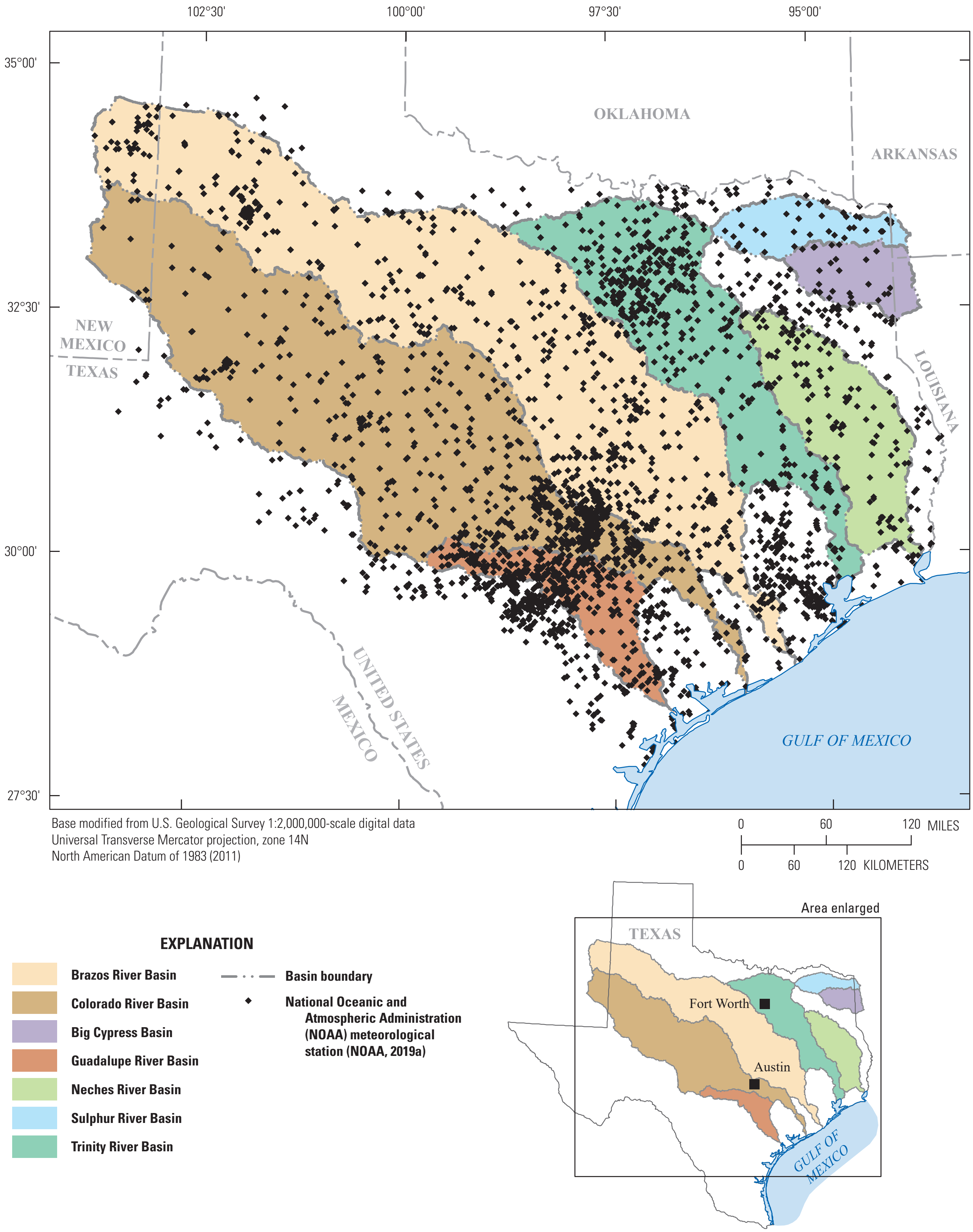

Figure 2. Locations of National Oceanic and Atmospheric Administration meteorological stations used for precipitation trend analyses within the Brazos, Colorado, Big Cypress, Guadalupe, Neches, Sulphur, and Trinity River Basins, 1900–2017.

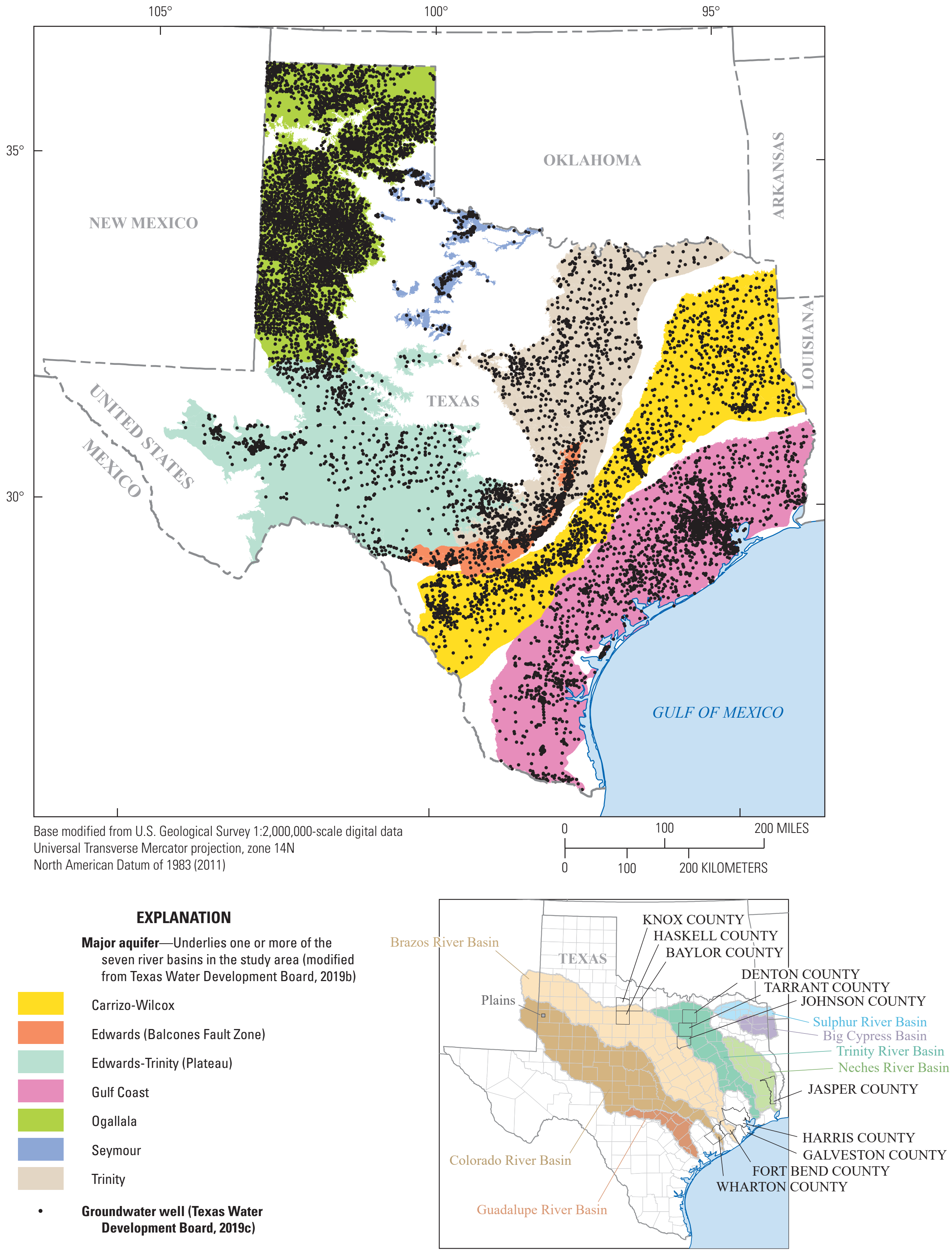

Figure 3. Locations of groundwater wells completed in seven major aquifers underlying the Brazos, Colorado, Big Cypress, Guadalupe, Neches, Sulphur, and Trinity River Basins.

Streamflow Trend Analysis

Many of the streamflow-gaging stations included in this report were used in previous USGS reports on trends in streamflow through 2003 (Asquith and others, 2007a, b) or 2007 (Asquith and Heitmuller, 2008). Trends identified in these previous reports were reanalyzed with the additional streamflow data collected in the intervening years since those earlier studies were done. This report summarizes trends in streamflow through calendar year 2017. Simulated-inflow data were provided by the USACE (2019b) for reservoirs managed by different entities in the study area (the USACE, Brazos River Authority, Lower Colorado River Authority, San Angelo Parks and Recreation Department, Tarrant Regional Water District, and the City of Dallas) and were used in conjunction with streamflow data obtained from USGS streamflow-gaging stations to evaluate trends in streamflow (USGS, 2019b). In cases where a USGS streamflow-gaging station is immediately downstream from a simulated-inflow station, the simulated-inflow station takes precedence in visualization of any trends. Additionally, streamflow monitored by USGS streamflow-gaging stations downstream from reservoirs with regulated releases will be inversely affected according to distance from the reservoirs; streamflow at stations closer to the reservoirs will be more affected by the releases. The USACE (2019b) calculates the simulated inflow as a mass balance over a 24-hour period to each reservoir by using the following equation:

$$Qinflow = \Delta S + E + Qgateout + Qpumpout - Qpumpin \quad (1)$$

where

- ΔS is the change in storage volume in the reservoir;
- E is the amount of reservoir evaporation;
- $Qinflow$ is the simulated surface-water inflow to the reservoir;
- $Qgateout$ is the amount of water released from the reservoir from its gates;
- $Qpumpout$ is the amount of water pumped out of the reservoir; and
- $Qpumpin$ is the amount of water pumped into the reservoir.

The change in storage volume is computed from reservoir water-surface elevation data and stage-storage relations for a reservoir. Evaporation is estimated from various methods such as pan evaporation data and applicable pan coefficients. *Qpumpout* and *Qpumpin* are known by the USACE for each reservoir. The amount of simulated inflow (*Qinflow*) to the reservoir is the only remaining unknown, and thus can be determined by using equation 1. Simulated-inflow data for USACE-managed reservoirs are available from the USACE Fort Worth District water management website (USACE, 2019b).

Historical precipitation and streamflow-volume data were analyzed to determine the association between streamflow volumes and precipitation. Because streamflow volumes normally increase as precipitation increases and decrease as precipitation decreases, stations with no association between streamflow volumes and precipitation may indicate something unique to the basin and explain temporal trends in streamflow observed at these stations.

Temporal trends in the ratio of streamflow volume to precipitation volume may indicate a change in the way a given basin responds to precipitation events by indicating that the amount of water leaving a basin for a given precipitation volume is changing over time. The relation between potential flood storage volumes and streamflow volumes was analyzed as a possible explanation of temporal trends in streamflow volumes. Negative associations between potential flood storage and streamflow volumes indicate that streamflow volumes decrease with increases in potential flood storage. Negative associations between potential flood storage and streamflow in conjunction with downward temporal trends in streamflow and downward trends in the ratio of streamflow volume to potential flood storage indicate that the addition of potential flood storage in a basin may be responsible for downward trends in streamflow volumes.

Annual, Seasonal, and Monthly Analysis

A total of 114 USGS streamflow-gaging stations and 36 simulated-inflow stations distributed among the 7 river basins were selected for streamflow trend analyses. USGS streamflow-gaging stations provide daily mean streamflow data, whereas simulated-inflow data are used to approximate streamflow at simulated-inflow stations immediately upstream from reservoirs. Stations were chosen to characterize streamflow in each basin by their length of period of record (more than 20 years) and their location relative to other stations (widely dispersed stations within each basin were desired). Monthly mean streamflow was computed from daily mean streamflow at each USGS and simulated-inflow station for the period of record at each station. Monthly mean streamflow was converted to a volume of water passing the station during a given month (monthly streamflow volume) by multiplying the daily mean streamflow in cubic feet per second by 86,400 (number of seconds in 1 day) and then by the number of days in a given month. The number of days in February during leap years (29) was accounted for when computing volumes. Volumes in cubic feet were converted to acre-feet to use in analyses of changes in volumes over time and when computing the ratios of streamflow volume to precipitation and potential flood storage volume. Monthly streamflow volumes were summed to compute annual volumes and seasonal volumes.

The area-weighted daily mean precipitation totals for each of the sections in the seven basins were used to analyze for temporal trends in precipitation-related variables such as the ratio of streamflow volume to precipitation volume. Monthly precipitation volume was computed by summing the daily values for a month to obtain monthly precipitation depth and multiplying the monthly precipitation depth by the contributing drainage area to the station. Monthly precipitation volume was converted to acre-feet to compute the ratio of monthly streamflow volume to monthly precipitation volume. Ratios of streamflow volume to precipitation volume were also computed for annual and seasonal time steps. Changes over time in the ratio of streamflow volume to precipitation volume would indicate a change in the way the system responds to precipitation events and possibly explain trends in streamflow.

Annual Minimum and Peak Flow Analysis

Temporal trends of annual minimum streamflow and annual peak streamflow are included in this report through water year 2017. A water year is defined as the 12-month period from October 1 through September 30 and is designated by the calendar year in which it ends. Some of the streamflow-gaging stations, particularly in the western part of Texas are characterized by extremes in streamflow. Daily mean streamflow at many western stations frequently is zero. The same basin may receive as much as 10 to 15 in. of precipitation in a single day, resulting in large runoff events that account for a large percentage of the annual streamflow volume. In a basin where a few large runoff events account for a large percentage of streamflow volume, the annual streamflow volume can vary markedly depending on the presence or absence of large rain events during a given year. Therefore, any changes to annual peak streamflow could correspond to changes in annual streamflow volumes.

Potential Flood Storage Trend Analysis

Surface-water storage affects annual peak streamflow. Benson (1964) determined that about 50 acre-feet per square mile of flood storage reduces the annual peak streamflow by about 10 percent in arid areas. Asquith (2001) studied reservoirs for 96 streamflow-gaging stations in Texas and found that as potential flood storage in a basin increases, the annual mean peak streamflow decreases nonlinearly.

Surface-water storage structures (dams) listed on the USACE NID and within the drainage area of the 114 USGS streamflow-gaging stations and the 36 reservoir stations were compiled. The NID database lists 4,861 dams within the 7 basins (fig. 4; USACE, 2019a; McDowell and others, 2020). The NID database includes storage information for each dam, such as normal storage and maximum storage. The normal storage is the volume of storage in a reservoir below the normal retention level, and maximum storage is the volume of storage in a reservoir below the maximum attainable water-surface elevation. The potential flood storage, defined as the difference between maximum storage and normal storage, was computed for each dam and accumulated basin-wide over time based on the completion date of the dam.

The associations of potential flood storage and streamflow volumes were analyzed by using Kendall’s *tau* to determine their relations as a possible explanation of temporal trends in streamflow. Negative associations between potential flood storage and streamflow volumes indicate that streamflow volumes decrease with increases in potential flood storage. Negative associations between potential flood storage and streamflow in conjunction with downward temporal trends (also determined by Kendall’s *tau*) in streamflow and downward trends in the ratio of streamflow volume to potential flood storage indicate that the addition of potential flood storage in a watershed may be responsible for downward trends in streamflow volumes.

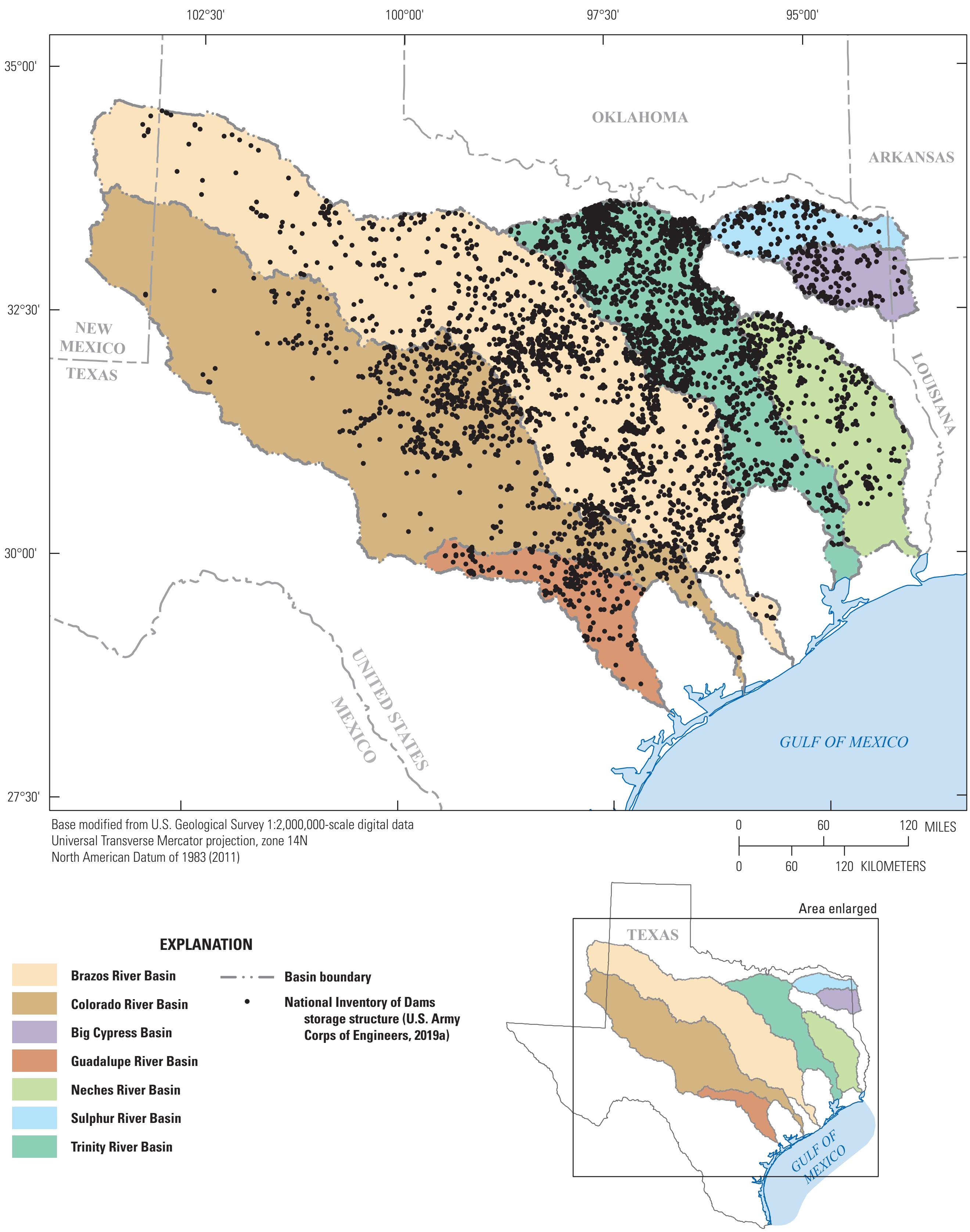

Figure 4. Locations of surface-water storage structures (dams) in the Brazos, Colorado, Big Cypress, Guadalupe, Neches, Sulphur, and Trinity River Basins.

Precipitation and Temperature Trends by Climate Division

Results of precipitation trend analyses indicated moderate upward trends in the Upper Coast and East Texas Climate Divisions analyzed on an annual time step from 1900 through 2017 (fig. 5; table 1). These two climate divisions are in the eastern and southeastern parts of the State, and they receive more mean annual precipitation (45.88 and 46.09 in., respectively) than the other climate divisions (table 1).

None of the climate division data indicated seasonal trends in precipitation. Results of precipitation trend analyses on a monthly time step indicated eight moderate upward trends and one moderate downward trend (table 1), or 8.0 percent of the months had upward trends and 1.0 percent had downward trends. Months with upward (positive) trends were January, March, June, and September within four different climate divisions. April was the only month with a downward trend.

No trends in any climate division were found in annual precipitation during drought conditions, normal conditions, or moist conditions (table 2), which were indicated by the annual mean PDSI. Drought conditions included years with annual mean PDSI values <–2.00, and moist conditions included years with annual mean PDSI values >2.00. Although the Upper Coast and East Texas Climate Division data indicated upward trends in precipitation, the results indicated no trends in drought or moist conditions.

Table 3 presents the results of using multiple regression analysis with periodic functions to analyze for temporal trends in annual mean air temperature within the eight climate divisions. The results indicated upward trends in annual mean air temperature within all climate divisions, with a mean slope of 0.02 degree Fahrenheit per year, or 1 degree every 50 years. The slope of the curve is the coefficient of the time variable, t.

Increases in air temperature correspond to decreases in the amount of energy required for evaporation to occur. This energy required is called latent heat of vaporization, and it decreases slightly with increases in water temperature (Shuttleworth, 1993). Similarly, as air temperature increases, the saturated vapor pressure increases, which results in a greater capacity of the air to hold water vapor.

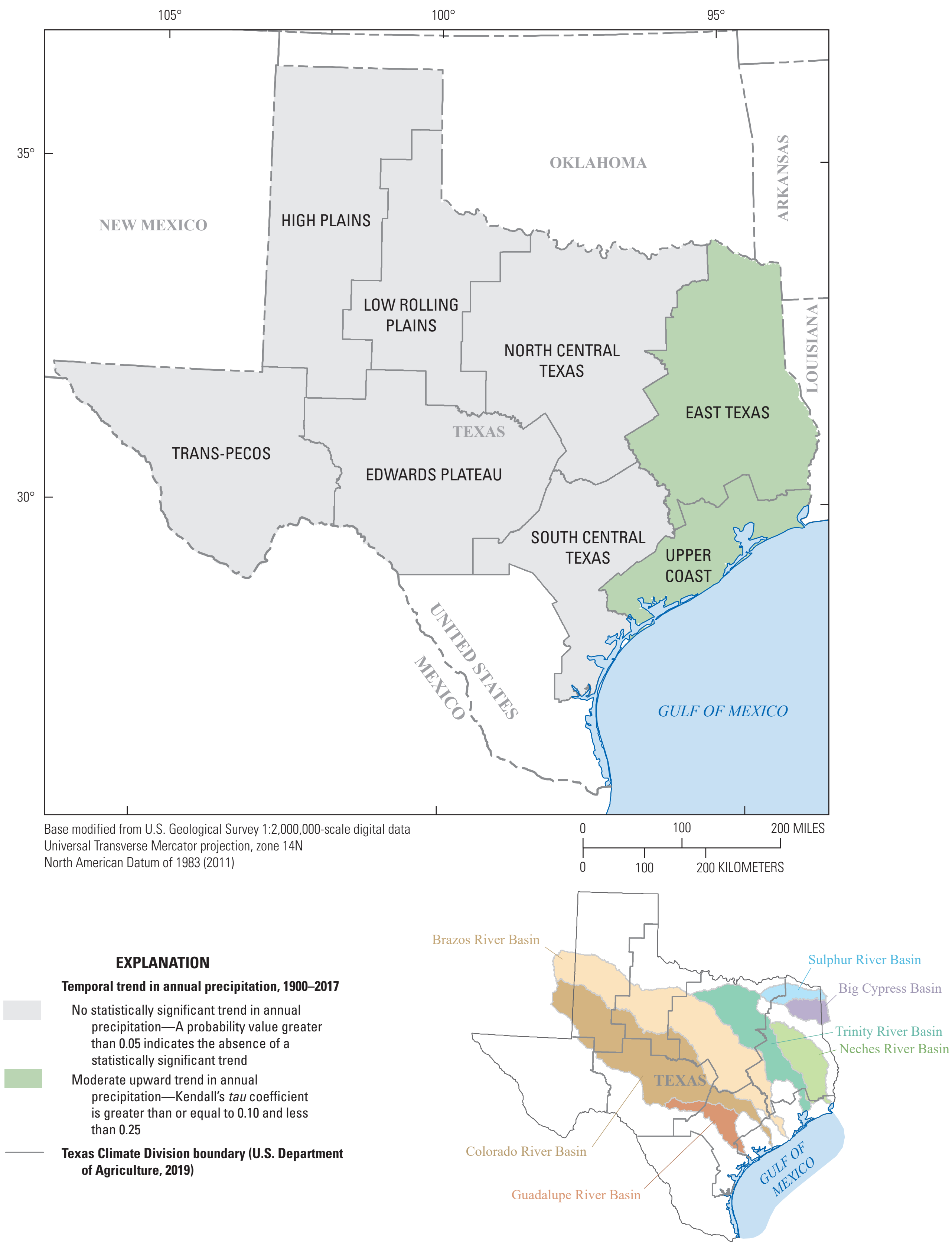

Figure 5. The eight Texas Climate Divisions that include the Brazos, Colorado, Big Cypress, Guadalupe, Neches, Sulphur, and Trinity River Basins with annual trends in precipitation identified, 1900–2017.

Table 1. Summary of annual, seasonal, and monthly precipitation trends during 1900–2017 within eight U.S. Department of Agriculture (USDA; 2019) Texas Climate Divisions that include the Brazos, Colorado, Big Cypress, Guadalupe, Neches, Sulphur, and Trinity River Basins.

[*p*-value, probability value (considered statistically significant if less than 0.05); red shaded cells indicate statistically significant downward trends; green shaded cells indicate statistically significant upward trends]

Time step	USDA Texas Climate Division (fig. 5)							
	High Plains				Trans-Pecos			
	Kendall's *tau*	*p*-value	Mean precipitation (inches)	Percentage[1]	Kendall's *tau*	*p*-value	Mean precipitation (inches)	Percentage[1]
Annual	0.0033	0.9592	18.59	100	0.0328	0.6007	12.62	100
Season 1[2]	0.0130	0.8376	2.53	13.6	0.0291	0.6443	1.99	15.8
Season 2[3]	0.0052	0.9351	7.37	39.7	−0.0104	0.8688	3.53	28.0
Season 3[4]	−0.0041	0.9499	8.69	46.8	0.0309	0.6219	7.09	56.2
January	0.0685	0.2732	0.52	2.8	0.0658	0.2930	0.48	3.8
February	0.0603	0.3343	0.60	3.2	0.0150	0.8106	0.46	3.6
March	0.0972	0.1196	0.87	4.7	0.0299	0.6334	0.39	3.1
April	−0.0966	0.1219	1.35	7.3	−0.0367	0.5577	0.56	4.4
May	−0.0558	0.3705	2.54	13.7	0.0078	0.9000	1.14	9.1
June	0.0697	0.2632	2.61	14.0	0.0628	0.3138	1.45	11.5
July	−0.0411	0.5104	2.42	13.0	0.0042	0.9462	1.95	15.5
August	0.0023	0.9703	2.46	13.2	0.0605	0.3321	1.90	15.0
September	0.0116	0.8524	2.17	11.7	0.0519	0.4050	1.99	15.8
October	−0.0592	0.3426	1.65	8.8	−0.0226	0.7167	1.25	9.9
November	−0.0500	0.4236	0.78	4.2	−0.0324	0.6053	0.55	4.4
December	0.0387	0.5360	0.63	3.4	0.0450	0.4722	0.49	3.9

Time step	USDA Texas Climate Division (fig. 5)							
	Low Rolling Plains				Edwards Plateau			
	Kendall's *tau*	*p*-value	Mean precipitation (inches)	Percentage[1]	Kendall's *tau*	*p*-value	Mean precipitation (inches)	Percentage[1]
Annual	0.0700	0.2622	23.04	100	0.0154	0.8071	23.57	100
Season 1[2]	0.0734	0.2417	3.91	17.0	0.0404	0.5202	4.84	20.5
Season 2[3]	0.0294	0.6385	9.67	42.0	−0.0057	0.9296	9.19	39.0
Season 3[4]	0.0188	0.7641	9.47	41.1	0.0030	0.9629	9.54	40.5
January	0.0799	0.2008	0.79	3.4	0.0810	0.1943	1.05	4.5
February	0.1187	0.0574	0.99	4.3	0.0630	0.3127	1.24	5.2
March	0.1104	0.0767	1.23	5.3	0.1084	0.0823	1.33	5.7
April	−0.0869	0.1635	2.07	9.0	−0.1270	0.0416	2.14	9.1
May	−0.0360	0.5640	3.43	14.9	−0.0421	0.5000	3.16	13.4
June	0.0721	0.2477	2.94	12.8	0.0832	0.1818	2.55	10.8
July	−0.0345	0.5799	2.16	9.4	−0.1202	0.0538	1.99	8.5
August	0.0744	0.2328	2.24	9.7	0.0548	0.3793	2.13	9.0
September	0.0235	0.7063	2.75	11.9	−0.0022	0.9722	2.93	12.4
October	−0.0432	0.4882	2.31	10.0	0.0010	0.9870	2.49	10.6
November	−0.0277	0.6568	1.20	5.2	−0.0097	0.8762	1.43	6.1
December	0.0642	0.3039	0.93	4.0	−0.0254	0.6839	1.12	4.8

Table 1. Summary of annual, seasonal, and monthly precipitation trends during 1900–2017 within eight U.S. Department of Agriculture (USDA; 2019) Texas Climate Divisions that include the Brazos, Colorado, Big Cypress, Guadalupe, Neches, Sulphur, and Trinity River Basins.—Continued

[*p*-value, probability value (considered statistically significant if less than 0.05); red shaded cells indicate statistically significant downward trends; green shaded cells indicate statistically significant upward trends]

Time step	USDA Texas Climate Division (fig. 5)							
	North Central Texas				South Central Texas			
	Kendall's *tau*	*p*-value	Mean precipitation (inches)	Percentage[1]	Kendall's *tau*	*p*-value	Mean precipitation (inches)	Percentage[1]
Annual	0.1043	0.0945	33.19	100	0.0953	0.1265	33.49	100
Season 1[2]	0.1029	0.1006	8.64	26.0	0.0304	0.6292	9.14	27.3
Season 2[3]	0.0496	0.4277	13.78	41.5	0.0270	0.6670	12.38	37.0
Season 3[4]	0.0765	0.2203	10.78	32.5	0.0919	0.1409	11.96	35.7
January	0.0896	0.1506	1.89	5.7	0.1470	0.0183	2.11	6.3
February	0.0857	0.1692	2.11	6.4	−0.0058	0.9259	2.14	6.4
March	0.1319	0.0345	2.51	7.6	0.0625	0.3161	2.19	6.5
April	−0.0950	0.1276	3.43	10.3	−0.1105	0.0763	2.88	8.6
May	−0.0225	0.7185	4.53	13.6	0.0132	0.8324	4.06	12.1
June	0.1025	0.1001	3.31	10.0	0.1307	0.0361	3.26	9.7
July	−0.0479	0.4427	2.25	6.8	−0.0993	0.1111	2.50	7.5
August	0.0677	0.2774	2.20	6.6	0.0494	0.4277	2.46	7.4
September	0.0431	0.4897	3.05	9.2	0.0922	0.1391	3.72	11.1
October	0.0720	0.2477	3.27	9.8	0.0355	0.5688	3.28	9.8
November	0.0392	0.5300	2.43	7.3	0.0245	0.6942	2.52	7.5
December	0.0278	0.6552	2.20	6.6	−0.1000	0.1090	2.37	7.1

Time step	USDA Texas Climate Division (fig. 5)							
	East Texas				Upper Coast			
	Kendall's *tau*	*p*-value	Mean precipitation (inches)	Percentage[1]	Kendall's *tau*	*p*-value	Mean precipitation (inches)	Percentage[1]
Annual	0.1229	0.0488	46.09	100	0.1504	0.0159	45.88	100
Season 1[2]	0.0747	0.2333	15.70	34.1	0.0383	0.5418	14.03	30.6
Season 2[3]	0.0413	0.5089	16.93	36.7	0.0703	0.2603	15.04	32.8
Season 3[4]	0.1041	0.0954	13.46	29.2	0.1204	0.0535	16.81	36.6
January	0.0865	0.1650	3.69	8.0	0.1553	0.0127	3.42	7.5
February	0.0017	0.9777	3.56	7.7	−0.0299	0.6318	2.95	6.4
March	0.0562	0.3668	3.84	8.3	0.0631	0.3116	2.95	6.4
April	−0.1146	0.0661	4.31	9.4	−0.0510	0.4129	3.30	7.2
May	0.0216	0.7289	4.90	10.6	0.0361	0.5625	4.43	9.7
June	0.1257	0.0437	3.87	8.4	0.1344	0.0311	4.36	9.5
July	−0.0873	0.1614	3.39	7.4	−0.0660	0.2899	4.21	9.2
August	0.0149	0.8107	2.95	6.4	0.0806	0.1959	4.00	8.7
September	0.1321	0.0341	3.39	7.3	0.1534	0.0139	4.56	9.9
October	0.1151	0.0648	3.74	8.1	0.0245	0.6943	4.05	8.8
November	0.0867	0.1642	4.08	8.8	0.0658	0.2910	3.77	8.2
December	−0.0225	0.7185	4.37	9.5	−0.0904	0.1473	3.89	8.5

[1]Percentage of the total precipitation within the season or month during 1900–2017.

[2]Season 1 includes November, December, January, and February.

[3]Season 2 includes March, April, May, and June.

[4]Season 3 includes July, August, September, and October.

Table 2. Trends in annual precipitation during different moisture conditions during 1900–2017 within eight U.S. Department of Agriculture (USDA; 2019) Texas Climate Divisions that include the Brazos, Colorado, Big Cypress, Guadalupe, Neches, Sulphur, and Trinity River Basins.

[PDSI, Palmer Drought Severity Index; drought conditions, years with a mean PDSI less than −2.00; normal conditions, years with a mean PDSI between −1.99 and 1.99; moist conditions, years with a mean PDSI greater than 2.00; *p*-value, probability value (considered statistically significant if less than 0.05)]

Moisture condition from PDSI	USDA Texas Climate Division (fig. 5)							
	High Plains		Trans-Pecos		Low Rolling Plains		Edwards Plateau	
	Kendall's *tau*	*p*-value	Kendall's *tau*	*p*-value	Kendall's *tau*	*p*-value	Kendall's *tau*	*p*-value
Annual precipitation during drought conditions	−0.3143	0.1133	−0.0314	0.8348	−0.1895	0.2561	−0.1389	0.3689
Annual precipitation during normal conditions	−0.0115	0.8887	−0.1061	0.1961	0.0995	0.2187	0.0350	0.6647
Annual precipitation during moist conditions	−0.2422	0.0709	−0.1818	0.2634	−0.0371	0.8083	−0.2863	0.0667

Moisture condition from PDSI	USDA Texas Climate Division (fig. 5)							
	North Central Texas		South Central Texas		East Texas		Upper Coast	
	Kendall's *tau*	*p*-value	Kendall's *tau*	*p*-value	Kendall's *tau*	*p*-value	Kendall's *tau*	*p*-value
Annual precipitation during drought conditions	0.1605	0.2721	−0.0317	0.8280	0.1775	0.2594	−0.0838	0.5849
Annual precipitation during normal conditions	−0.0379	0.6443	0.1386	0.0886	0.0776	0.3202	−0.0009	0.9959
Annual precipitation during moist conditions	−0.1735	0.2713	−0.1579	0.3630	−0.0175	0.9442	−0.1873	0.1987

Table 3. Summary of multiple regression analysis done with periodic functions to analyze for temporal trends during 1900–2017 in annual mean air temperature in degrees Fahrenheit in eight U.S. Department of Agriculture (USDA; 2019) Texas Climate Divisions that include the Brazos, Colorado, Big Cypress, Guadalupe, Neches, Sulphur, and Trinity River Basins.

[*p*-value, probability value (considered statistically significant if less than 0.05); <, less than; PAMAT, predicted annual mean air temperature in degrees Fahrenheit; *, multiplication symbol; θ, theta; *t*, time, in units of years; green shaded cells indicate statistically significant upward trends]

USDA Texas Climate Division[1]	Regression equation	*p*-value for time coefficient[2]	Adjusted r-squared	Period analyzed
High Plains	PAMAT = 56.89 + (0.16*$cos\theta$) + (0.82*$sin\theta$) + (0.03*t)	<0.001	30.0	1900–2017
Trans-Pecos	PAMAT = 61.74 + (0.33*$cos\theta$) + (0.46*$sin\theta$) + (0.03*t)	<0.001	34.7	1900–2017
Low Rolling Plains	PAMAT = 61.13 + (0.20*$cos\theta$) + (0.95*$sin\theta$) + (0.03*t)	<0.001	20.6	1900–2017
Edwards Plateau	PAMAT = 64.25 + (0.47*$cos\theta$) + (0.92*$sin\theta$) + (0.02*t)	<0.001	22.8	1900–2017
North Central Texas	PAMAT = 63.61 + (0.37*$cos\theta$) + (0.84*$sin\theta$) + (0.02*t)	<0.001	15.8	1900–2017
South Central Texas	PAMAT = 67.50 + (0.42*$cos\theta$) + (0.83*$sin\theta$) + (0.02*t)	<0.001	24.9	1900–2017
East Texas	PAMAT = 64.77 + (0.45*$cos\theta$) + (0.73*$sin\theta$) + (0.02*t)	<0.001	17.8	1900–2017
Upper Coast	PAMAT = 67.42 + (0.50*$cos\theta$) + (0.73*$sin\theta$) + (0.02*t)	<0.001	32.8	1900–2017

[1]Refer to figure 5 for location of Texas Climate Divisions.

[2]Only *p*-value for time variable reported. If at least one *p*-value for either the *sin* or *cos* coefficients was less than 0.05, then both *sin* and *cos* functions were included in the regression equation.

Groundwater-Level Elevation Trends for Major Aquifers

The purpose of including trends in annual mean groundwater-level elevation data in the seven major aquifers of Texas is to identify possible causes for temporal trends identified in streamflow at the stations evaluated in this study. Graphs of annual mean groundwater-level elevations within the seven major aquifers are illustrated (fig. 6, *A*–*G*); years when the number of annual groundwater-level elevation measurements was either ≥20 or <20 are identified. For analysis of groundwater-level elevation data, Kendall's *tau* was only computed for years during which the number of groundwater-level elevation measurements was greater than or equal to 20.

From 1928 through 2017, the Carrizo-Wilcox aquifer groundwater-level elevation data indicated a downward trend, and Kendall's *tau* equaled –0.6672 (p-value ≤0.05) (fig. 6*A*). For this period of record, the mean number of measurements per year was 953. The downward trend is consistent with groundwater-level declines illustrated in figure 2-1 of a report by the TWDB (2016) that indicate declines as much as several hundred feet in some parts of the aquifer. The Carrizo-Wilcox aquifer is identified in the TWDB report (2016) as having the potential to discharge groundwater directly to the rivers and tributaries within the Colorado, Big Cypress, Guadalupe, Neches, Sulphur, and Trinity River Basins. The amount of streamflow over the aquifer outcrop area attributable to groundwater discharge from the Carrizo-Wilcox aquifer is 25 percent (TWDB, 2016). Therefore, groundwater-level trends in the aquifer in areas that contribute to the rivers and tributaries within the basins may explain streamflow trends, if present.

From 1929 through 2017, the Edwards (Balcones Fault Zone) aquifer groundwater-level elevation data indicated a downward trend, and Kendall's *tau* equaled –0.4479 (p-value ≤0.05) (fig. 6*B*). For this period of record, the mean number of measurements per year was 1,622. The Edwards aquifer is not a homogenous aquifer, however; it is a karst system composed of different limestones and is heterogenic. Groundwater-level elevations therefore vary considerably across the Edwards aquifer because of its high permeability and rapid response to rainfall, pumping, and drought (George and others, 2011; Eckhardt, 2019). Changes, or trends, in groundwater-level elevation data are less meaningful for the Edwards aquifer because of the rapid recharge and discharge characteristics of the aquifer. The Edwards aquifer is identified in the TWDB report (2016) as having the potential to discharge groundwater directly to the rivers and tributaries within the Guadalupe Basin. The amount of streamflow over the aquifer outcrop area attributable to groundwater discharge from the Edwards aquifer is 72 percent (TWDB, 2016). Therefore, groundwater-level trends in the aquifer in areas that contribute to the rivers and tributaries within the Guadalupe Basin may explain streamflow trends, if present.

From 1949 through 2017, the Edwards-Trinity (Plateau) aquifer groundwater-level elevation data indicated no trend, and Kendall's *tau* equaled –0.0394 (p-value equals 0.6522) (fig. 6*C*). For this period of record, the mean number of measurements per year was 101. For the trend analysis of the Edwards-Trinity (Plateau) aquifer, the first measurements in December for each well were used. This was done to include data that represented ambient aquifer conditions with minimal effects from pumpage discharge as was done for the groundwater availability model for the aquifer by the TWDB (Anaya and Jones, 2009). According to a report by the TWDB, groundwater-level elevations have remained fairly stable because recharge has kept pace with relatively low amounts of pumping withdrawals across the extent of the aquifer (George and others, 2011). More recent publications by the TWDB (2016) indicate that there are areas in the northern and western plateau where groundwater levels have declined from increased pumping. The Edwards-Trinity (Plateau) aquifer is identified in the TWDB report (2016) as having the potential to discharge groundwater directly to the rivers and tributaries within the Colorado and Guadalupe Basins. The amount of streamflow over the aquifer outcrop area attributable to groundwater discharge from the Edwards-Trinity (Plateau) aquifer is 55 percent (TWDB, 2016). Therefore, groundwater-level trends in the aquifer in areas that contribute to the rivers and tributaries within the basins may explain streamflow trends, if present.

From 1930 through 2017, the Gulf Coast aquifer groundwater-level elevation data indicated a downward trend, and Kendall's *tau* equaled –0.4045 (p-value ≤0.05) (fig. 6*D*). For this period of record, the mean number of measurements per year was 2,065. A report by the TWDB indicates that groundwater-level declines of as much as 350 feet (ft) have led to land subsidence in Harris, Galveston, Fort Bend, Jasper, and Wharton Counties (fig. 3; George and others, 2011; Shah and others, 2018). In 1976 the Harris-Galveston Coastal Subsidence District, created by the Texas Legislature to regulate groundwater withdrawals as they relate to land-surface subsidence, adopted the 1976 Regulatory Plan as its first regulatory effort (Mace and others, 2006). The 1976 Plan called upon permittees to voluntarily do whatever they could to reduce groundwater withdrawals, and cities and industries started to change to alternative water supplies. Since the 1976 regulatory plan was adopted, the Gulf Coast aquifer data indicated an overall upward trend, and for the period from 1976 through 2017, Kendall's *tau* equaled 0.7375 (p-value ≤0.05) (fig. 6*D*). However, in areas and north and west of Houston, groundwater withdrawals have increased, and groundwater-level elevations have declined more than 100 ft between 2000 and 2015 (TWDB, 2016). The Gulf Coast aquifer is identified in the TWDB report (2016) as having the potential to discharge groundwater directly to the rivers and tributaries within the Colorado, Guadalupe, and Neches Basins. The amount of streamflow over the aquifer outcrop area attributable to groundwater discharge from the Gulf Coast aquifer is 27 percent (TWDB, 2016). Therefore, groundwater-level trends in the aquifer in areas that contribute to the rivers and tributaries within the basins may explain streamflow trends, if present.

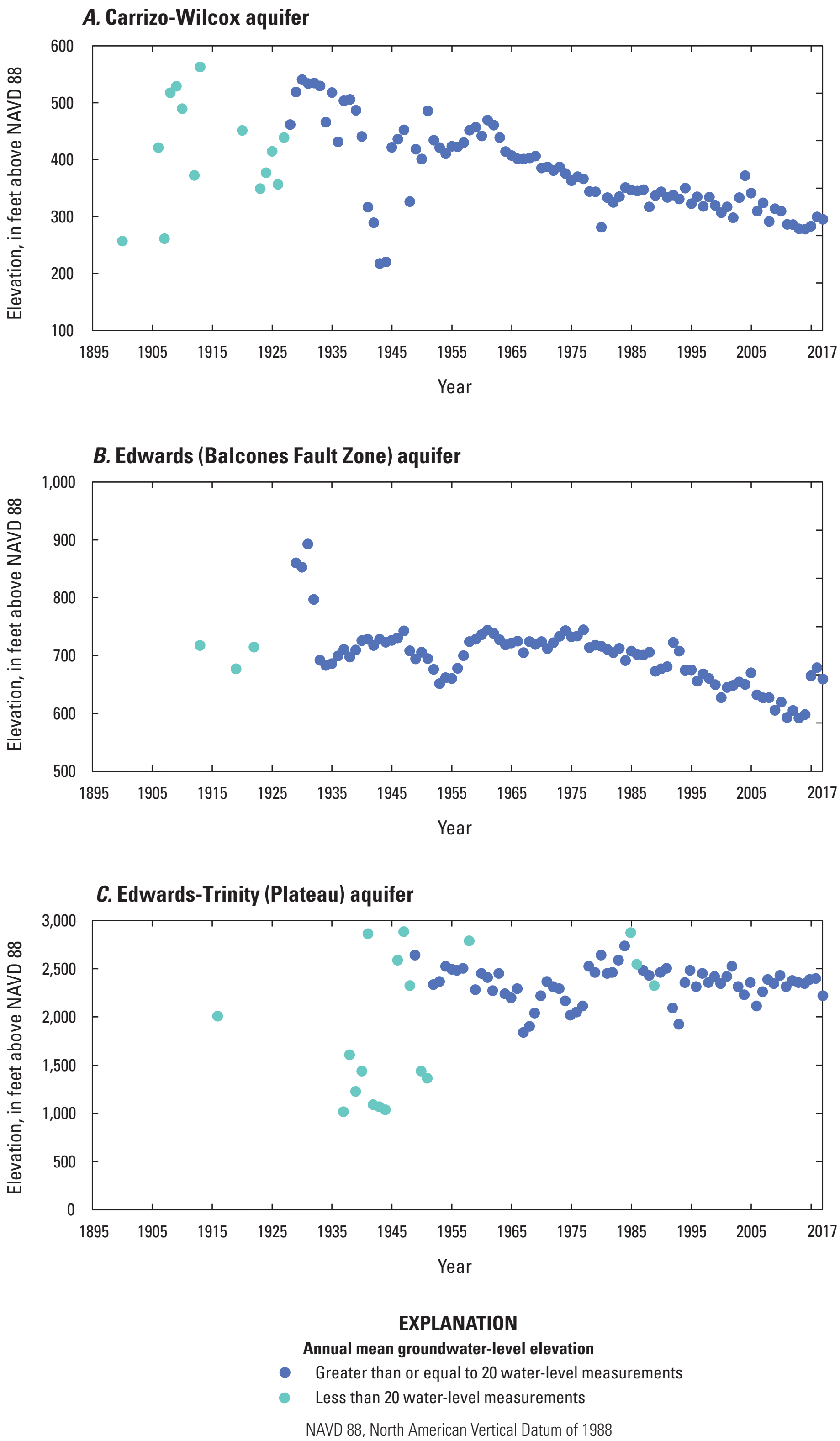

Figure 6. Annual mean groundwater-level elevations in the *A*, Carrizo-Wilcox aquifer, 1900–2017, *B*, Edwards (Balcones Fault Zone) aquifer, 1913–2017, *C*, Edwards-Trinity (Plateau) aquifer, 1916–2017, *D*, Gulf Coast aquifer, 1985–2017, *E*, Ogallala aquifer, 1910–2017, *F*, Seymour aquifer, 1897–2017, and *G*, Trinity aquifer, 1900–2017.

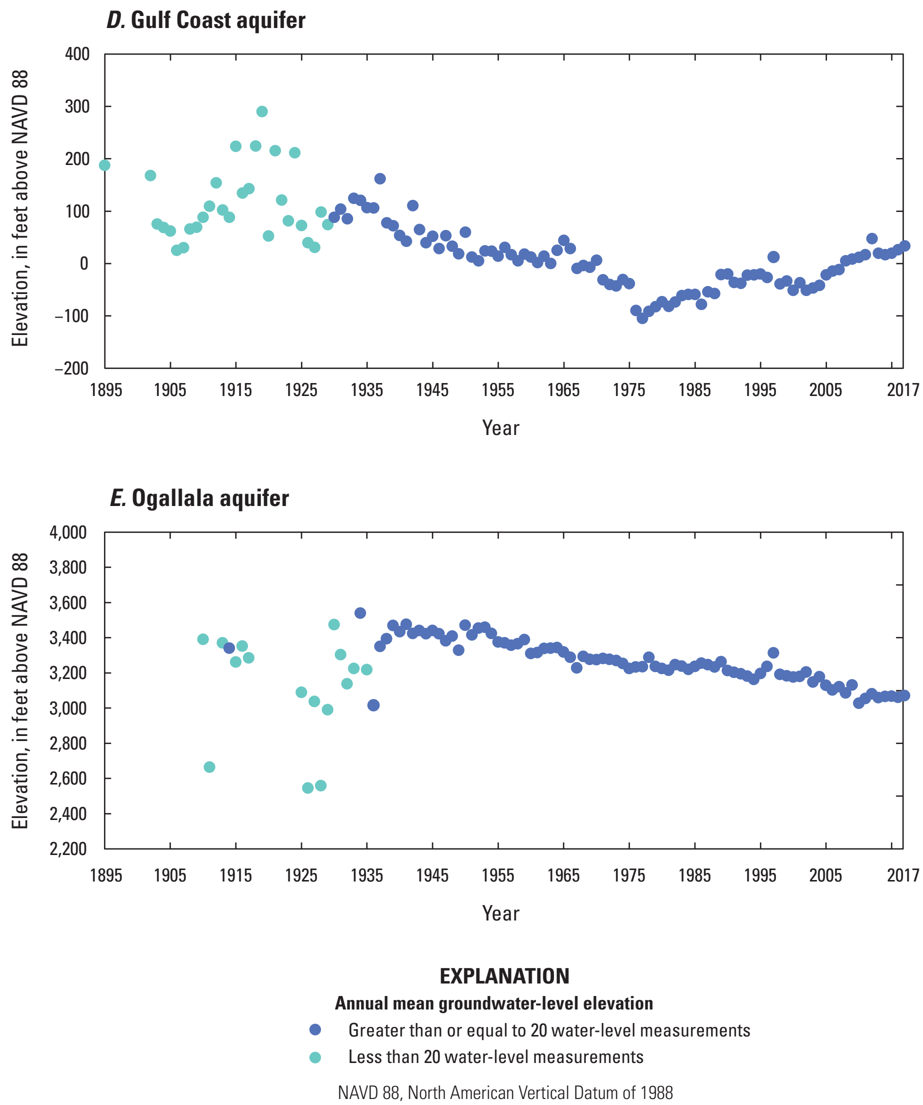

Figure 6. Annual mean groundwater-level elevations in the *A*, Carrizo-Wilcox aquifer, 1900–2017, *B*, Edwards (Balcones Fault Zone) aquifer, 1913–2017, *C*, Edwards-Trinity (Plateau) aquifer, 1916–2017, *D*, Gulf Coast aquifer, 1985–2017, *E*, Ogallala aquifer, 1910–2017, *F*, Seymour aquifer, 1897–2017, and *G*, Trinity aquifer, 1900–2017.—Continued

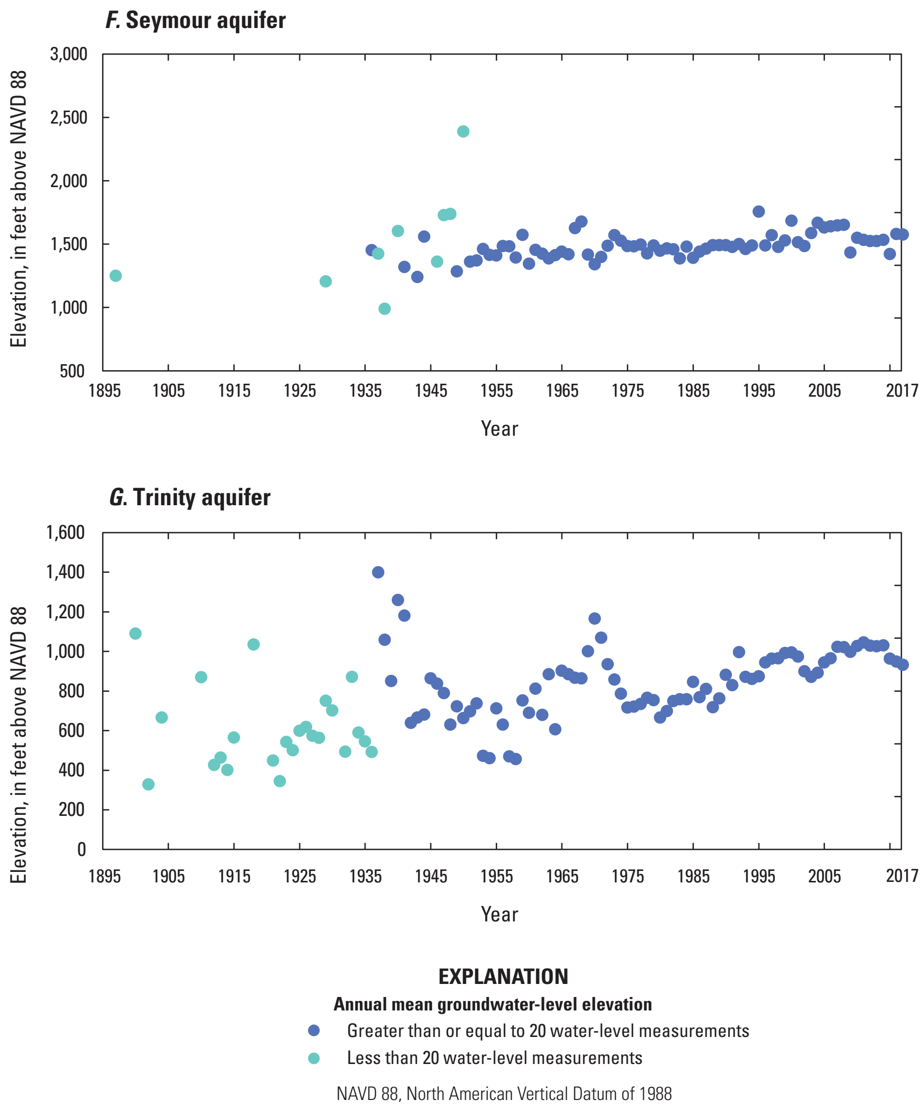

Figure 6. Annual mean groundwater-level elevations in the *A*, Carrizo-Wilcox aquifer, 1900–2017, *B*, Edwards (Balcones Fault Zone) aquifer, 1913–2017, *C*, Edwards-Trinity (Plateau) aquifer, 1916–2017, *D*, Gulf Coast aquifer, 1985–2017, *E*, Ogallala aquifer, 1910–2017, *F*, Seymour aquifer, 1897–2017, and *G*, Trinity aquifer, 1900–2017.—Continued

From 1914 through 2017, the Ogallala aquifer groundwater-level elevation data indicated a downward trend, and Kendall's *tau* equaled –0.7667 (p-value ≤0.05) (fig. 6*E*). For this period of record, the mean number of measurements per year was 3,011. The downward trend is expected, given the well-documented declines in groundwater-level elevations in the Ogallala aquifer throughout much of its extent in Texas (Gutentag and others, 1984; McGuire, 2014; Thomas and others, 2016). Groundwater-level changes in the Ogallala aquifer vary spatially. From predevelopment (about 1950) through 2013, average groundwater levels have declined about 41 ft in Texas, but some groundwater levels in some parts of the State increased about 19 ft from 2011 through 2013 (McGuire, 2014). Thomas and others (2016) reported 66-ft increases in groundwater-level elevations northeast of Plains, Texas (fig. 3). Irrigation withdrawals have in general lowered the water table of the Ogallala aquifer, affected groundwater-flow directions, and caused streams and draws that were once fed by springs and aquifer discharge to have reduced flow or no flow (Deeds and others, 2015). Historical springs and seeps of the region are summarized in Appendix 1A of the Llano Estacado 2016 regional water plan (TWDB, 2015); the information in Appendix 1A of this regional water plan is summarized from Brune (2002). Brune documented at least 65 springs that historically flowed within the upper Brazos River Basin from the Ogallala aquifer that no longer flow. Brune also noted many other seep areas that are now dry. Although many of these springs and seeps may have produced minimal flow that only continued for a few miles downstream, their demise could contribute to decreased streamflows within the upper Brazos River Basin because their presence kept areas moist to very wet so that less inputs from precipitation would be required to generate meaningful downstream flow.

From 1936 through 2017, the Seymour aquifer groundwater-level elevation data indicated an upward trend, and Kendall's *tau* equaled 0.4340 (p-value ≤0.05) (fig. 6*F*). For this period of record, the mean number of measurements per year was 220. The outcrop area for the Seymour aquifer within the upper parts of the Brazos River Basin includes Haskell, southern Knox, and western Baylor Counties (fig. 3). Although groundwater-level elevation data in the Seymour aquifer indicated an upward trend among the years with more than 20 measurements, groundwater-level elevation data in the Seymour aquifer within Baylor, Haskell, and Knox Counties indicated downward trends, with Kendall's *tau* values of –0.2724, –0.2389, and –0.2372, respectively (all p-values ≤0.05) (TWDB, 2019c). For individual county groundwater-level elevation data analyses, the threshold was set to 5 groundwater-level elevation measurements per year within the county instead of 20 for the entire aquifer. Within Baylor County, the mean number of measurements per year was 35 for the period from 1955 through 2017. Within Haskell County, the mean number of measurements per year was 57 for the period from 1944 through 2017. Within Knox County, the mean number of measurements per year was 46 for the period from 1936 through 2017. The downward trends in groundwater-level elevations in many of the wells within these three counties and the continued increase in pumping for irrigation and municipal supply could cause further declines in groundwater-level elevations and contribute to decreasing streamflow. The most recent report from the TWDB on the Seymour aquifer provides some summary information on spring discharge from the Seymour aquifer (Jones and others, 2012). The report states that for springs with more than one measurement, spring discharge has generally declined over time. The decline, as stated by Brune (2002), is attributed to pumping from the Seymour aquifer for irrigation.

From 1937 through 2017, an upward trend in the mean groundwater-level elevations of the Trinity aquifer was detected, with a Kendall's *tau* of 0.3525 (p-value ≤0.05) (fig. 6*G*). For this period of record, the mean number of measurements per year was 1,613. Although annual mean groundwater-level elevation data in the Trinity aquifer indicated an upward trend among all the available data, groundwater-level elevation data in the Trinity aquifer within counties along the Interstate 35 corridor in counties such as Denton, Tarrant, and Johnson (fig. 3) indicated downward trends, with Kendall's *tau* values of –0.6953, –0.3400 and –0.4918, respectively (all p-values ≤0.05) for the period from 1912 through 2017. A 2011 report by the TWDB identifies the Trinity aquifer as the aquifer in Texas with the largest groundwater-level declines, particularly in the Dallas-Fort Worth and Waco areas, with some areas experiencing 350 to more than 1,000 ft of declines (George and others, 2011). The declines were primarily attributed by TWDB to municipal pumping, but declines have slowed in the past 10 years because of increased reliance on surface water. The Trinity aquifer is identified in the TWDB report (2016) as having the potential to discharge groundwater directly to the rivers and tributaries within the Colorado, Guadalupe, Sulphur, and Trinity Basins. The amount of streamflow over the aquifer outcrop area attributable to groundwater discharge from the Trinity aquifer is 34 percent (TWDB, 2016). Therefore, groundwater-level trends in the aquifer in areas that contribute to these rivers may explain streamflow trends, if present.

Precipitation, Streamflow, and Potential Flood Storage Trends by River Basin

Long-term records of precipitation, streamflow, and potential flood storage within the Brazos, Colorado, Big Cypress, Guadalupe, Neches, Sulphur, and Trinity River Basins were evaluated through 2017 for statistically significant changes over time (trends). Trends in long-term streamflow data at 114 selected USGS streamflow-gaging stations and 36 simulated-inflow stations in the seven river basins are presented.

Brazos River Basin

The Brazos River Basin covers 45,573 mi^2; it begins in eastern New Mexico and is the largest basin in this study (fig. 7; TWDB, 2019a). Within the Brazos River Basin, 19 USGS streamflow-gaging stations and 12 simulated-inflow stations were selected for streamflow trend analyses (table 4). The periods of record for these 31 stations range from 24 to 117 years, with a mean period of record of 66 years. The mean percentage of complete and continuous record was 95 percent. Thirteen of the stations (10 USGS and 3 simulated-inflow) are on the main stem of the Brazos River. The most downstream station, USGS streamflow-gaging station 08116650 Brazos River near Rosharon, Texas, is on the main stem of the Brazos River about 58 miles (mi) upstream from where the river empties into the Gulf of Mexico; because of its proximity to the mouth of the river, this station drains most of the basin (45,339 mi^2).

In the Brazos River Basin, the associations between precipitation and streamflow were strong for most time steps and were all positive, indicating an increase in streamflow as precipitation increases (table 5, available at https://doi.org/10.3133/sir20195137). Of the 496 possible associations, 465 were significant.

Precipitation Trends

Results of precipitation trend analyses on an annual time step indicated an upward trend in section 4 of the Brazos River Basin (table 6). For precipitation in section 1, a p-value of 0.0502 was determined, which only slightly exceeded the probability value of 0.05 used in this report to define a statistically significant trend. Sections 4 and 5 had upward trends in precipitation during dry years. Results also indicated upward trends in precipitation during three seasons: two within section 4 and one within section 2. Results of precipitation trend analyses on a monthly time step indicated 13 monthly trends, 12 of which were upward and 1 of which was downward. No precipitation trends were indicated for section 6, which does not include any streamflow-gaging or simulated-inflow stations and was created for precipitation analysis only. Section 6 mostly includes nearly flat parts of west Texas in the High Plains Climate Division and is effectively a noncontributing area for streamflow in the Brazos River Basin. If precipitation has changed over time in the Brazos River Basin from 1900 through 2017, then precipitation amounts have most likely increased in the lower section of the basin (section 1 near the coast) and within section 4, based on these results and observed precipitation trends within the climate divisions (table 1).

Possible trends in the sum of precipitation on the day of annual peak streamflow, for different numbers of days before the annual peak streamflow (365, 180, 90, 60, and 30), and for the 5 days before, the day of, and the day after annual peak streamflow for each of the 31 stations in the Brazos River Basin are summarized in table 7 (available at https://doi.org/10.3133/sir20195137). Of the 31 stations and 217 possible trends in peak streamflow-related precipitation, 26 trends were significant, consisting of 21 upward trends and 5 downward trends. No patterns in peak streamflow-related precipitation were evident.

Streamflow Trends

Temporal trends in streamflow volume on annual, seasonal, and monthly time steps are summarized in table 8 (available at https://doi.org/10.3133/sir20195137). The trends in annual streamflow at the 31 stations within the Brazos River Basin are also depicted for the areal extent of the basin (fig. 7). At the 16 stations in the lower or downstream sections of the basin (sections 1 and 2), no trends in annual streamflow were indicated. At 7 of the 15 stations in the upper or upstream sections of the basin (sections 3, 4, and 5), moderate to strong downward trends in annual streamflow were indicated. Of the 17 seasonal trends in the Brazos River Basin, 16 were downward and 1 was upward (table 8). Ten of the 17 downward trends were at stations in the upper sections of the basin during seasons 2 and 3, which account for about 50 and 32 percent of the total annual streamflow, respectively. Of the 54 monthly trends in the Brazos River Basin, 40 were downward and 14 were upward, and more than one-half of the months with upward monthly trends were at stations in the upper sections of the basin. Particularly in the upper sections of the basin, months with upward trends (January, February, and March) accounted for small amounts (< 8 percent) of annual streamflow, and months with downward trends (May and June) accounted for large amounts (between 18 and 16 percent, respectively).

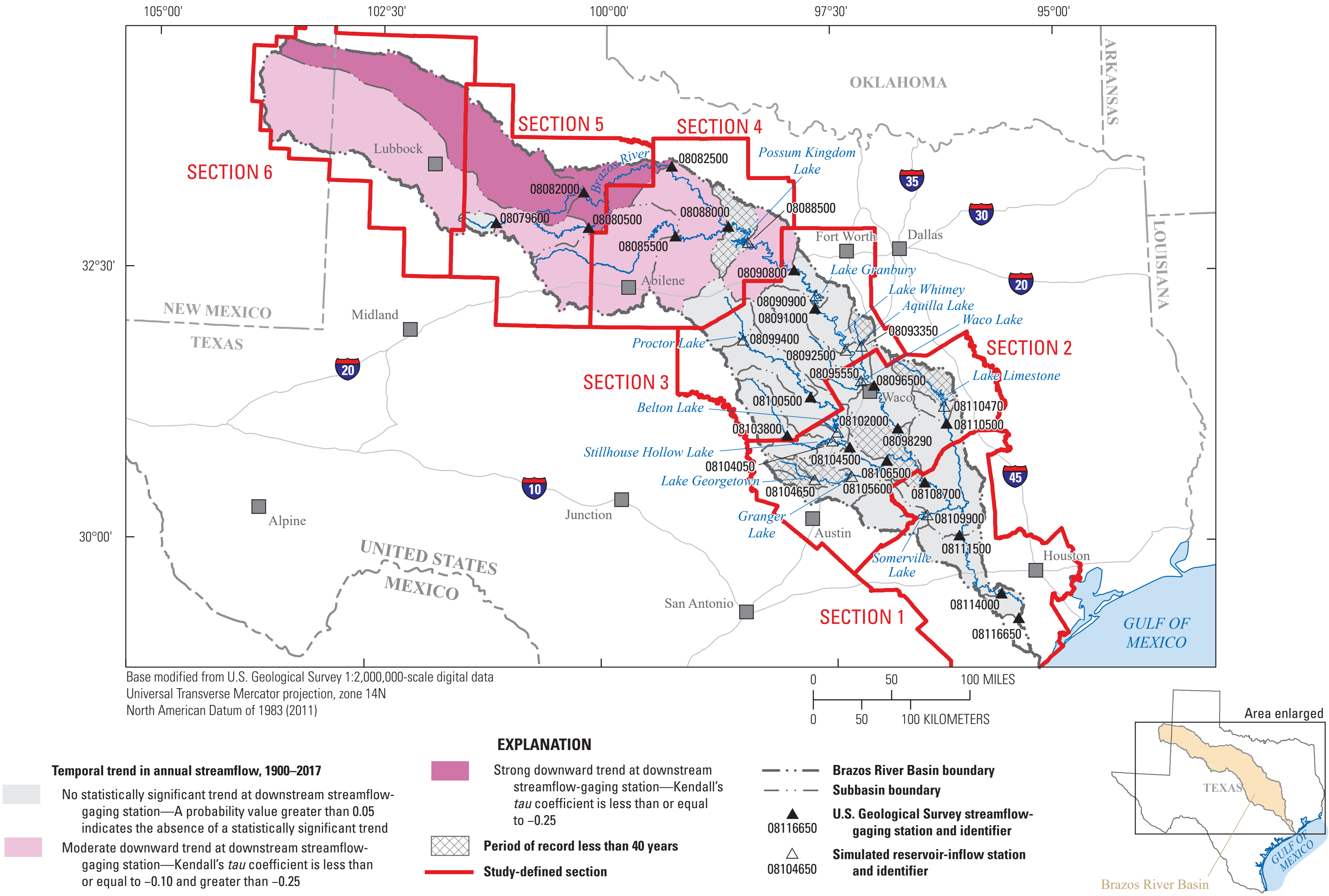

Figure 7. Temporal trends in annual streamflow at 19 U.S. Geological Survey streamflow-gaging stations and 12 simulated reservoir-inflow stations in the Brazos River Basin, 1900–2017.

Table 4. Summary information for 19 U.S. Geological Survey streamflow-gaging stations and 12 simulated reservoir-inflow stations analyzed for trends in the Brazos River Basin, 1900–2017.

[mi², square mile]

Section number[1]	Station number, name[2]	Total drainage area (mi²)	Contributing drainage area (mi²)	Period of record by calendar year[3]	Number of years of record	Percentage of record complete
1	08116650, Brazos River near Rosharon, Texas	45,339	35,773	1967–2017	50	93.0
	08114000, Brazos River at Richmond, Texas	45,107	35,541	1903–2017	114	85.9
	08111500, Brazos River near Hempstead, Texas	43,880	34,314	1938–2017	79	84.9
	08109900, Somerville Lake near Somerville, Texas	1,007	1,007	1966–2017	51	100
	08108700, Brazos River at State Highway 21 near Bryan, Texas	39,049	29,483	1993–2017	24	100
2	08110500, Navasota River near Easterly, Texas	968	968	1924–2017	93	100
	08110470, Lake Limestone near Marquez, Texas	675	675	1981–2017	36	84.5
	08106500, Little River near Cameron, Texas	7,065	7,065	1916–2017	101	100
	08105600, Granger Lake near Granger, Texas	730	730	1980–2017	37	100
	08104650, Lake Georgetown near Georgetown, Texas	247	247	1980–2017	37	100
	08104500, Little River near Little River, Texas	5,228	5,228	1923–2017	94	64.7
	08104050, Stillhouse Hollow Lake near Belton, Texas	1,313	1,313	1966–2017	51	100
	08102000, Belton Lake near Belton, Texas	3,570	3,570	1953–2017	64	100
	08098290, Brazos River near Highbank, Texas	30,436	20,870	1965–2017	52	100
	08096500, Brazos River at Waco, Texas	29,559	19,993	1900–2017	117	100
	08095550, Waco Lake near Waco, Texas	1,652	1,652	1965–2017	52	100
3	08103800, Lampasas River near Kempner, Texas	818	818	1962–2017	55	100
	08100500, Leon River at Gatesville, Texas	2,342	2,342	1950–2017	67	100
	08099400, Proctor Lake near Proctor, Texas	1,259	1,259	1963–2017	54	100
	08093350, Aquilla Lake above Aquilla, Texas	255	255	1983–2017	34	97.9
	08092500, Whitney Lake near Whitney, Texas	27,189	17,623	1952–2017	65	100
	08091000, Brazos River near Glen Rose, Texas	25,818	16,252	1923–2017	94	99.9
	08090900, Lake Granbury near Granbury, Texas	25,679	16,113	1981–2017	36	84.3
	08090800, Brazos River near Dennis, Texas	25,237	15,671	1968–2017	49	94.0
4	08088500, Possum Kingdom Lake near Graford, Texas	23,596	14,030	1981–2017	36	84.0
	08088000, Brazos River near South Bend, Texas	22,673	13,107	1938–2017	79	95.0
	08085500, Clear Fork Brazos River at Fort Griffin, Texas	3,988	3,988	1924–2017	93	100
	08082500, Brazos River at Seymour, Texas	15,538	5,972	1923–2017	94	100
5	08082000, Salt Fork Brazos River near Aspermont, Texas	5,130	2,496	1924–2017	93	85.3
	08080500, Double Mountain Fork Brazos River near Aspermont, Texas	8,796	1,864	1924–2017	93	94.9
	08079600, Double Mountain Fork Brazos River at Justiceburg, Texas	1,466	244	1961–2017	56	100

[1]Refer to figure 7 for map of sections within the Brazos River Basin.

[2]Shaded cells are U.S. Geological Survey streamflow-gaging stations with measured streamflow data (U.S. Geological Survey, 2019b), and cells that are not shaded are lake and reservoir stations with simulated reservoir-inflow data provided by the U.S. Army Corps of Engineers (2019b) or the Brazos River Authority.

[3]Period of record includes the calendar year when daily mean streamflow data collection began to the end of 2017.

Table 6. Summary of annual, seasonal, and monthly precipitation trends for the period 1900–2017 within six sections of the Brazos River Basin.

[wet, years with precipitation totals above long-term mean; dry, years with precipitation totals below long-term mean; NA, not applicable; season 1, November, December, January, and February; season 2, March, April, May, and June; season 3, July, August, September, and October; *p*-value, probability value (considered statistically significant if less than 0.05); green shaded cells indicate statistically significant upward trends; red shaded cells indicate statistically significant downward trends]

Time step	Brazos River Basin section number[1]											
	Section 1				Section 2				Section 3			
	1900–2017				1900–2017				1900–2017			
	Kendall's *tau*	*p*-value	Mean precipitation (inches)	Percentage[3]	Kendall's *tau*	*p*-value	Mean precipitation (inches)	Percentage[3]	Kendall's *tau*	*p*-value	Mean precipitation (inches)	Percentage[3]
Annual	0.1222	0.0502	43.34	100	0.1019	0.1020	35.72	100	0.1063	0.0882	31.90	100
Annual (wet)	0.0937	0.3211	NA	NA	0.0951	0.2817	NA	NA	−0.0095	0.9178	NA	NA
Annual (dry)	0.0988	0.2513	NA	NA	0.1222	0.1817	NA	NA	0.0039	0.9718	NA	NA
Season 1	0.0395	0.5278	13.31	30.7	0.0850	0.1741	10.69	29.9	0.0696	0.2662	8.23	25.8
Season 2	0.0607	0.3298	14.84	34.2	0.0301	0.6285	14.06	39.4	0.0920	0.1397	13.40	42.0
Season 3	0.1139	0.0675	15.19	35.0	0.1322	0.0339	10.97	30.7	0.0894	0.1513	10.27	32.2
January	0.1448	0.0201	3.16	7.3	0.1460	0.0192	2.40	6.7	0.0933	0.1348	1.84	5.8
February	−0.0457	0.4637	2.91	6.7	0.0283	0.6501	2.53	7.1	0.0708	0.2563	2.08	6.5
March	0.0583	0.3498	2.84	6.6	0.1180	0.0583	2.69	7.5	0.1254	0.0442	2.39	7.5
April	−0.0822	0.1872	3.46	8.0	−0.1476	0.0179	3.58	10.0	−0.0936	0.1329	3.36	10.5
May	0.0296	0.6351	4.55	10.5	0.0215	0.7307	4.54	12.7	−0.0116	0.8524	4.47	14.0
June	0.1737	0.0053	3.98	9.2	0.1171	0.0602	3.24	9.1	0.1444	0.0205	3.18	10.0
July	−0.0779	0.2116	3.48	8.0	−0.0245	0.6942	2.14	6.0	−0.0096	0.8780	2.09	6.6
August	0.0561	0.3680	3.45	8.0	0.0626	0.3150	2.19	6.1	0.0918	0.1409	2.09	6.6
September	0.1289	0.0387	4.32	10.0	0.0697	0.2632	3.19	8.9	0.0207	0.7394	2.98	9.3
October	0.0446	0.4737	3.94	9.1	0.1095	0.0791	3.45	9.7	0.0620	0.3195	3.11	9.7
November	0.0687	0.2702	3.63	8.4	0.0854	0.1707	2.90	8.1	0.0202	0.7465	2.30	7.2
December	−0.0828	0.1841	3.61	8.3	−0.0347	0.5783	2.85	8.0	−0.0052	0.9333	2.02	6.3

Table 6. Summary of annual, seasonal, and monthly precipitation trends for the period 1900–2017 within six sections of the Brazos River Basin.—Continued

[wet, years with precipitation totals above long-term mean; dry, years with precipitation totals below long-term mean; NA, not applicable; season 1, November, December, January, and February; season 2, March, April, May, and June; season 3, July, August, September, and October; *p*-value, probability value (considered statistically significant if less than 0.05); green shaded cells indicate statistically significant upward trends; red shaded cells indicate statistically significant downward trends]

Time step	Brazos River Basin section number[1]											
	Section 4				Section 5				Section 6			
	1900–2017				1900–2017				[2]1901–2017			
	Kendall's *tau*	*p*-value	Mean precipitation (inches)	Percentage[3]	Kendall's *tau*	*p*-value	Mean precipitation (inches)	Percentage[3]	Kendall's *tau*	*p*-value	Mean precipitation (inches)	Percentage[3]
Annual	0.1706	0.0062	26.88	100	0.0984	0.1148	21.94	100	0.0279	0.6589	17.83	100
Annual (wet)	0.1364	0.1478	NA	NA	−0.0840	0.3892	NA	NA	−0.0126	0.9030	NA	NA
Annual (dry)	0.2243	0.0090	NA	NA	0.1751	0.0367	NA	NA	0.1025	0.2300	NA	NA
Season 1	0.1390	0.0263	5.61	20.9	0.0768	0.2197	3.66	16.7	−0.0027	0.9662	2.38	13.3
Season 2	0.1205	0.0532	11.24	41.8	0.0614	0.3240	8.89	40.5	0.0225	0.7204	6.59	36.9
Season 3	0.1033	0.0972	10.03	37.3	0.0162	0.7945	9.38	42.8	−0.0077	0.9025	8.87	49.7
January	0.0963	0.1230	1.15	4.3	0.0982	0.1163	0.75	3.4	0.0828	0.1878	0.48	2.7
February	0.1746	0.0051	1.41	5.3	0.1364	0.0291	0.91	4.2	0.0930	0.1389	0.56	3.1
March	0.1694	0.0066	1.70	6.3	0.1040	0.0954	1.10	5.0	0.1160	0.0634	0.73	4.1
April	−0.0030	0.9610	2.56	9.5	−0.0699	0.2622	1.89	8.6	−0.1084	0.0823	1.16	6.5
May	−0.0261	0.6755	3.89	14.5	−0.0206	0.7412	3.16	14.4	−0.0159	0.7992	2.24	12.6
June	0.1459	0.0193	3.10	11.5	0.1228	0.0488	2.75	12.5	0.1000	0.1085	2.46	13.8
July	0.0078	0.9000	2.13	7.9	−0.0390	0.5315	2.22	10.1	−0.0534	0.3920	2.44	13.7
August	0.1238	0.0470	2.20	8.2	0.0791	0.2049	2.24	10.2	−0.0403	0.5179	2.44	13.7
September	0.0725	0.2448	2.97	11.0	0.0490	0.4318	2.69	12.3	0.0144	0.8179	2.33	13.0
October	0.0516	0.4076	2.73	10.2	−0.0589	0.3450	2.23	10.2	−0.0179	0.7756	1.66	9.3
November	0.0194	0.7553	1.70	6.3	−0.0263	0.6737	1.12	5.1	−0.0394	0.5283	0.72	4.0
December	0.0739	0.2364	1.35	5.0	0.0554	0.3755	0.88	4.0	0.0342	0.5846	0.62	3.5

[1]Refer to figure 7 for map of sections within the Brazos River Basin.

[2]Section 6 precipitation data does not include 1900 because of a lack of data in that area for that year.

[3]Percentage of the total precipitation within the season or month for the time period specified.

Overall, many downward trends in streamflow were indicated in the upper sections of the Brazos River Basin. In the lower sections of the basin, some seasonal and monthly trends (upward or downward) in streamflow were indicated, without affecting annual volumes. The downward streamflow trends did not coincide with downward trends in precipitation in the upper sections of the basin. Springs that historically flowed within the upper Brazos River Basin from the Ogallala aquifer that no longer flow (Brune, 2002) could be contributing to decreased streamflows because their presence kept areas moist to very wet so that less inputs from precipitation would be required to generate meaningful downstream flow. Similarly, decreasing groundwater-level elevations in many of the Seymour aquifer wells within Baylor, Haskell, and Knox Counties and the continued increase in pumping for irrigation and municipal supply could cause further declines in groundwater-level elevations and contribute to decreasing streamflow (Brune, 2002; Jones and others, 2012).

The ratios of streamflow volume to precipitation volume were analyzed as part of this study (fig. 8; table 9, available at https://doi.org/10.3133/sir20195137). Temporal trends in the ratio of streamflow volume to precipitation volume indicate a change in the way the system responds to precipitation events and possibly explain downward trends in streamflow if the ratios are also downward. The analyses indicate that trends in streamflow and trends in the ratio of streamflow volume to precipitation volume are similar (figs. 7 and 8; tables 8 and 9). Some seasonal and monthly downward trends in the ratio of streamflow volume to precipitation volume were indicated in the lower sections of the Brazos River Basin without any corresponding downward trends in annual streamflow. The only station in sections 1 and 2 with a downward trend evident in the annual ratio of streamflow volume to precipitation volume is USGS streamflow-gaging station 08096500 Brazos River at Waco, Texas. Although a downward trend in annual streamflow at this station was not detected, the *p*-value of 0.0696 only slightly exceeded the 0.05 *p*-value threshold used in this report for determining a statistically significant trend (table 8). At 7 of the 15 stations in the upper sections of the basin, downward trends in annual streamflow and downward trends in the ratio of streamflow volume to precipitation volume on an annual time step were indicated.

The Kendall's *tau* and *p*-values for trends in two extreme streamflow regimes, annual minimum and annual peak streamflow, were calculated (table 10, available at https://doi.org/10.3133/sir20195137), and any trends that were indicated for these two streamflow regimes are depicted for the areal extent of the basin (figs. 9–10). In the lower sections of the basin, an upward trend in annual minimum streamflow was indicated at one station, whereas downward trends in annual minimum streamflow were indicated at five stations. In the upper sections of the basin, upward trends in annual minimum streamflow were indicated at four stations, and a downward trend in annual minimum streamflow was indicated at one station.

A downward trend in annual peak streamflow was indicated at one station in the lower sections of the basin and at six stations in the upper sections of the basin. Upward trends in annual peak streamflow were not indicated at any of the stations in the Brazos River Basin.

Potential Flood Storage Trends

Results of the analyses of the associations between potential flood storage volume and annual streamflow volume and the trends in the ratio of annual streamflow volume to potential flood storage volume for the Brazos River Basin are summarized in table 10, and the annual results are illustrated in figures 11 and 12, respectively.

No statistically significant associations between potential flood storage volume and annual streamflow volume were indicated at the stations in sections 1 and 2 (the lower sections of the basin) (fig. 11). In contrast, downward trends were frequently detected for the ratio of annual streamflow volume to potential flood storage volume (fig. 12). At the same seven stations in the upper sections of the basin where there were downward trends in annual streamflow (fig. 7; table 8), there were also downward trends in the ratio of streamflow volume to precipitation volume measured on an annual time step. Data from these same seven stations indicate negative associations between potential flood storage volume and annual streamflow volume and downward trends in the ratio of annual streamflow volume to potential flood storage volume. With the known addition of 13,006,394 acre-ft of potential flood storage between 1900 and 2010 in the subbasins analyzed (USACE, 2019a), streamflow volumes have decreased in sections of the Brazos River Basin.

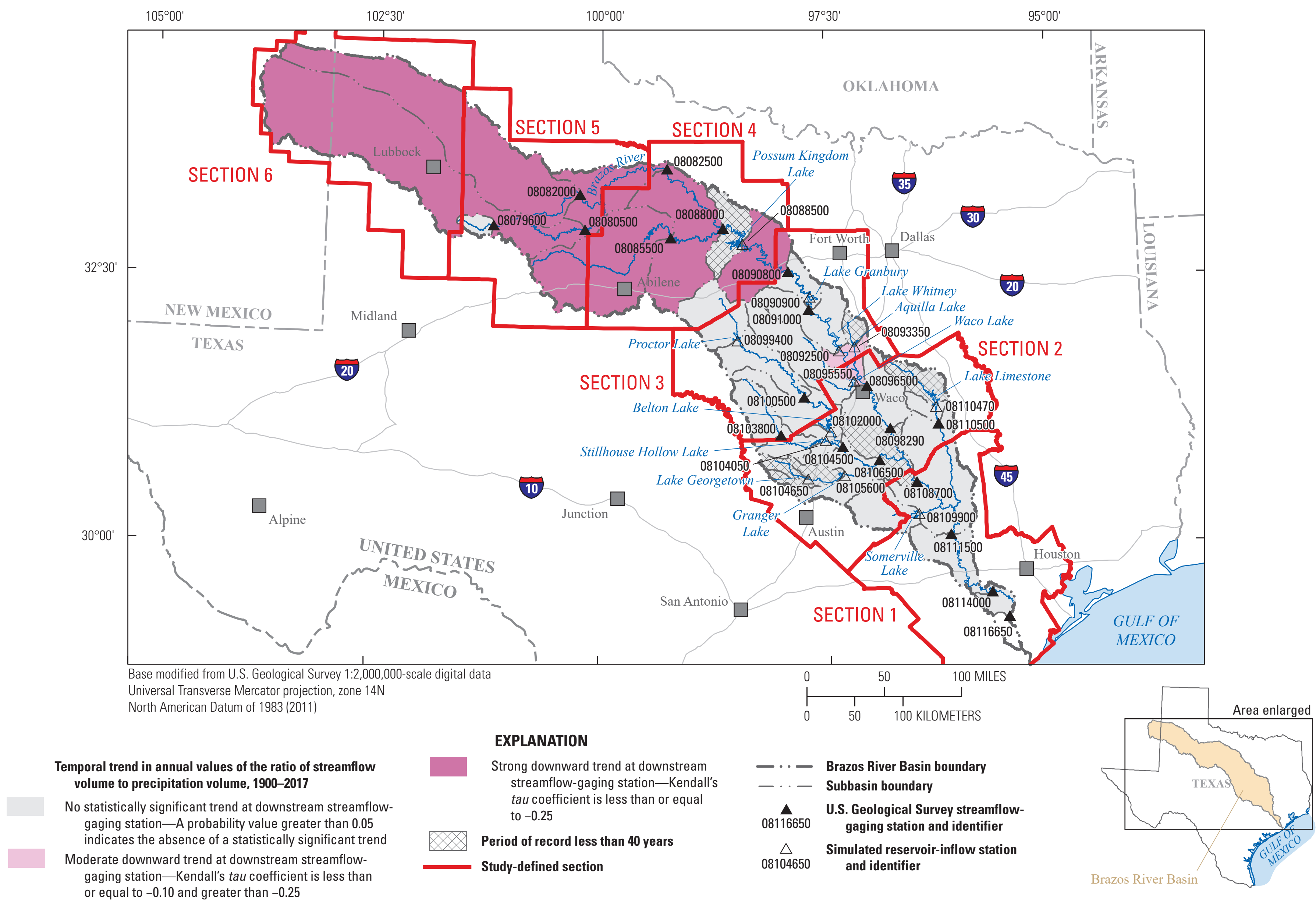

Figure 8. Temporal trends in annual values of the ratio of streamflow volume to precipitation volume at 19 U.S. Geological Survey streamflow-gaging stations and 12 simulated reservoir-inflow stations in the Brazos River Basin, 1900–2017.

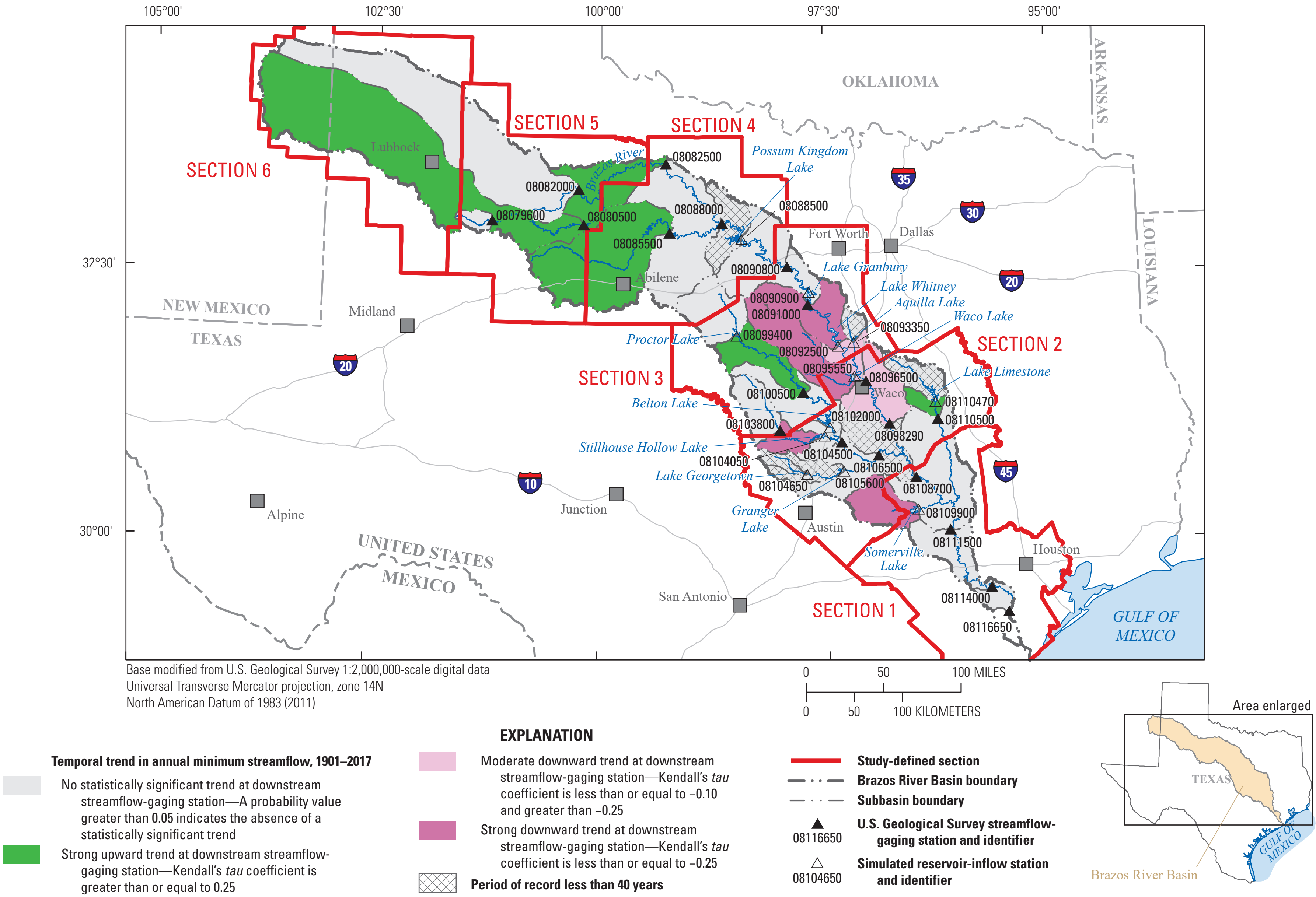

Figure 9. Temporal trends in annual minimum streamflow at 19 U.S. Geological Survey streamflow-gaging stations and 12 simulated reservoir-inflow stations in the Brazos River Basin, 1901–2017.

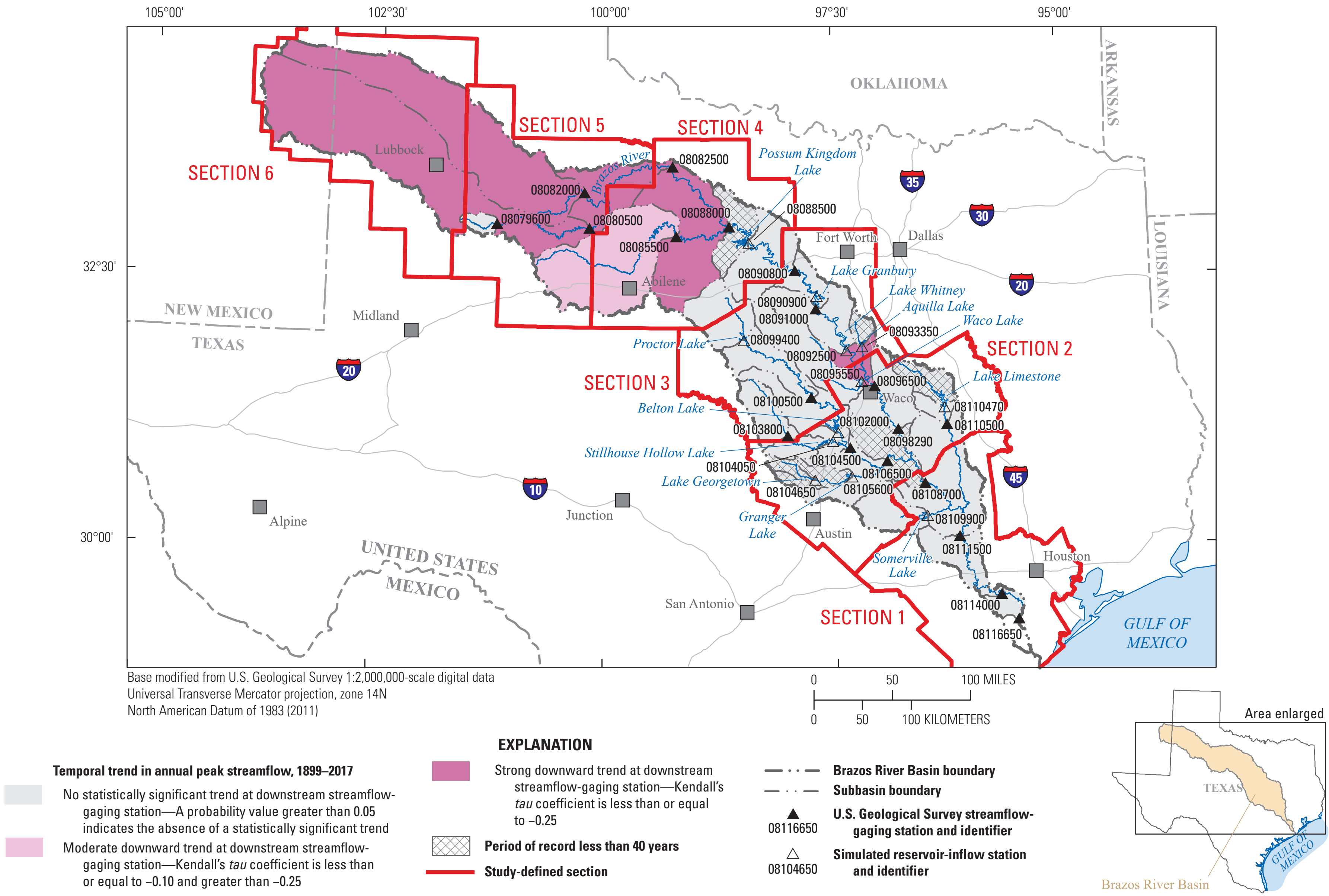

Figure 10. Temporal trends in annual peak streamflow at 19 U.S. Geological Survey streamflow-gaging stations and 12 simulated reservoir-inflow stations in the Brazos River Basin, 1899–2017.

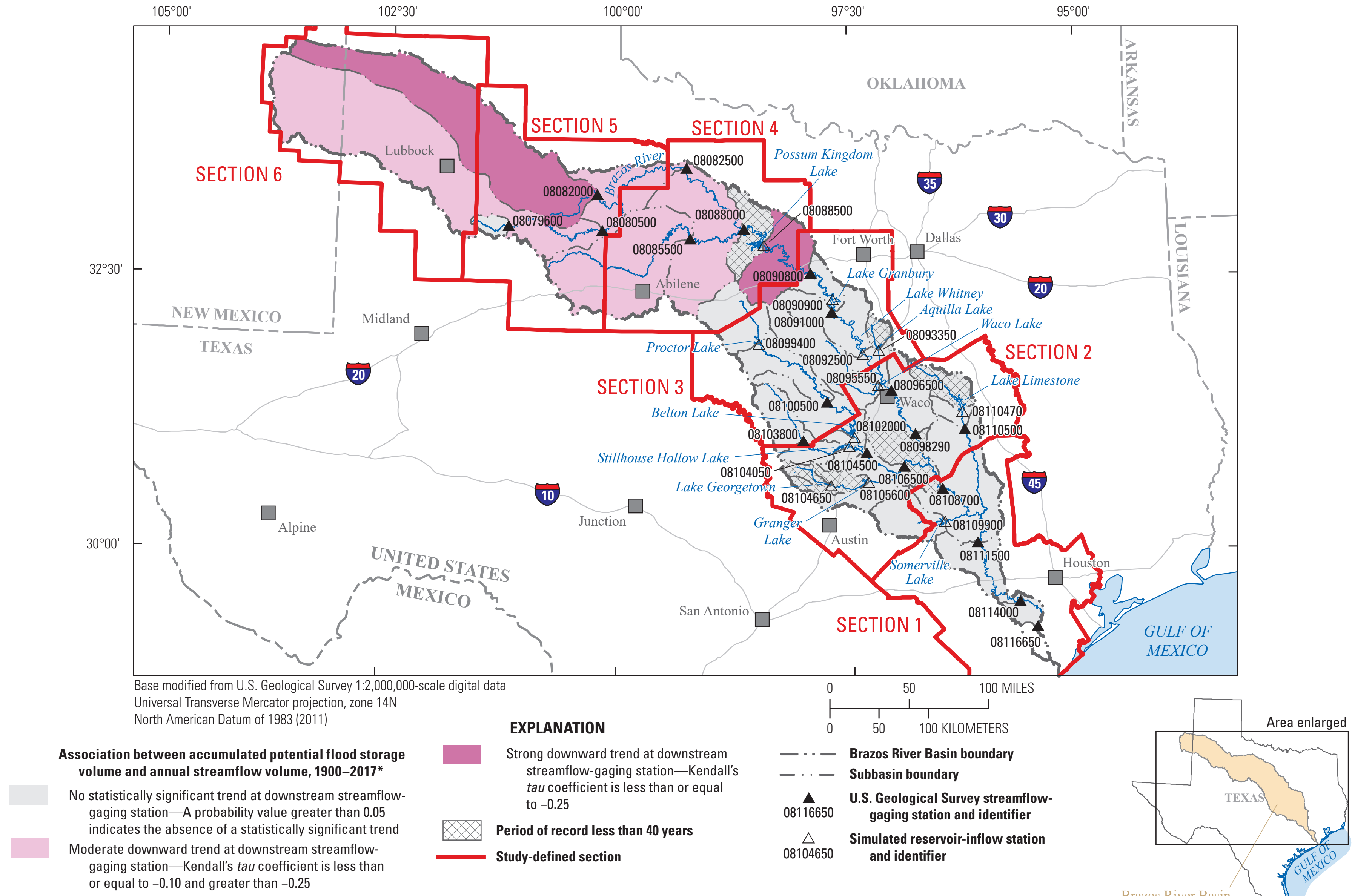

* The association between accumulated potential flood storage volume and annual streamflow volume was analyzed by using Kendall's *tau* to determine the direction and magnitude of streamflow change.

Figure 11. Association between accumulated potential flood storage volume and annual streamflow volume at 19 U.S. Geological Survey streamflow-gaging stations and 12 simulated reservoir-inflow stations in the Brazos River Basin, 1900–2017.

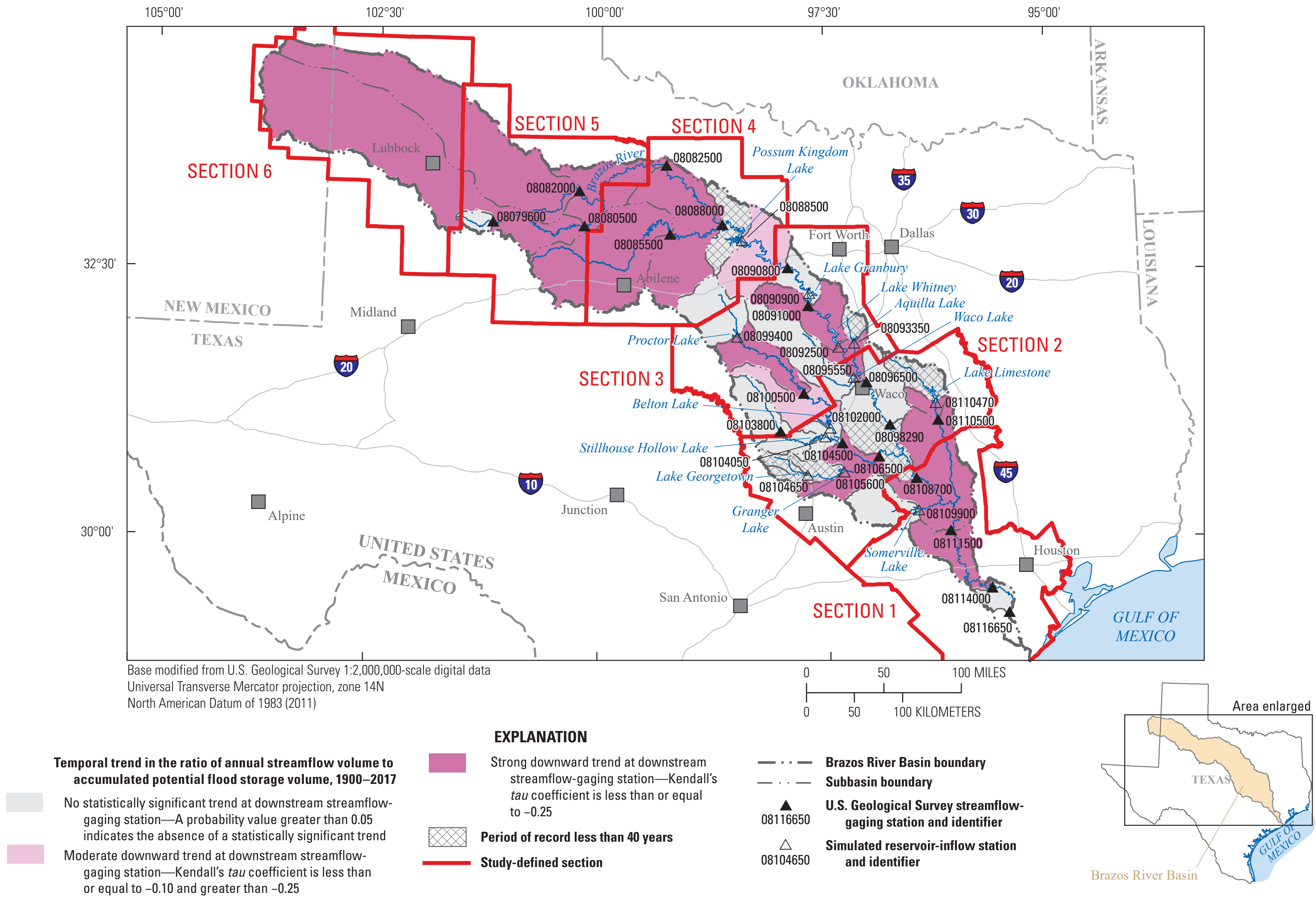

Figure 12. Temporal trends in the ratio of annual streamflow volume to accumulated potential flood storage volume at 19 U.S. Geological Survey streamflow-gaging stations and 12 simulated reservoir-inflow stations in the Brazos River Basin, 1900–2017.

Colorado River Basin

The Colorado River Basin covers 42,318 mi^2 and begins in eastern New Mexico (fig. 13; TWDB, 2019a). Within the Colorado River Basin, 26 USGS streamflow-gaging stations and 4 simulated-inflow stations were selected for streamflow trend analyses (table 11). The periods of record for these 30 stations range from 35 to 117 years, with a mean period of record of 79 years. The mean percentage of complete and continuous record was 93 percent. Eleven of the stations (10 USGS and 1 simulated inflow) are on the main stem of the Colorado River. The most downstream station, USGS streamflow-gaging station 08162500 Colorado River near Bay City, Texas, is on the main stem of the Colorado River about 32 mi upstream from where the river empties into the Gulf of Mexico and has a total drainage area of 42,240 mi^2.

In the Colorado River Basin, the associations between precipitation and streamflow were strong for most time steps and were all positive, indicating an increase in streamflow as precipitation increases (table 5). Of the 480 possible associations, 404 were significant.

Precipitation Trends

Results of precipitation trend analyses on an annual time step indicated no trends in any of the five sections of the Colorado River Basin (table 12). Note that section 5 does not include any streamflow-gaging or simulated-inflow stations and was created for precipitation analysis only. Section 5 mostly includes the nearly flat parts of west Texas in the High Plains Climate Division, and the area is effectively a noncontributing area of the Colorado River Basin. Section 3 had an upward trend in precipitation during dry years. Results also indicated no trends in precipitation during the three seasons. Results of precipitation trend analyses on a monthly time step indicated 10 monthly trends, of which 7 were upward and 3 were downward. The results indicated that precipitation did not change in the Colorado River Basin from 1900 through 2017.

Possible trends in the sum of precipitation on the day of the annual peak, for different numbers of days before the annual peak streamflow (365, 180, 90, 60, and 30), and for the 5 days before, the day of, and the day after annual peak streamflow for each of the 30 stations in the Colorado River Basin are summarized in table 7. Of the 30 stations and 210 possible trends in peak streamflow-related precipitation, 15 trends were significant, consisting of 13 upward trends and 2 downward trends. No patterns in peak streamflow-related precipitation were evident.

Streamflow Trends

Temporal trends in streamflow volume on annual, seasonal, and monthly time steps are summarized in table 8. The trends in annual streamflow at the 30 stations within the Colorado River Basin are also depicted for the areal extent of the basin (fig. 13). Data from 16 of the 28 stations in the upper sections of the basin (sections 2, 3, and 4) indicated moderate to strong downward trends in annual streamflow. Data from one small subbasin on USGS streamflow-gaging station 08129300 Spring Creek near San Angelo, Texas, indicated an upward trend in streamflow between 1960 and 1995 when data collection stopped. Data from the farthest downstream section of the basin (section 1) indicated no trends in annual streamflow. Of the 42 seasonal trends in the Colorado River Basin, 40 were downward and 2 were upward. Fourteen of the 40 downward trends were during season 2, which accounted for the greatest percentage (mean of 43 percent) of total annual streamflow. Seventeen of the 40 downward trends were during season 3, which accounted for 36 percent of total annual streamflow. Of the 149 monthly trends in the Colorado River Basin, 127 were downward and 22 were upward.

On an overall basis, many downward trends in streamflow were indicated in the upper sections of the basin, whereas data from the lower section of the basin indicated some monthly trends in streamflow without affecting annual volumes. The downward streamflow trends did not coincide with downward trends in precipitation in the basin. Despite downward trends in the Carrizo-Wilcox and Gulf Coast aquifers, streamflow volumes downstream from the outcrop areas in the basin are not decreasing. Downward groundwater-level trends in the Trinity aquifer near Austin coincided with some downward streamflow trends in the Colorado River Basin.

The ratios of streamflow volume to precipitation volume were analyzed as part of this study (fig. 14; table 9). Temporal trends in the ratio of streamflow volume to precipitation volume indicate a change in the way the system responds to precipitation events and possibly explain downward trends in streamflow if the ratios are also downward. The analyses indicated that trends in streamflow and trends in the ratio of streamflow volume to precipitation volume were similar (figs. 13 and 14; tables 8 and 9). Sixteen of the 28 stations in the upper sections of the basin with data that indicated downward trends in annual streamflow also indicated downward trends in the ratio of streamflow volume to precipitation volume on an annual time step.

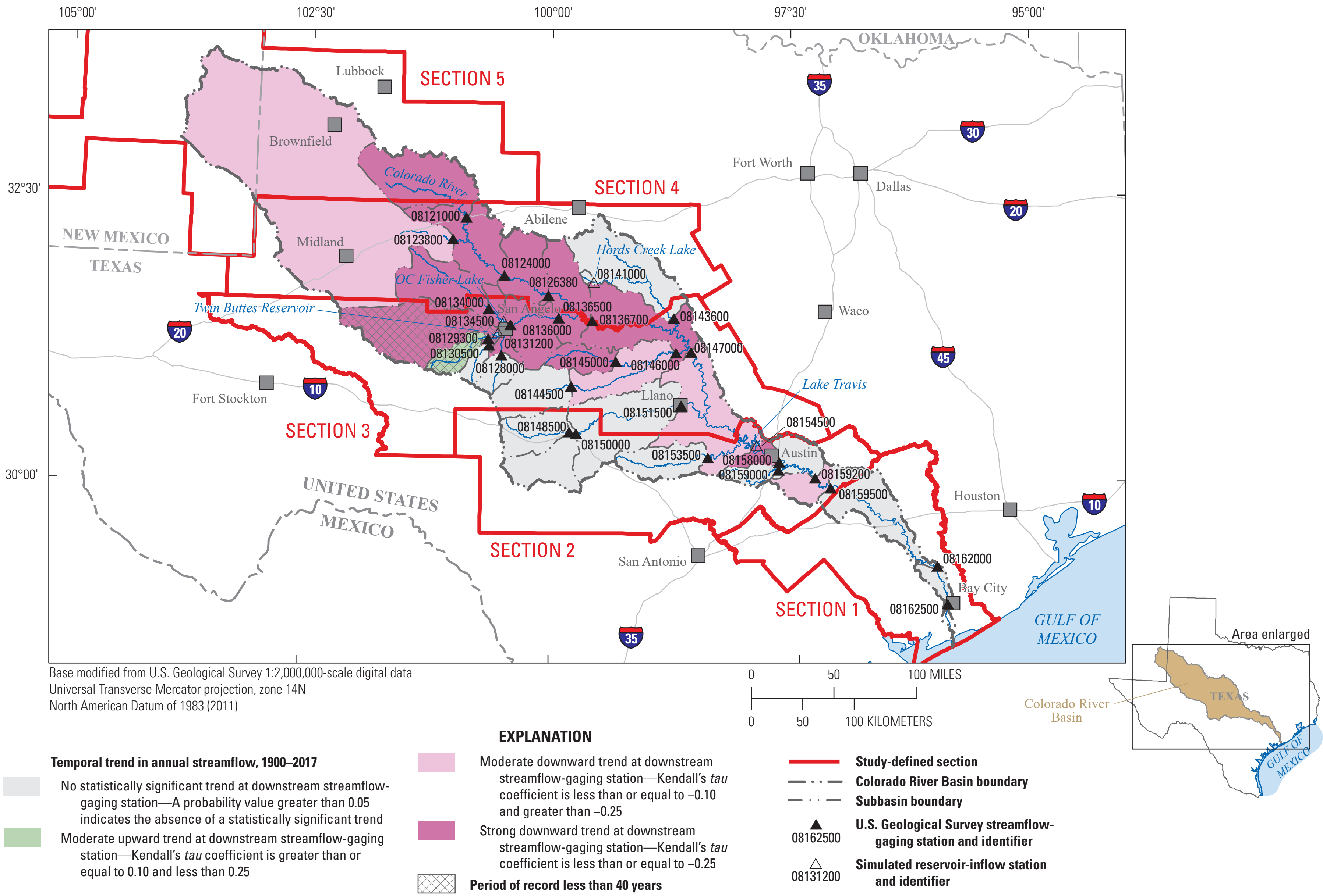

Figure 13. Temporal trends in annual streamflow at 26 U.S. Geological Survey streamflow-gaging stations and 4 simulated reservoir-inflow stations in the Colorado River Basin, 1900–2017.

Table 11. Summary information for 26 U.S. Geological Survey streamflow-gaging stations and 4 simulated reservoir-inflow stations analyzed for trends in the Colorado River Basin, 1900–2017.

[mi², square mile]

Section number[1]	Station number, name[2]	Total drainage area (mi²)	Contributing drainage area (mi²)	Period of record by calendar year[3]	Number of years of record	Percentage of record complete
1	08162500, Colorado River near Bay City, Texas	42,240	30,837	[4]1948–2007	59	100
	08162000, Colorado River at Wharton, Texas	42,003	30,600	[5]1938–2017	79	100
2	08159500, Colorado River at Smithville, Texas	40,371	28,968	1930–2017	87	74.8
	08159200, Colorado River at Bastrop, Texas	39,979	28,576	1960–2017	57	100
	08159000, Onion Creek at US Hwy 183, Austin, Texas	321	321	1924–2017	93	50.8
	08158000, Colorado River at Austin, Texas	39,009	27,606	1900–2017	117	100
	08154500, Lake Travis near Austin, Texas	38,755	27,352	1965–2017	52	100
	08153500, Pedernales River near Johnson City, Texas	901	901	1939–2017	78	100
	08150000, Llano River near Junction, Texas	1,854	1,849	1915–2017	102	95.7
	08148500, North Llano River near Junction, Texas	914	914	1915–2017	102	76.9
3	08151500, Llano River at Llano, Texas	4,197	4,192	1939–2017	78	100
	08147000, Colorado River near San Saba, Texas	31,217	19,819	1915–2017	102	98.6
	08146000, San Saba River at San Saba, Texas	3,046	3,039	1915–2017	102	96.1
	08145000, Brady Creek at Brady, Texas	588	588	1939–2017	78	81.5
	08144500, San Saba River at Menard, Texas	1,135	1,128	1915–2017	102	96.1
	08143600, Pecan Bayou near Mullin, Texas	2,073	2,073	1967–2017	50	99.9
	08136500, Concho River at Paint Rock, Texas	6,574	5,443	1915–2017	102	100
	08136000, Concho River at San Angelo, Texas	5,542	4,411	1915–2017	102	100
	08134500, O. C. Fisher Lake at San Angelo, Texas	1,488	1,383	1952–2017	65	100
	08134000, North Concho River near Carlsbad, Texas	1,266	1,191	1924–2017	93	100
	08131200, Twin Buttes Reservoir near San Angelo, Texas	3,868	2,813	1981–2017	36	97.5
	08130500, Dove Creek at Knickerbocker, Texas	226	218	1960–2009	49	73.1
	08129300, Spring Creek above Tankersley, Texas	425	405	1960–1995	35	100
	08128000, South Concho River at Christoval, Texas	413	354	1930–2017	87	93.6
4	08141000, Hords Creek Lake near Valera, Texas	48	48	1948–2017	69	100
	08136700, Colorado River near Stacy, Texas	24,193	12,802	1968–2017	49	100
	08126380, Colorado River near Ballinger, Texas	16,358	6,098	1907–2017	110	100
	08124000, Colorado River at Robert Lee, Texas	15,307	5,047	1923–2017	94	74.8
	08123800, Beals Creek near Westbrook, Texas	9,802	1,988	1958–2017	59	100
	08121000, Colorado River at Colorado City, Texas	3,966	1,585	1923–2017	94	77.9

[1]Refer to figure 13 for map of sections within the Colorado River Basin.

[2]Shaded cells are U.S. Geological Survey streamflow-gaging stations with measured streamflow data (U.S. Geological Survey, 2019b), and cells that are not shaded are lake and reservoir stations with simulated reservoir-inflow data provided by the U.S. Army Corps of Engineers (2019b), the Lower Colorado River Authority, or the San Angelo Parks and Recreation Department.

[3]Period of record includes the calendar year when daily mean streamflow data collection began to the end of 2017 or when data collection ended (if applicable).

[4]Became partial record station in 2008; therefore, continuous streamflow data after 2007 are not available, but annual peak streamflow are available through 2017. Streamflow analyses are through 2007, and annual peak streamflow data analyses are through 2017.

[5]Annual peak streamflow data collection began in 1919, but continuous streamflow data began in 1938.

Table 12. Summary of annual, seasonal, and monthly precipitation trends for the period 1900–2017 within five sections of the Colorado River Basin.

[wet, years with precipitation totals above long-term mean; dry, years with precipitation totals below long-term mean; NA, not applicable; season 1, includes November, December, January, and February; season 2, includes March, April, May, and June; season 3, includes July, August, September, and October; *p*-value, probability value (considered statistically significant if less than 0.05); green shaded cells indicate statistically significant upward trends; red shaded cells indicate statistically significant downward trends]

Time step	Colorado River Basin section number[1]											
	Section 1				Section 2				Section 3			
	1900–2017				1900–2017				1900–2017			
	Kendall's *tau*	*p*-value	Mean precipitation (inches)	Percentage[2]	Kendall's *tau*	*p*-value	Mean precipitation (inches)	Percentage[2]	Kendall's *tau*	*p*-value	Mean precipitation (inches)	Percentage[2]
Annual	0.0922	0.1397	38.64	100	0.0875	0.1608	30.36	100	0.0597	0.3391	22.28	100
Annual (wet)	0.1440	0.1262	NA	NA	0.1027	0.2761	NA	NA	0.0036	0.9732	NA	NA
Annual (dry)	0.0645	0.4548	NA	NA	−0.0055	0.9538	NA	NA	0.1898	0.0326	NA	NA
Season 1	0.0208	0.7398	11.25	29.1	0.0622	0.3202	7.60	25.0	0.0563	0.3682	4.99	22.4
Season 2	0.0472	0.4483	13.87	35.9	0.0035	0.9555	11.79	38.8	0.0771	0.2159	8.55	38.4
Season 3	0.0929	0.1360	13.53	35.0	0.0904	0.1467	10.97	36.1	0.0486	0.4359	8.74	39.2
January	0.1469	0.0185	2.63	6.8	0.1097	0.0787	1.69	5.6	0.0978	0.1169	1.10	4.9
February	−0.0515	0.4090	2.55	6.6	0.0251	0.6874	1.86	6.1	0.0688	0.2702	1.25	5.6
March	0.0600	0.3356	2.55	6.6	0.1031	0.0982	1.94	6.4	0.1307	0.0361	1.30	5.8
April	−0.0951	0.1270	3.24	8.4	−0.1381	0.0268	2.88	9.5	−0.1259	0.0435	1.97	8.9
May	0.0280	0.6535	4.38	11.3	0.0180	0.7730	3.92	12.9	−0.0006	0.9926	2.96	13.3
June	0.1574	0.0115	3.69	9.5	0.1160	0.0628	3.04	10.0	0.1685	0.0069	2.32	10.4
July	−0.0706	0.2573	2.94	7.6	−0.1247	0.0455	2.28	7.5	−0.0569	0.3619	1.75	7.8
August	0.0490	0.4318	2.91	7.5	0.0948	0.1282	2.30	7.6	0.0915	0.1422	1.97	8.8
September	0.1239	0.0467	3.91	10.1	0.0578	0.3534	3.29	10.8	0.0071	0.9093	2.74	12.3
October	0.0207	0.7394	3.76	9.7	0.0610	0.3275	3.10	10.2	0.0270	0.6653	2.29	10.3
November	0.0206	0.7412	3.14	8.1	0.0416	0.5044	2.15	7.1	−0.0258	0.6789	1.46	6.5
December	−0.1000	0.1085	2.93	7.6	−0.0538	0.3882	1.90	6.2	−0.0042	0.9462	1.18	5.3

Table 12. Summary of annual, seasonal, and monthly precipitation trends for the period 1900–2017 within five sections of the Colorado River Basin.—Continued

[wet, years with precipitation totals above long-term mean; dry, years with precipitation totals below long-term mean; NA, not applicable; season 1, includes November, December, January, and February; season 2, includes March, April, May, and June; season 3, includes July, August, September, and October; *p*-value, probability value (considered statistically significant if less than 0.05); green shaded cells indicate statistically significant upward trends; red shaded cells indicate statistically significant downward trends]

Time step	Colorado River Basin section number[1]							
	Section 4				Section 5			
	1900–2017				1900–2017			
	Kendall's *tau*	*p*-value	Mean precipitation (inches)	Percentage[2]	Kendall's *tau*	*p*-value	Mean precipitation (inches)	Percentage[2]
Annual	0.0186	0.7677	21.30	100	0.0643	0.3028	16.94	100
Annual (wet)	−0.1455	0.1150	NA	NA	−0.0138	0.8851	NA	NA
Annual (dry)	0.1356	0.1214	NA	NA	0.0967	0.2734	NA	NA
Season 1	0.0403	0.5202	4.12	19.3	0.0187	0.7648	2.50	14.8
Season 2	0.0210	0.7359	8.44	39.6	0.0489	0.4331	5.96	35.2
Season 3	0.0300	0.6302	8.74	41.0	0.0309	0.6203	8.48	50.0
January	0.0793	0.2040	0.91	4.3	0.0509	0.4155	0.53	3.1
February	0.0924	0.1390	1.04	4.9	0.1232	0.0488	0.59	3.5
March	0.0932	0.1353	1.20	5.7	0.0755	0.2273	0.70	4.1
April	−0.0975	0.1180	1.93	9.0	−0.0569	0.3619	1.11	6.5
May	−0.0736	0.2374	2.96	13.9	0.0419	0.5014	2.03	12.0
June	0.1407	0.0241	2.35	11.0	0.0882	0.1573	2.12	12.5
July	−0.0310	0.6186	1.97	9.2	−0.0054	0.9314	2.27	13.4
August	0.1166	0.0615	2.00	9.4	0.1014	0.1040	2.20	13.0
September	0.0386	0.5361	2.60	12.2	0.0490	0.4318	2.36	13.9
October	0.0052	0.9333	2.17	10.2	−0.0636	0.3083	1.65	9.7
November	−0.0360	0.5640	1.22	5.7	−0.0275	0.6602	0.75	4.5
December	0.0093	0.8817	0.95	4.5	0.0490	0.4330	0.63	3.7

[1]Refer to figure 13 for map of sections within the Colorado River Basin.

[2]Percentage of the total precipitation within the season or month for the time period specified.

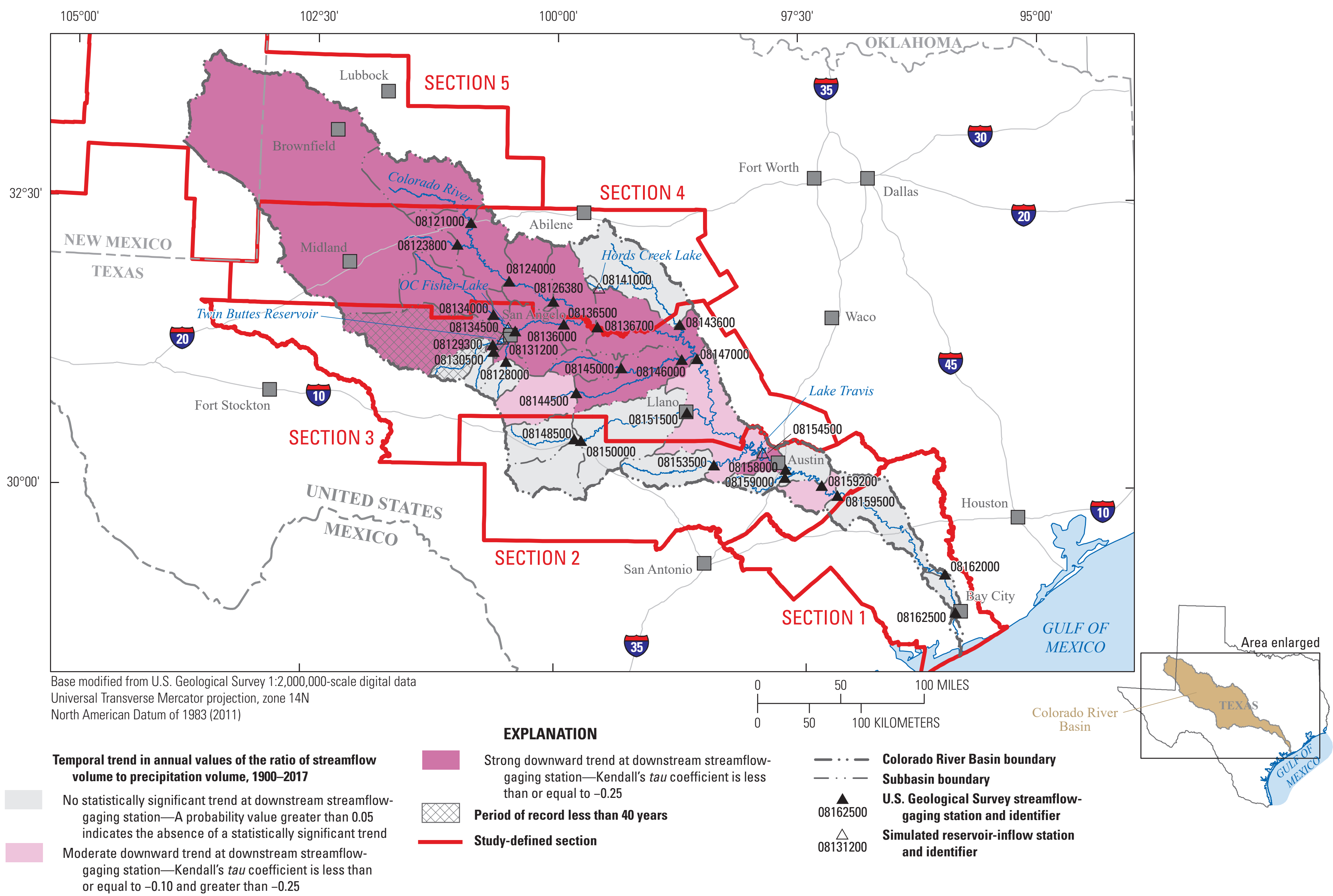

Figure 14. Temporal trends in annual values of the ratio of streamflow volume to precipitation volume at 26 U.S. Geological Survey streamflow-gaging stations and 4 simulated reservoir-inflow stations in the Colorado River Basin, 1900–2017.

The Kendall's *tau* and *p*-values for trends in two extreme streamflow regimes, annual minimum and annual peak streamflow, were calculated (table 10), and any trends that were indicated for these two streamflow regimes are depicted for the areal extent of the basin (figs. 15–16). In the lower section of the basin (section 1), data from one station operated as a continuous streamflow-gaging station through 2017 indicated a downward trend in annual minimum streamflow, and data from the other station (operated through 2007) indicated an upward trend in annual minimum streamflow. In the upper sections of the basin (sections 2, 3, and 4) data from seven stations indicated upward trends and data from six stations indicated downward trends in annual minimum streamflow.

Downward trends in annual peak streamflow were not indicated at either of the stations in section 1 of the basin. However, data from 18 stations in the upper sections of the basin indicated a downward trend in annual peak streamflow. Upward trends in annual peak streamflow were not indicated at any of the stations in the Colorado River Basin.

Potential Flood Storage Trends

Results of the analyses of the associations between potential flood storage volume and annual streamflow volume and the trends in the ratio of annual streamflow volume to potential flood storage volume for the Colorado River Basin are summarized in table 10, and the annual results are illustrated in figures 17 and 18, respectively.

In the lower section of the basin, potential flood storage volume and streamflow volume were not associated. Data from only one of the two stations indicated a trend in the ratio of annual streamflow volume to potential flood storage volume, and data from neither of the two stations indicated a downward trend in annual streamflow. Thirteen of the 16 stations in the upper sections of the basin with data that indicated downward trends in annual streamflow (table 8) also indicated downward trends in the ratio of streamflow volume to precipitation volume on an annual time step (table 9). Data from the same 13 stations indicated negative associations between potential flood storage volume and annual streamflow volume and downward trends in the ratio of annual streamflow volume to potential flood storage volume (table 10). With the known addition of 7,193,147 acre-ft of potential flood storage between 1891 and 2014 in the subbasins analyzed (USACE, 2019a), streamflow volumes have decreased in the upper sections of the Colorado River Basin.

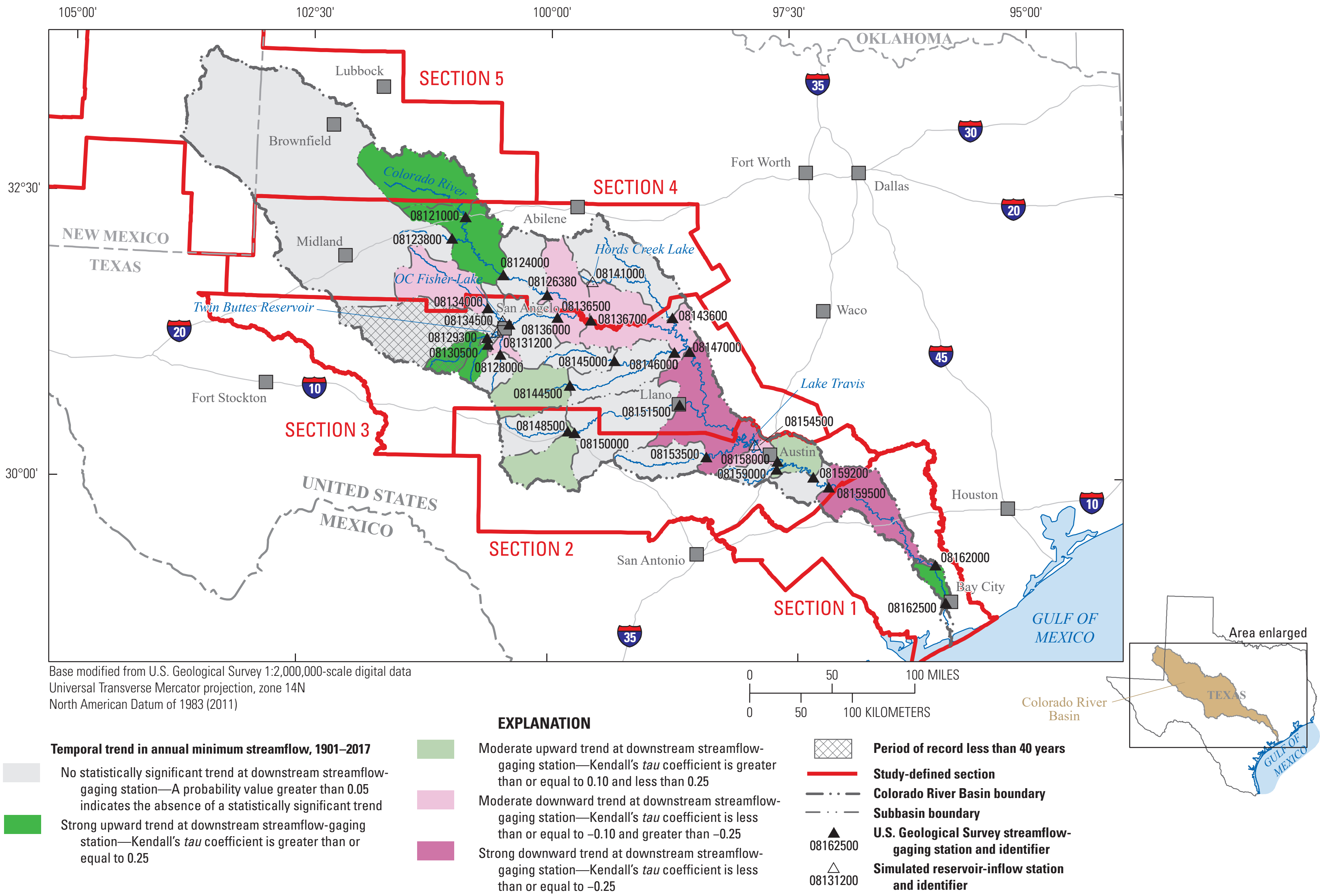

Figure 15. Temporal trends in annual minimum streamflow at 26 U.S. Geological Survey streamflow-gaging stations and 4 simulated reservoir-inflow stations in the Colorado River Basin, 1901–2017.

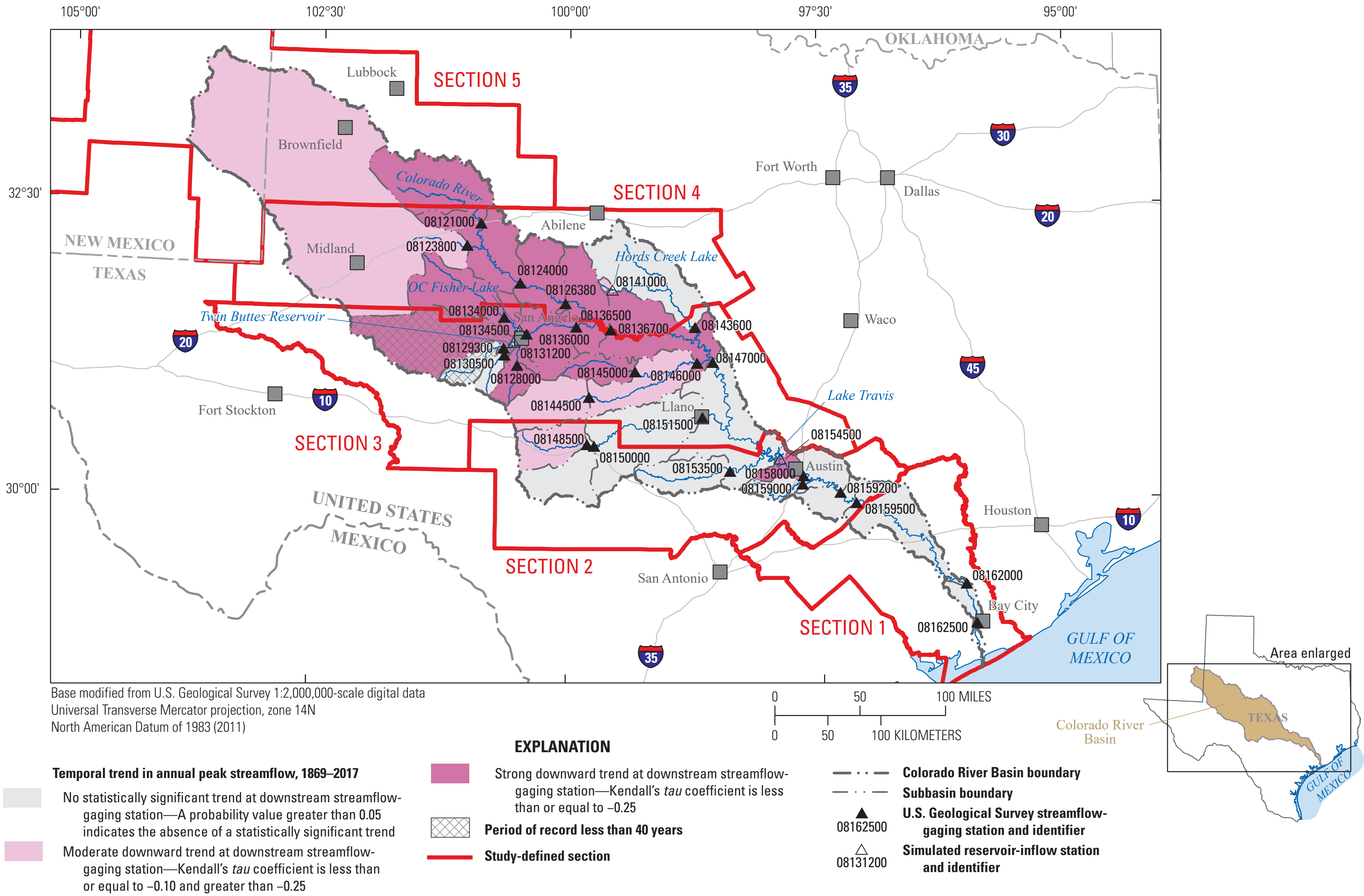

Figure 16. Temporal trends in annual peak streamflow at 26 U.S. Geological Survey streamflow-gaging stations and 4 simulated reservoir-inflow stations in the Colorado River Basin, 1869–2017.

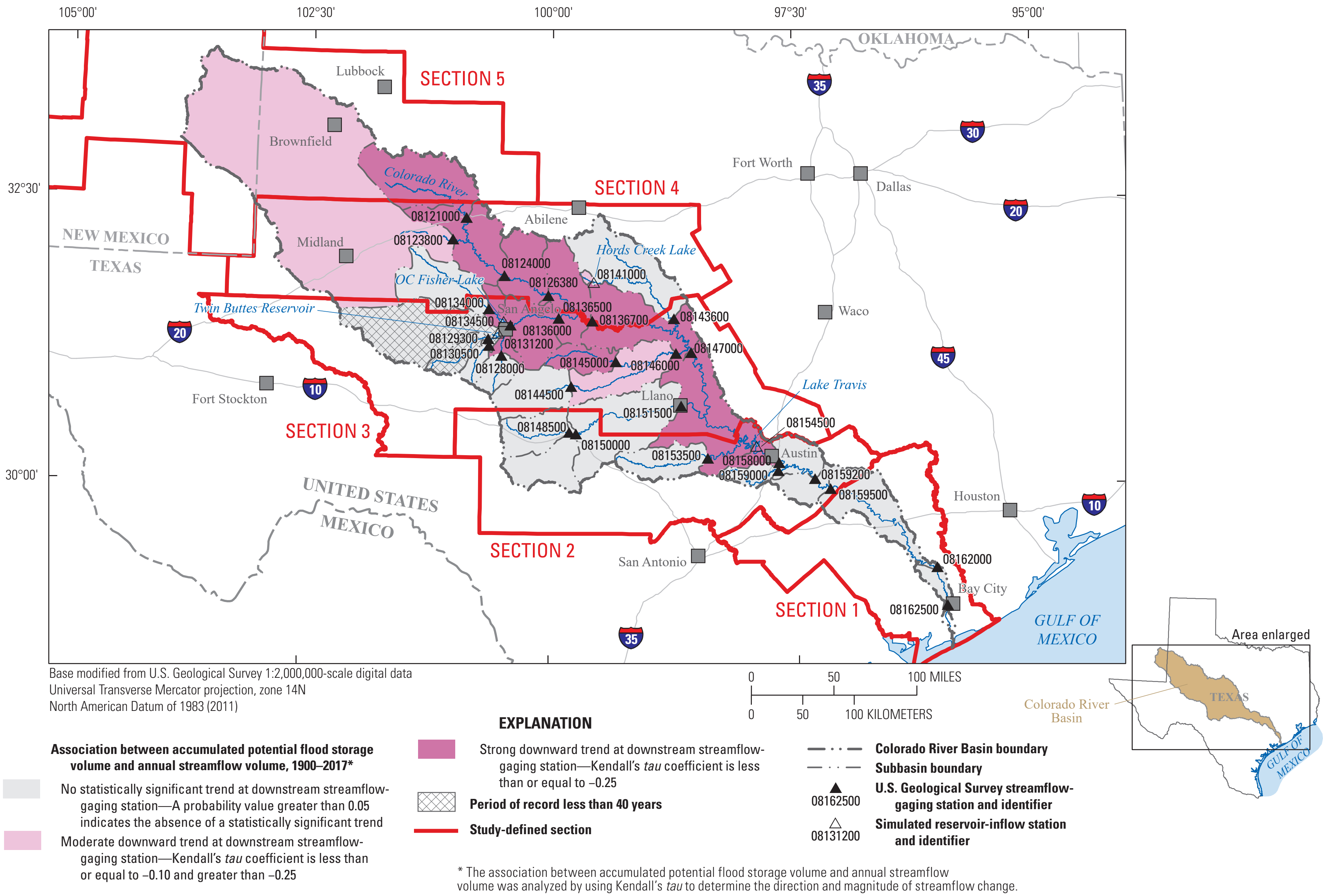

Figure 17. Association between accumulated potential flood storage volume and annual streamflow volume at 26 U.S. Geological Survey streamflow-gaging stations and 4 simulated reservoir-inflow stations in the Colorado River Basin, 1900–2017.

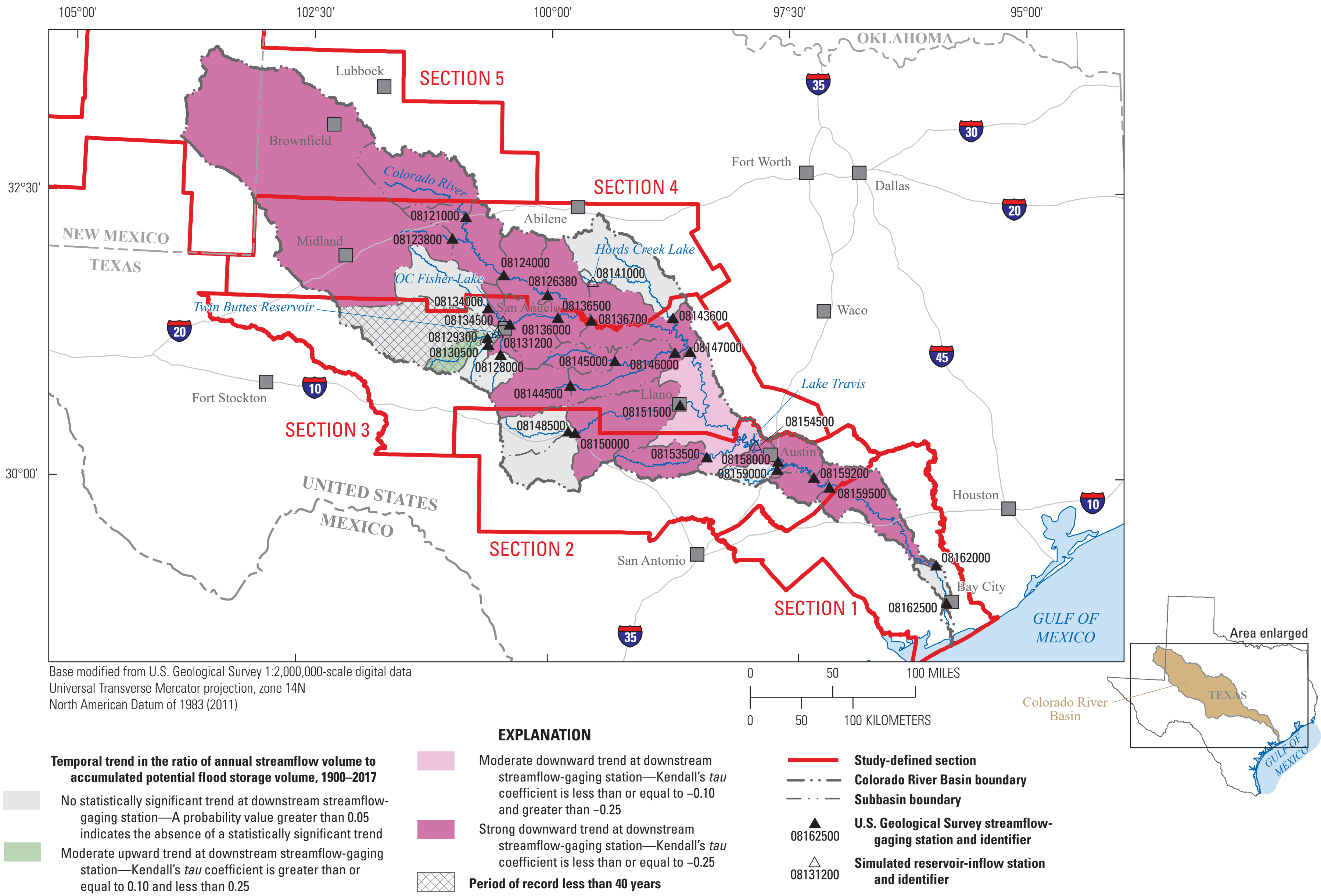

Figure 18. Temporal trends in the ratio of annual streamflow volume to accumulated potential flood storage volume at 26 U.S. Geological Survey streamflow-gaging stations and 4 simulated reservoir-inflow stations in the Colorado River Basin, 1900–2017.

Big Cypress Basin

The Big Cypress Basin, which includes Big Cypress Creek and Little Cypress Creek and their tributaries, in east Texas covers 3,552 mi^2 in Texas, Arkansas, and Louisiana and is the smallest basin in this study (fig. 19; TWDB, 2019a). Within the Big Cypress Basin, seven USGS streamflow-gaging stations and one simulated-inflow station were selected for streamflow trend analyses (table 13). The periods of record for these eight stations range from 27 to 93 years, with a mean period of record of 60 years. The mean percentage of complete and continuous record was 88 percent. Four of the stations (three USGS and one simulated-inflow) are on the main stem of Big Cypress Creek. The most downstream station, USGS streamflow-gaging station 07348000 Twelvemile Bayou near Dixie, Louisiana, is about 14 mi upstream from its confluence with the Red River and has a total drainage area of 3,137 mi^2.

In the Big Cypress Basin, the associations between precipitation and streamflow were strong for most time steps and were all positive, indicating an increase in streamflow as precipitation increases (table 5). Of the 128 possible trends, 125 were significant.

Precipitation Trends

Results of precipitation trend analyses on annual, seasonal, and monthly time steps indicated almost no trends in the Big Cypress Basin (table 14) as defined in this report (p-value ≤0.05), save for a moderate upward trend in the month of October. However, the annual precipitation p-value is 0.0582, which only slightly exceeds the 0.05 p-value threshold for a statistically significant trend, and therefore could be interpreted as indicative of an annual trend in precipitation in the basin. When the data were separated by wet and dry years, no trends were indicated. The lack of trends is somewhat inconsistent with the moderate upward trend in the East Texas Climate Division (table 1) because the East Texas Climate Division includes the Big Cypress Basin. However, the East Texas Climate Division also extends well beyond the extent of the Big Cypress Basin and farther south towards the Gulf of Mexico. Given the low p-value (0.0582) and the upward trend in the East Texas Climate Division, precipitation in the Big Cypress Basin may be increasing over time.

Possible trends in the sum of precipitation on the day of the annual peak, for different numbers of days before the annual peak streamflow (365, 180, 90, 60, and 30), and for the 5 days before, the day of, and the day after annual peak streamflow for each of the eight stations in the Big Cypress Basin are summarized in table 7. Of the 8 stations and 56 possible trends in peak streamflow-related precipitation, four trends were significant, consisting of three upward trends and one downward trend. No patterns in peak streamflow-related precipitation were evident.

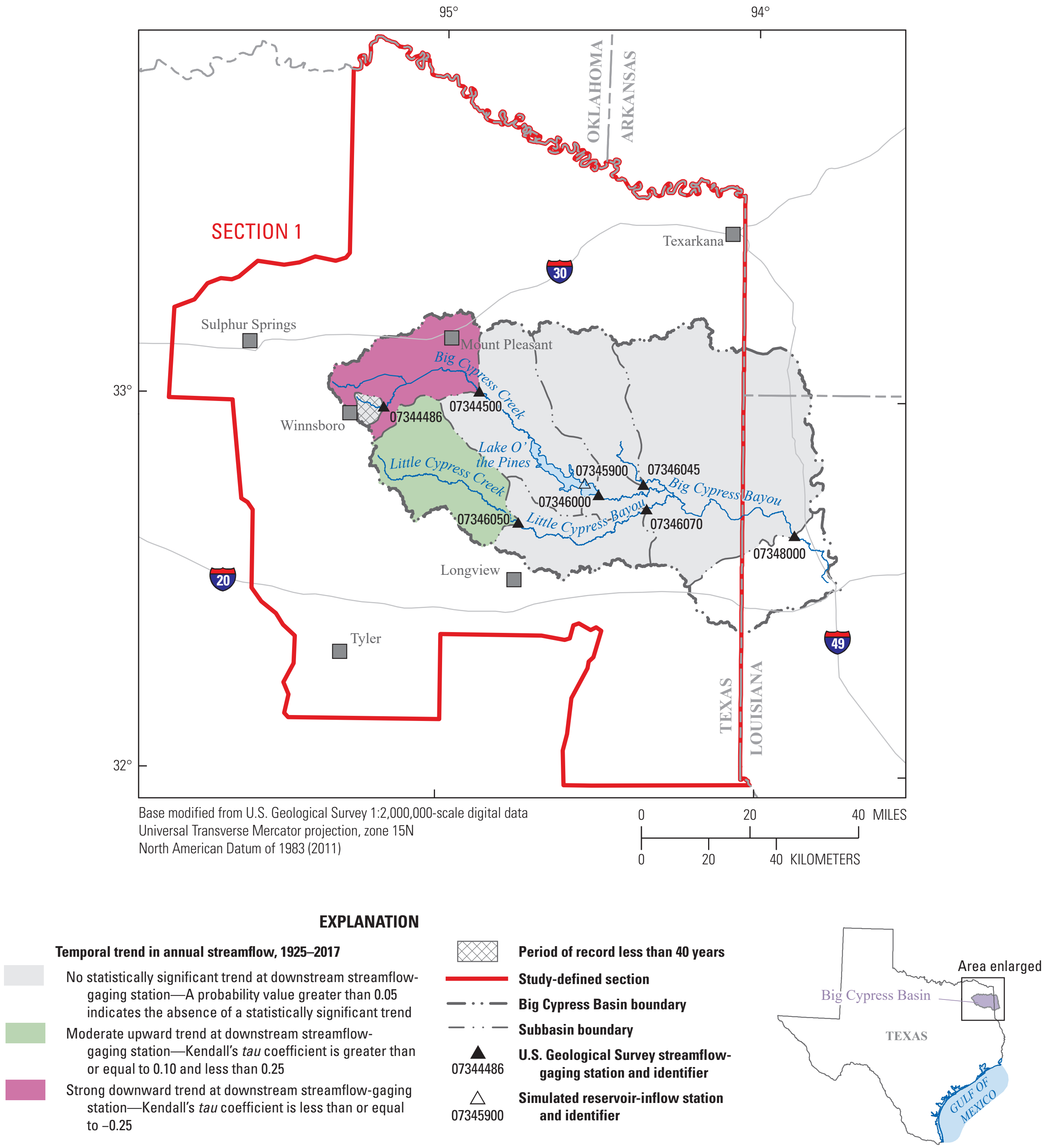

Figure 19. Temporal trends in annual streamflow at seven U.S. Geological Survey streamflow-gaging stations and one U.S. Army Corps of Engineers simulated reservoir-inflow station in the Big Cypress Basin, 1925–2017.

Table 13. Summary information for seven U.S. Geological Survey streamflow-gaging stations and one U.S. Army Corps of Engineers simulated reservoir-inflow station analyzed for trends in the Big Cypress Basin, 1924–2017.

[mi^2, square mile]

Section number[1]	Station number, name[2]	Total drainage area (mi^2)	Contributing drainage area (mi^2)	Period of record by calendar year[3]	Number of years of record	Percentage of record complete
1	07348000, Twelvemile Bayou near Dixie, Louisiana	3,137	3,137	1942–95	53	100
	07346070, Little Cypress Bayou near Jefferson, Texas	675	675	1946–2017	71	100
	07346050, Little Cypress Creek near Ore City, Texas	383	383	1962–2017	55	73.7
	07346045, Black Cypress Bayou at Jefferson, Texas	365	365	1968–2017	49	100
	07346000, Big Cypress Bayou near Jefferson, Texas	850	850	1924–2017	93	73.5
	07345900, Lake O' the Pines near Jefferson, Texas	850	850	1957–2017	60	100
	07344500, Big Cypress Creek near Pittsburg, Texas	370	370	1943–2017	74	65.6
	07344486, Brushy Creek at Scroggins, Texas	23.4	23.4	1977–2004	27	92.5

[1]Refer to figure 19 for map of Big Cypress Basin.

[2]Shaded cells are U.S. Geological Survey streamflow-gaging stations with measured streamflow data (U.S. Geological Survey, 2019b), and cells that are not shaded are lake and reservoir stations with simulated inflow data provided by the U.S. Army Corps of Engineers (2019b).

[3]Period of record includes the calendar year when daily mean streamflow data collection began to the end of 2017 or when data collection ended (if applicable).

Table 14. Summary of annual, seasonal, and monthly precipitation trends for the period 1900–2017 within the Big Cypress Basin.

[wet, years with precipitation totals above long-term mean; dry, years with precipitation totals below long-term mean; NA, not applicable; season 1, includes November, December, January, and February; season 2, includes March, April, May, and June; season 3, includes July, August, September, and October; *p*-value, probability value (considered statistically significant if less than 0.05); green shaded cells indicate statistically significant upward trends]

Time step	Big Cypress Basin[1]			
	Kendall's *tau*	*p*-value	Mean precipitation (inches)	Percentage[2]
Annual	0.1192	0.0582	45.53	100
Annual (wet)	0.0820	0.3584	NA	NA
Annual (dry)	0.0156	0.8709	NA	NA
Season 1	0.0912	0.1475	15.26	33.5
Season 2	0.0559	0.3747	17.46	38.3
Season 3	0.0750	0.2314	12.81	28.1
January	0.0568	0.3644	3.46	7.6
February	0.0894	0.1534	3.53	7.8
March	0.0864	0.1674	4.17	9.2
April	−0.1005	0.1081	4.67	10.3
May	0.0319	0.6089	4.86	10.7
June	0.0936	0.1330	3.76	8.2
July	−0.0787	0.2066	3.25	7.1
August	−0.0213	0.7324	2.69	5.9
September	0.1131	0.0708	3.15	6.9
October	0.1396	0.0251	3.72	8.2
November	0.1074	0.0848	3.95	8.7
December	0.0321	0.6076	4.31	9.5

[1]Refer to figure 19 for map of Big Cypress Basin.

[2]Percentage of the total precipitation within the season or month for the time period specified.

Streamflow Trends

Temporal trends in streamflow volume on annual, seasonal, and monthly time steps are summarized in table 8. The trends in annual streamflow at the eight stations within the Big Cypress Basin are also depicted for the areal extent of the basin (fig. 19). The two statistically significant annual trends, one upward and one downward, in the Big Cypress Basin were both at stations in the upstream part of the basin. The upward trend was on Little Cypress Creek, a tributary of Big Cypress Creek, and the downward trend was on the main stem at the farthest upstream station downstream from Mount Pleasant, Texas. Three of the 24 possible seasonal trends were significant, 2 upward and 1 downward. Of the 18 monthly streamflow trends in the Big Cypress Basin, 5 were downward and 13 were upward. The upstream parts of the basin in the outcrop areas of the Carrizo-Wilcox aquifer, particularly the area contributing to the station on the main stem downstream from Mount Pleasant, could be affected by the downward groundwater-level trends in the aquifer.

The ratios of streamflow volume to precipitation volume were analyzed as part of this study (fig. 20; table 9). Temporal trends in the ratio of streamflow volume to precipitation volume indicate a change in the way the system responds to precipitation events and possibly explain downward trends in streamflow if the ratios are also downward. The only station with a strong downward trend in annual streamflow also indicated a strong downward trend in the ratio of streamflow volume to precipitation volume on an annual time step and is on the main stem at the farthest upstream station downstream from Mount Pleasant, Texas, with no trend in annual precipitation.

The Kendall's *tau* and *p*-values for trends in two extreme streamflow regimes, annual minimum and annual peak streamflow, were calculated (table 10), and any trends that were indicated for these two streamflow regimes are depicted for the areal extent of the basin (figs. 21–22). In cases where a USGS streamflow-gaging station is immediately downstream from a simulated-inflow station, the simulated-inflow station takes precedence in visualization of any trends. Data from USGS streamflow-gaging station 07346000 Big Cypress Bayou near Jefferson, Texas, indicated an upward trend in annual minimum streamflow and a downward trend in annual peak streamflow (table 10). The station is immediately downstream from Lake O' the Pines; presumably, minimums have increased because of regulated releases, and annual peaks have decreased because of storage from the lake for flood control.

Potential Flood Storage Trends

Results of the analyses of the associations between potential flood storage volume and annual streamflow volume and the trends in the ratio of annual streamflow volume to potential flood storage volume for the Big Cypress Basin are summarized in table 10, and the annual results are illustrated in figures 23 and 24, respectively.

Data from the farthest upstream station on the main stem downstream from Mount Pleasant, Texas, with a strong downward trend in annual streamflow, also indicated a strong downward trend in the ratio of streamflow volume to precipitation volume on an annual time step. Data from the station also indicated a negative association between potential flood storage volume and annual streamflow volume and a downward trend in the ratio of annual streamflow volume to potential flood storage volume. However, despite the known addition of 2,737,154 acre-ft of potential flood storage between 1898 and 2011 in the subbasins analyzed (USACE, 2019a), there have not been widespread reductions in streamflow volumes in the Big Cypress Basin.

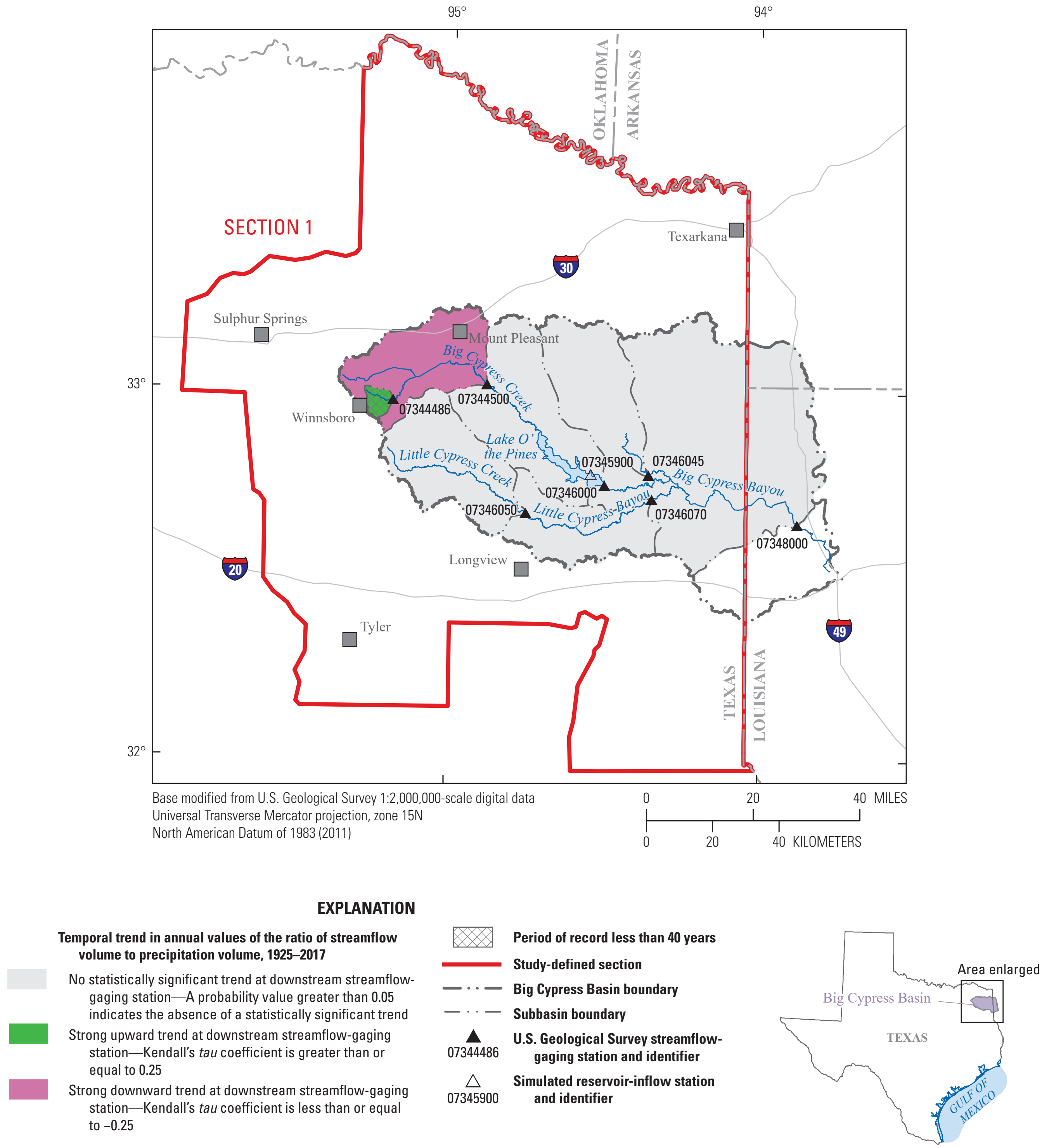

Figure 20. Temporal trends in annual values of the ratio of streamflow volume to precipitation volume at seven U.S. Geological Survey streamflow-gaging stations and one U.S. Army Corps of Engineers simulated reservoir-inflow station in the Big Cypress Basin, 1925–2017.

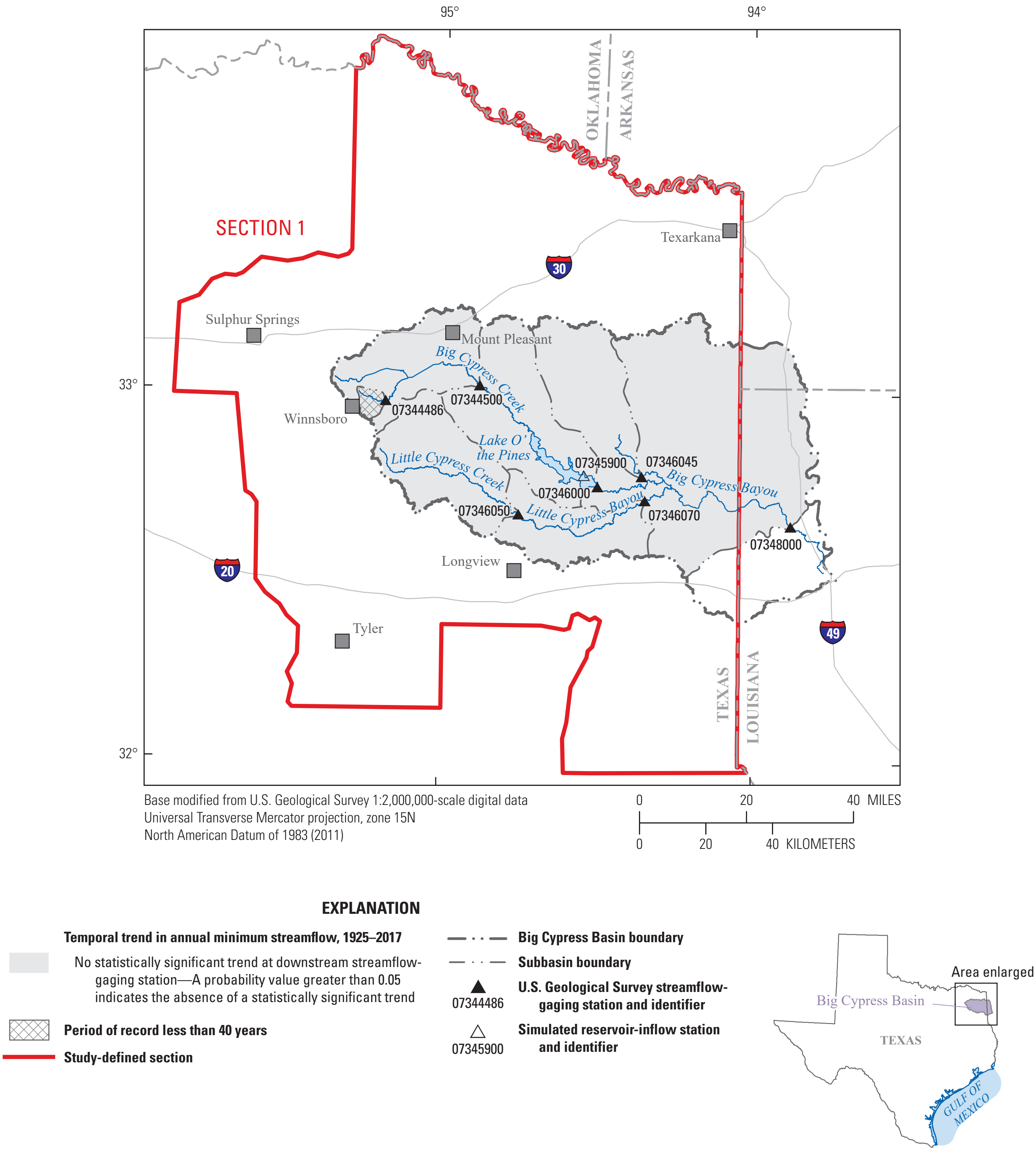

Figure 21. Temporal trends in annual minimum streamflow at seven U.S. Geological Survey streamflow-gaging stations and one U.S. Army Corps of Engineers simulated reservoir-inflow station in the Big Cypress Basin, 1925–2017.

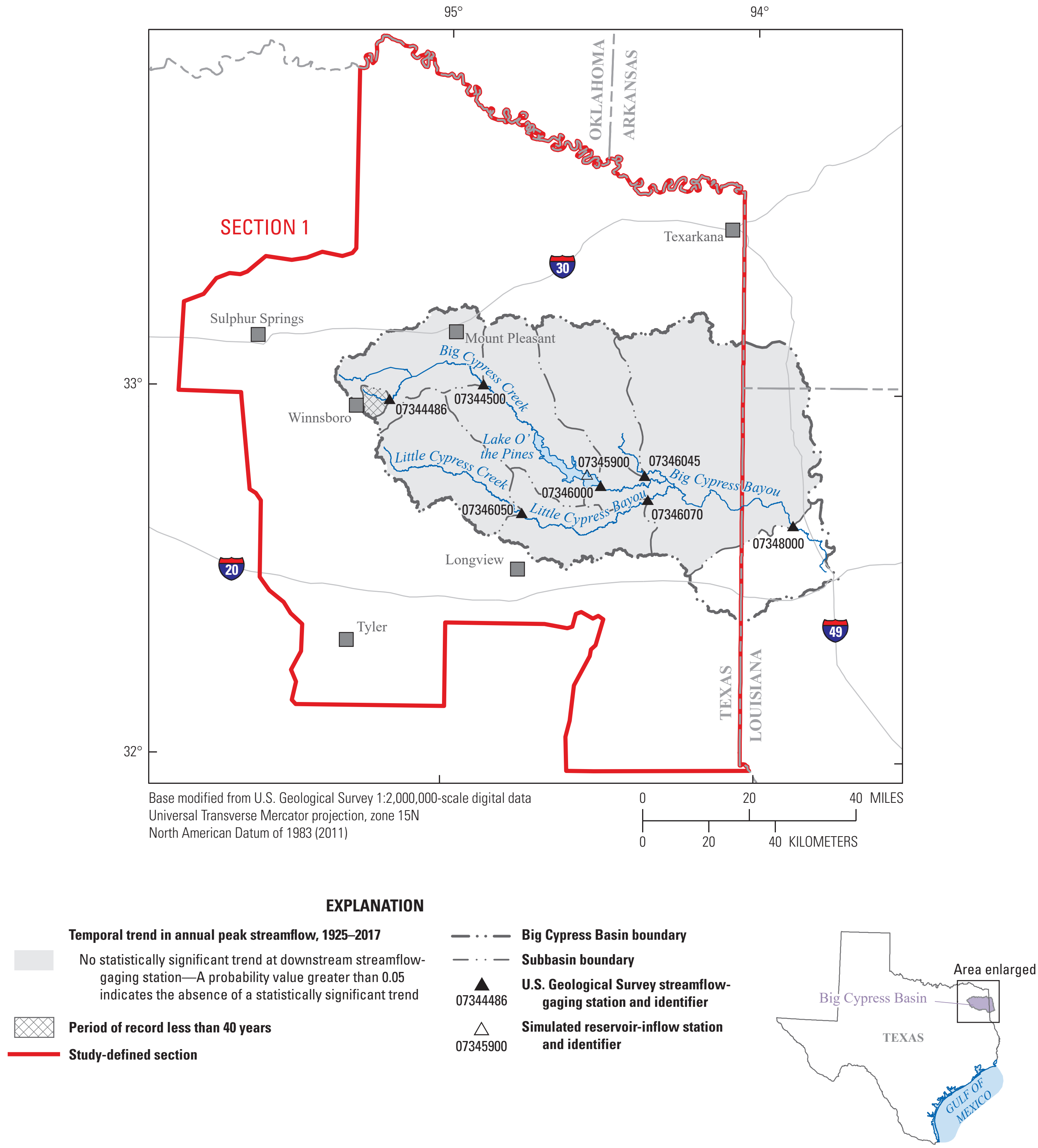

Figure 22. Temporal trends in annual peak streamflow at seven U.S. Geological Survey streamflow-gaging stations and one U.S. Army Corps of Engineers simulated reservoir-inflow station in the Big Cypress Basin, 1925–2017.

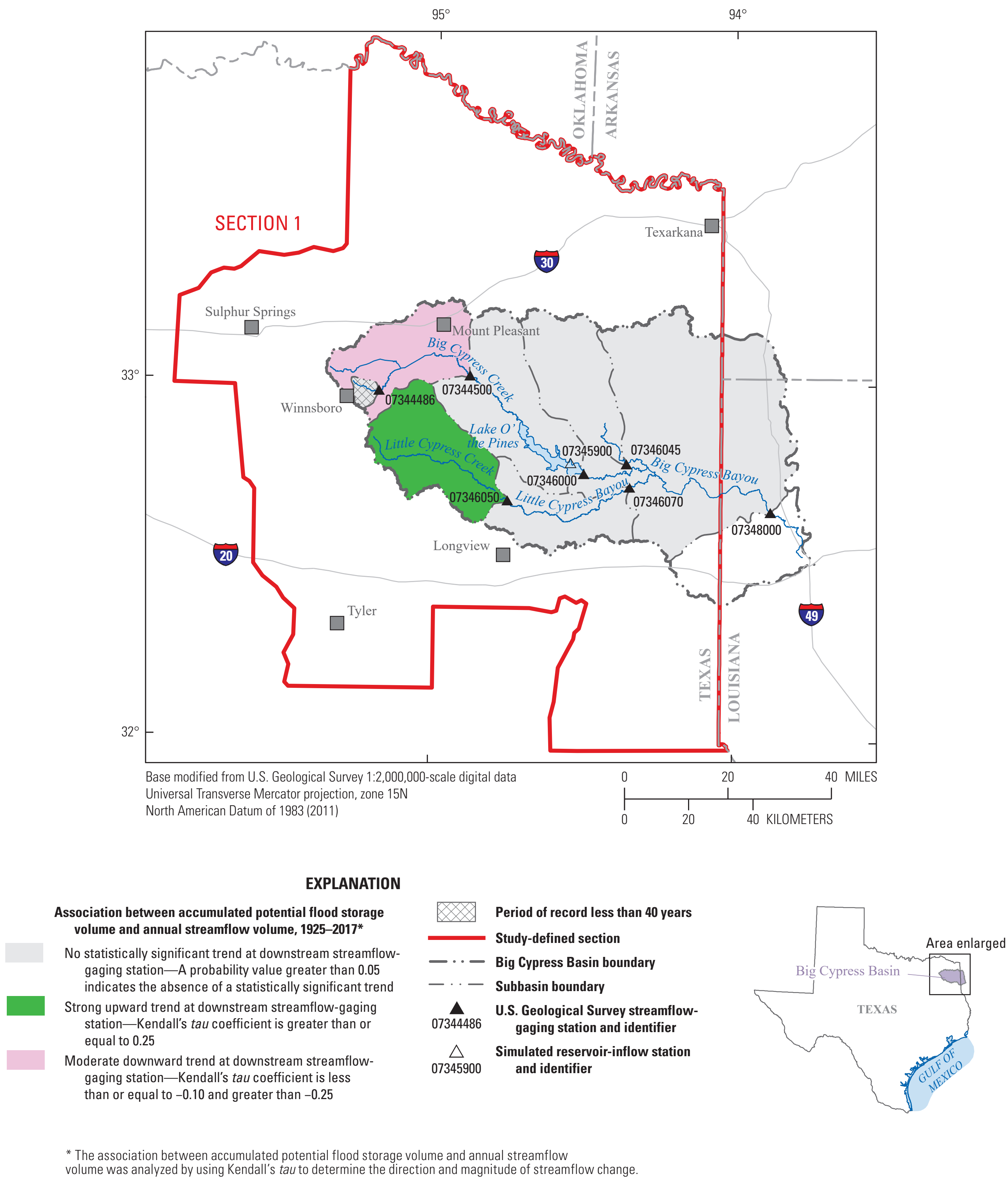

Figure 23. Association between accumulated potential flood storage volume and annual streamflow volume at seven U.S. Geological Survey streamflow-gaging stations and one U.S. Army Corps of Engineers simulated reservoir-inflow station in the Big Cypress Basin, 1925–2017.

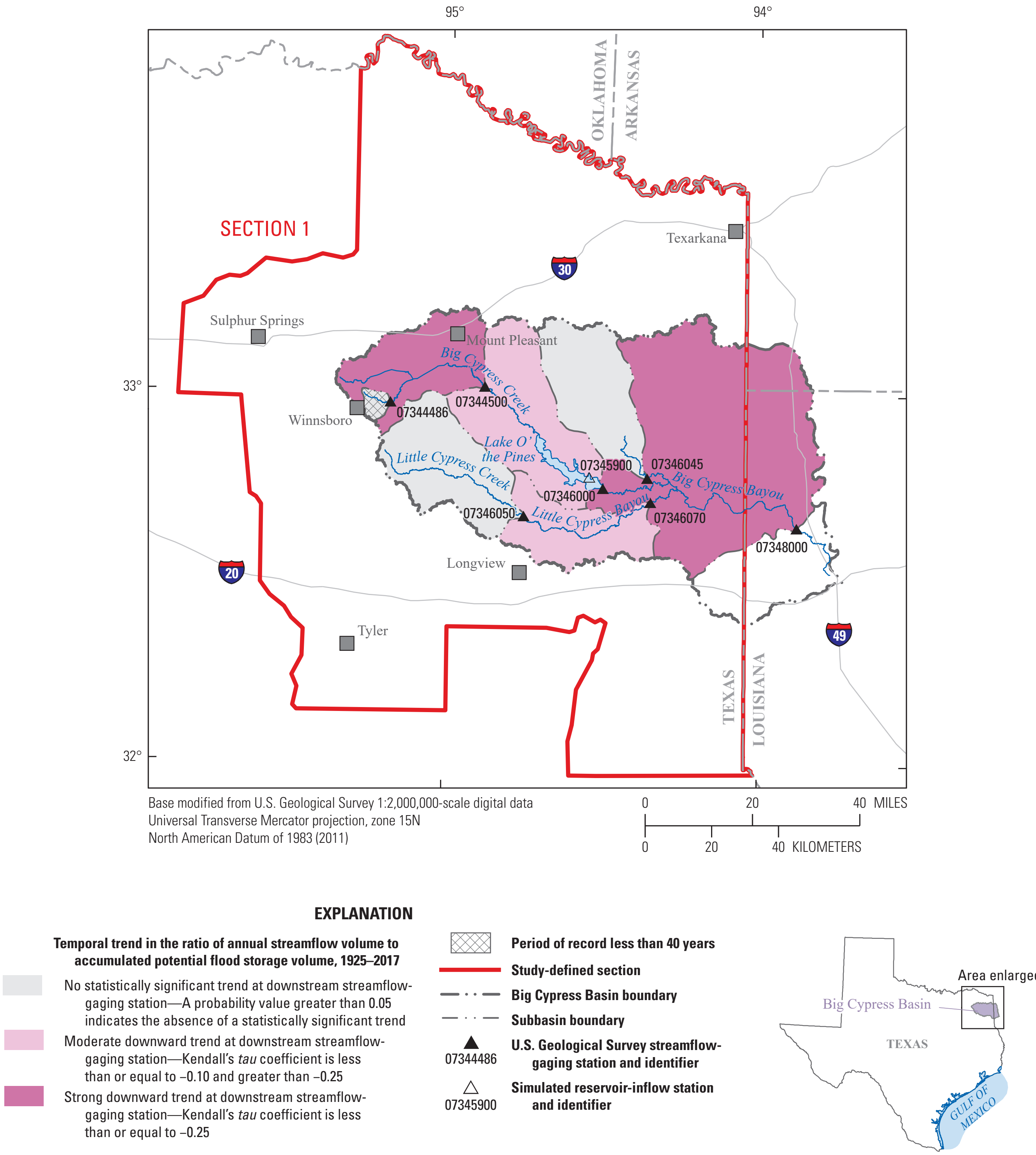

Figure 24. Temporal trends in the ratio of annual streamflow volume to accumulated potential flood storage volume at seven U.S. Geological Survey streamflow-gaging stations and one U.S. Army Corps of Engineers simulated reservoir-inflow station in the Big Cypress Basin, 1925–2017.

Guadalupe River Basin

The Guadalupe River Basin covers 5,953 mi^2 and begins in central Texas (fig. 25; TWDB, 2019a). Within the Guadalupe River Basin, 17 USGS streamflow-gaging stations and 1 simulated-inflow station were selected for streamflow trend analyses (table 15). The periods of record for these 18 stations range from 53 to 95 years, with a mean period of record of 75 years. The mean percentage of complete and continuous record was 92 percent. Eight of the stations (seven USGS and one simulated-inflow) are on the main stem of the Guadalupe River. The most downstream main-stem station, USGS streamflow-gaging station 08176500 Guadalupe River at Victoria, Texas, is about 50 mi upstream from where the river empties into San Antonio Bay and has a total drainage area of 5,198 mi^2.

In the Guadalupe River Basin, the associations between precipitation and streamflow were strong for most time steps and were all positive, indicating an increase in streamflow as precipitation increases (table 5). Of the 288 possible associations, 269 were significant.

Precipitation Trends

Results of precipitation trend analyses on an annual time step indicated an upward trend in the lower section (section 1) of the Guadalupe River Basin (table 16), which is consistent with the upward trend in the Upper Coast Climate Division (table 1). When separated by wet and dry years, the data did not indicate trends in either section. Results also indicated no trends in precipitation on a seasonal time step. Results of precipitation trend analyses on a monthly time step indicated three trends, of which two were upward and one was downward (table 16).

Possible trends in the sum of precipitation on the day of the annual peak, for different numbers of days before the annual peak streamflow (365, 180, 90, 60, and 30), and for the 5 days before, the day of, and the day after annual peak streamflow for each of the 18 stations in the Guadalupe River Basin are summarized in table 7. Of the 18 stations and 126 possible trends in peak streamflow-related precipitation, 5 trends were significant. All five were upward trends and in section 2 of the basin. Four of the five trends were for precipitation on the day of the annual peak.

Streamflow Trends

Temporal trends in streamflow volume on annual, seasonal, and monthly time steps are summarized in table 8. The trends in annual streamflow at the 18 stations within the Guadalupe River Basin are also depicted for the areal extent of the basin (fig. 25). No trends in annual streamflow were indicated in the lower section of the basin (section 1). In the upper section of the basin (section 2), data from 1 of the 13 stations (USGS streamflow-gaging station 08166000 Johnson Creek near Ingram, Texas) in the northwest part of the basin indicated a strong upward trend in annual streamflow. Of the four seasonal trends in the Guadalupe River Basin, all were upward and in section 2 (table 8). Three seasonal trends were for USGS streamflow-gaging station 08166000 Johnson Creek near Ingram, Texas. Thirty of the 216 possible monthly trends in the Guadalupe River Basin were significant; 10 were downward and 20 were upward. Data from one station (USGS streamflow-gaging station 08166000 Johnson Creek near Ingram, Texas) indicated strong upward trends in streamflow during all 12 months, accounting for about 60 percent of all upward monthly trends. Similarly, data from one station (USGS streamflow-gaging station 08177500 Coleto Creek near Victoria, Texas) in section 1 indicated moderate downward trends in streamflow for six months, accounting for 60 percent of all downward monthly trends. The remaining monthly trends (upward and downward) were dispersed across eight different stations in both sections. Data from the lower section of the basin indicated only downward monthly trends, whereas data from the upper section of the basin indicated only a small number of downward trends (three monthly) and several seasonal and monthly (and one annual) upward trends in streamflow. Downward trends in groundwater-levels within the major aquifers with potential to discharge directly to the Guadalupe River (Carrizo-Wilcox and Gulf Coast) did not coincide with annual streamflow trends.

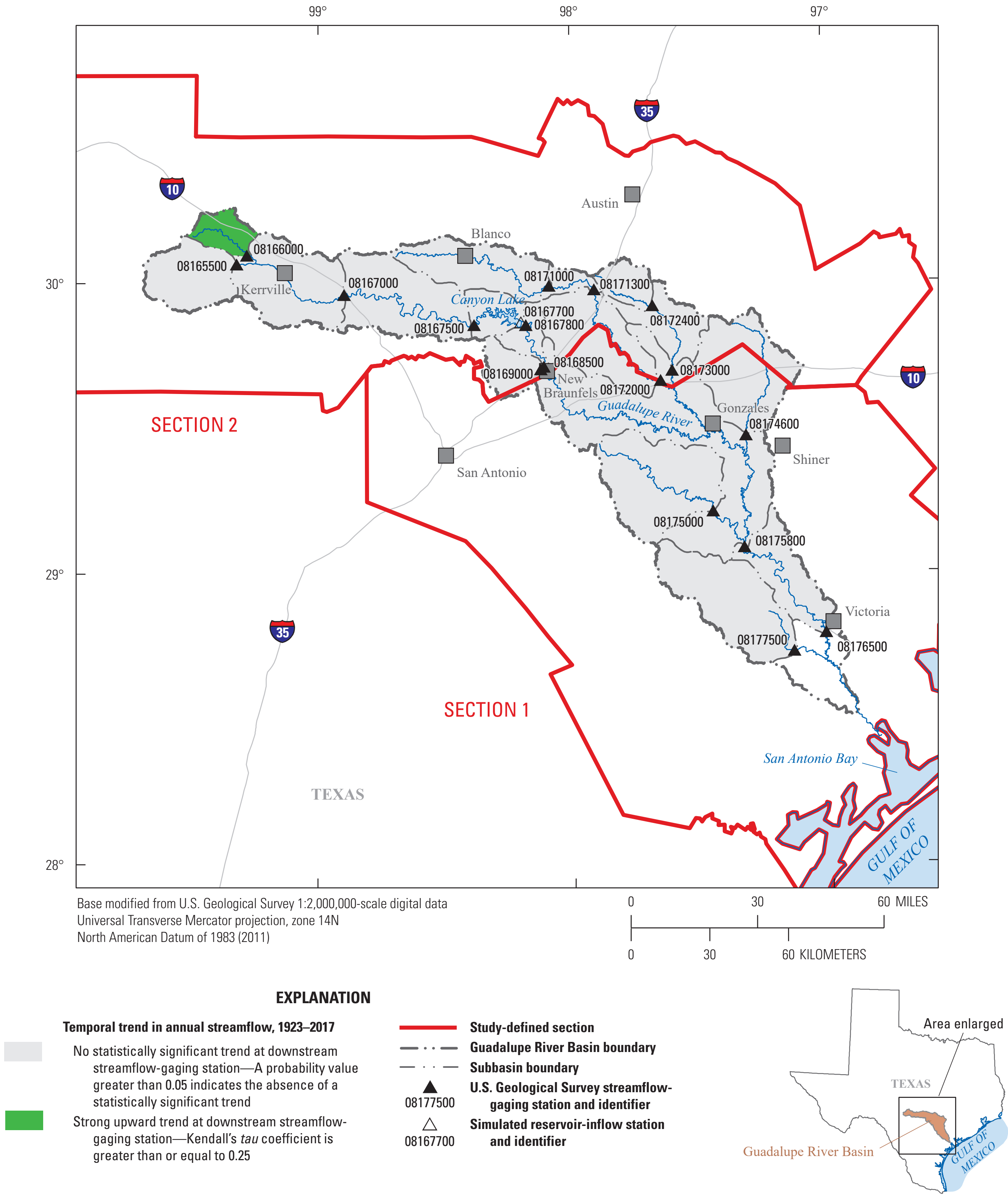

Figure 25. Temporal trends in annual streamflow at 17 U.S. Geological Survey streamflow-gaging stations and 1 U.S. Army Corps of Engineers simulated reservoir-inflow station in the Guadalupe River Basin, 1923–2017.

Table 15. Summary information for 17 U.S. Geological Survey streamflow-gaging stations and 1 U.S. Army Corps of Engineers simulated reservoir-inflow station analyzed for trends in the Guadalupe River Basin, 1922–2017.

[mi², square mile]

Section number[1]	Station number, name[2]	Total drainage area (mi²)	Contributing drainage area (mi²)	Period of record by calendar year[3]	Number of years of record	Percentage of record complete
1	08177500, Coleto Creek near Victoria, Texas	500	500	1939–2017	78	69.8
	08176500, Guadalupe River at Victoria, Texas	5,198	5,198	1934–2017	83	100
	08175800, Guadalupe River at Cuero, Texas	4,934	4,934	1964–2017	53	100
	08175000, Sandies Creek near Westhoff, Texas	549	549	1930–2017	87	71.8
	08174600, Peach Creek below Dilworth, Texas	460	460	1959–2017	58	64.2
2	08173000, Plum Creek near Luling, Texas	309	309	1930–2017	87	91.1
	08172400, Plum Creek at Lockhart, Texas	112	112	1959–2017	58	100
	08172000, San Marcos River at Luling, Texas	838	838	1939–2017	78	100
	08171300, Blanco River near Kyle, Texas	412	412	1956–2017	61	100
	08171000, Blanco River at Wimberley, Texas	355	355	1924–2017	93	97.4
	08169000, Comal River at New Braunfels, Texas	130	130	1927–2017	90	99.9
	08168500, Guadalupe River above Comal River at New Braunfels, Texas	1,518	1,518	1927–2017	90	100
	08167800, Guadalupe River at Sattler, Texas	1,436	1,436	1960–2017	57	100
	08167700, Canyon Lake near New Braunfels, Texas	1,432	1,432	1964–2017	53	100
	08167500, Guadalupe River near Spring Branch, Texas	1,315	1,315	1922–2017	95	100
	08167000, Guadalupe River at Comfort, Texas	839	839	1939–2017	78	100
	08166000, Johnson Creek near Ingram, Texas	114	114	1941–2017	76	90.3
	08165500, Guadalupe River at Hunt, Texas	288	288	1941–2017	76	79.4

[1]Refer to figure 25 for map of sections within the Guadalupe River Basin.

[2]Shaded cells are U.S. Geological Survey streamflow-gaging stations with measured streamflow data (U.S. Geological Survey, 2019b), and cells that are not shaded are lake and reservoir stations with simulated inflow data provided by the U.S. Army Corps of Engineers (2019b).

[3]Period of record includes the calendar year when daily mean streamflow data collection began to the end of 2017.

Table 16. Summary of annual, seasonal, and monthly precipitation trends for the period 1900–2017 within two sections of the Guadalupe River Basin.

[wet, years with precipitation totals above long-term mean; dry, years with precipitation totals below long-term mean; NA, not applicable; season 1, includes November, December, January, and February; season 2, includes March, April, May, and June; season 3, includes July, August, September, and October; *p*-value, probability value (considered statistically significant if less than 0.05); green shaded cells indicate statistically significant upward trends; red shaded cells indicate statistically significant downward trends]

Time step	Guadalupe River Basin section number[1]							
	Section 1				Section 2			
	1900–2017				1900–2017			
	Kendall's *tau*	*p*-value	Mean precipitation (inches)	Percentage[2]	Kendall's *tau*	*p*-value	Mean precipitation (inches)	Percentage[2]
Annual	0.1311	0.0355	33.82	100	0.0711	0.2544	31.04	100
Annual (wet)	0.1197	0.1909	NA	NA	0.1662	0.0715	NA	NA
Annual (dry)	0.0476	0.5925	NA	NA	0.0249	0.7799	NA	NA
Season 1	0.0453	0.4710	8.85	26.2	0.0559	0.3732	7.91	25.5
Season 2	0.0480	0.4427	12.21	36.1	0.0133	0.8324	12.03	38.8
Season 3	0.1060	0.0895	12.76	37.7	0.0739	0.2364	11.10	35.8
January	0.1698	0.0065	2.06	6.1	0.1040	0.0954	1.76	5.7
February	−0.0144	0.8179	2.07	6.1	0.0170	0.7855	1.92	6.2
March	0.0585	0.3486	2.12	6.3	0.1008	0.1060	2.00	6.4
April	−0.0802	0.1983	2.74	8.1	−0.1440	0.0209	2.92	9.4
May	0.0277	0.6568	3.95	11.7	0.0304	0.6252	4.01	12.9
June	0.1124	0.0714	3.40	10.0	0.1265	0.0425	3.10	10.0
July	−0.0384	0.5376	2.76	8.2	−0.1203	0.0535	2.32	7.5
August	0.0616	0.3229	2.67	7.9	0.0721	0.2477	2.28	7.4
September	0.0945	0.1294	4.07	12.0	0.0570	0.3607	3.32	10.7
October	0.0114	0.8542	3.26	9.6	0.0544	0.3831	3.17	10.2
November	0.0199	0.7500	2.44	7.2	0.0467	0.4539	2.24	7.2
December	−0.0779	0.2116	2.28	6.7	−0.0683	0.2733	1.98	6.4

[1]Refer to figure 25 for map of sections within the Guadalupe River Basin.

[2]Percentage of the total precipitation within the season or month for the time period specified.

The ratios of streamflow volume to precipitation volume were analyzed as part of this study (fig. 26; table 9). Temporal trends in the ratio of streamflow volume to precipitation volume indicate a change in the way the system responds to precipitation events and possibly explain upward trends in streamflow if the ratios are also upward. Data from the only station with an upward trend in annual streamflow (USGS streamflow-gaging station 08166000 Johnson Creek near Ingram, Texas) also indicated an upward trend in the ratio of streamflow volume to precipitation volume on an annual time step and is in the northwestern part of the basin. However, data from the section of the basin including this station (section 2) did not indicate an upward trend in annual precipitation.

The Kendall's *tau* and *p*-values for trends in two extreme streamflow regimes, annual minimum and annual peak streamflow, were calculated (table 10), and any trends that were indicated for these two streamflow regimes are depicted for the areal extent of the basin (figs. 27–28). None of the data from the stations in section 1 indicated trends in annual minimum streamflow or annual peak streamflow. Data from 6 of the 13 stations in section 2 indicated trends in annual minimum streamflow, with 4 upward and 2 downward trends. Data from 2 of the 13 stations in section 2 indicated downward trends in annual peak streamflow.

Potential Flood Storage Trends

Results of the analyses of the associations between potential flood storage volume and annual streamflow volume and the trends in the ratio of annual streamflow volume to potential flood storage volume for the Guadalupe River Basin are summarized in table 10, and the annual results are illustrated in figures 29 and 30, respectively.

Data from two of the stations in the upper section of the basin indicated positive associations between potential flood storage volume and streamflow volume (fig. 29), meaning that streamflow increased relative to and despite the addition of flood storage. Data from 9 of the 20 stations indicated downward trends in the ratio of streamflow volume to potential flood storage volume; however, without negative associations between potential flood storage volume and streamflow volume or decreasing streamflow volumes over time, this result is not meaningful. Despite the known addition of 2,016,534 acre-ft of potential flood storage between 1849 and 2013 in the subbasins analyzed (USACE, 2019a), streamflow volumes have not decreased in the Guadalupe River Basin.

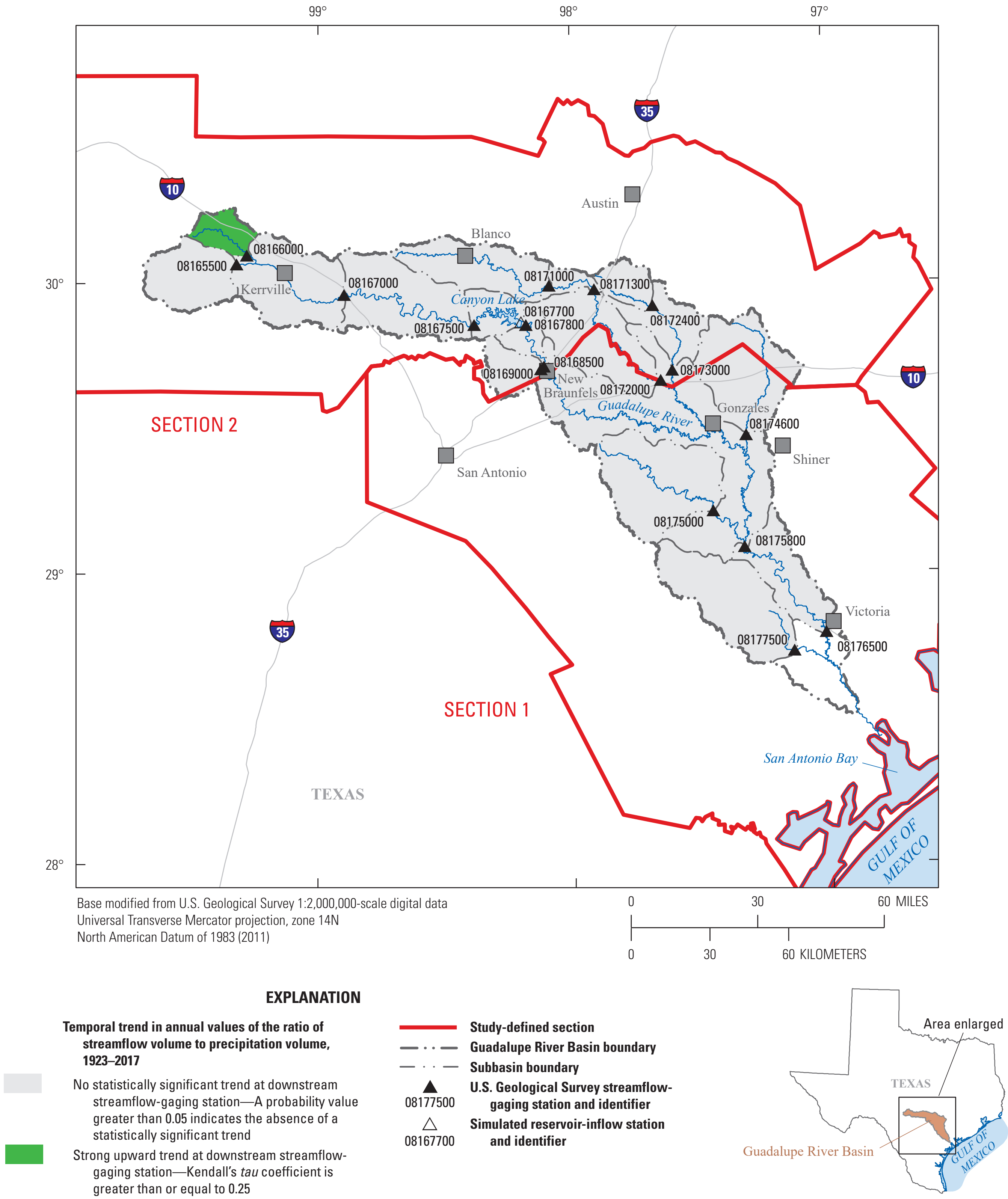

Figure 26. Temporal trends in annual values of the ratio of streamflow volume to precipitation volume at 17 U.S. Geological Survey streamflow-gaging stations and 1 U.S. Army Corps of Engineers simulated reservoir-inflow station in the Guadalupe River Basin, 1923–2017.

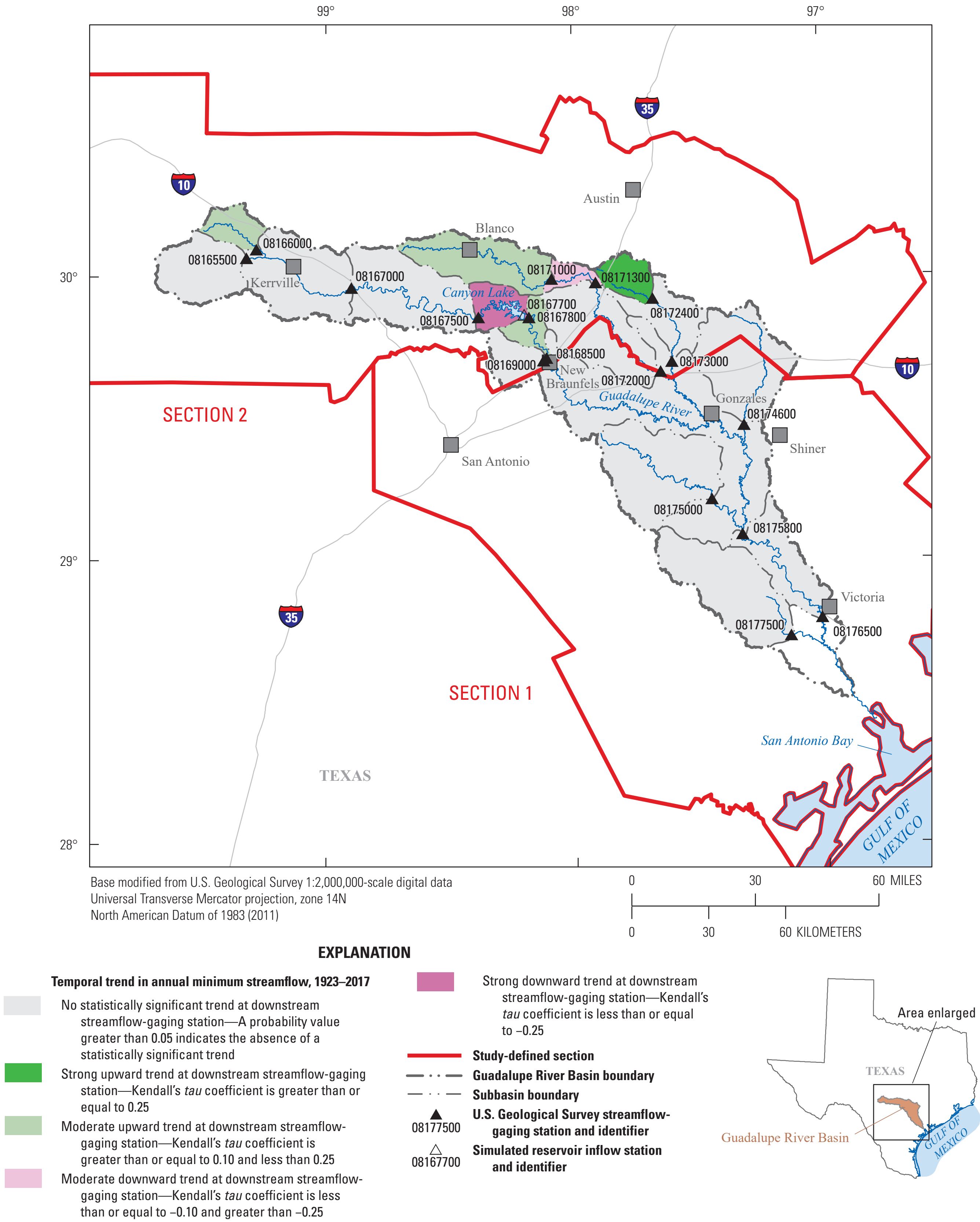

Figure 27. Temporal trends in annual minimum streamflow at 17 U.S. Geological Survey streamflow-gaging stations and 1 U.S. Army Corps of Engineers simulated reservoir-inflow station in the Guadalupe River Basin, 1923–2017.

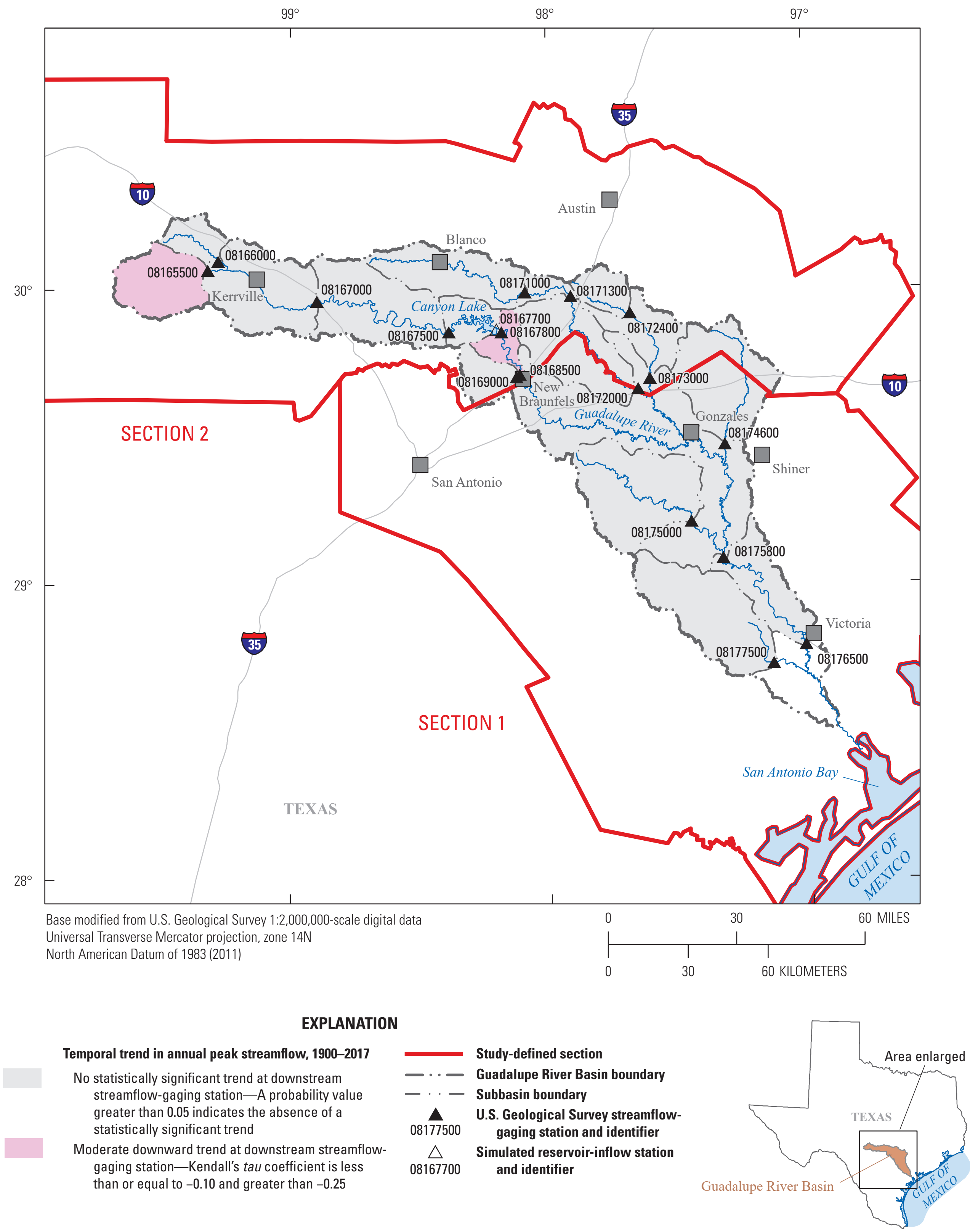

Figure 28. Temporal trends in annual peak streamflow at 17 U.S. Geological Survey streamflow-gaging stations and 1 U.S. Army Corps of Engineers simulated reservoir-inflow station in the Guadalupe River Basin, 1900–2017.

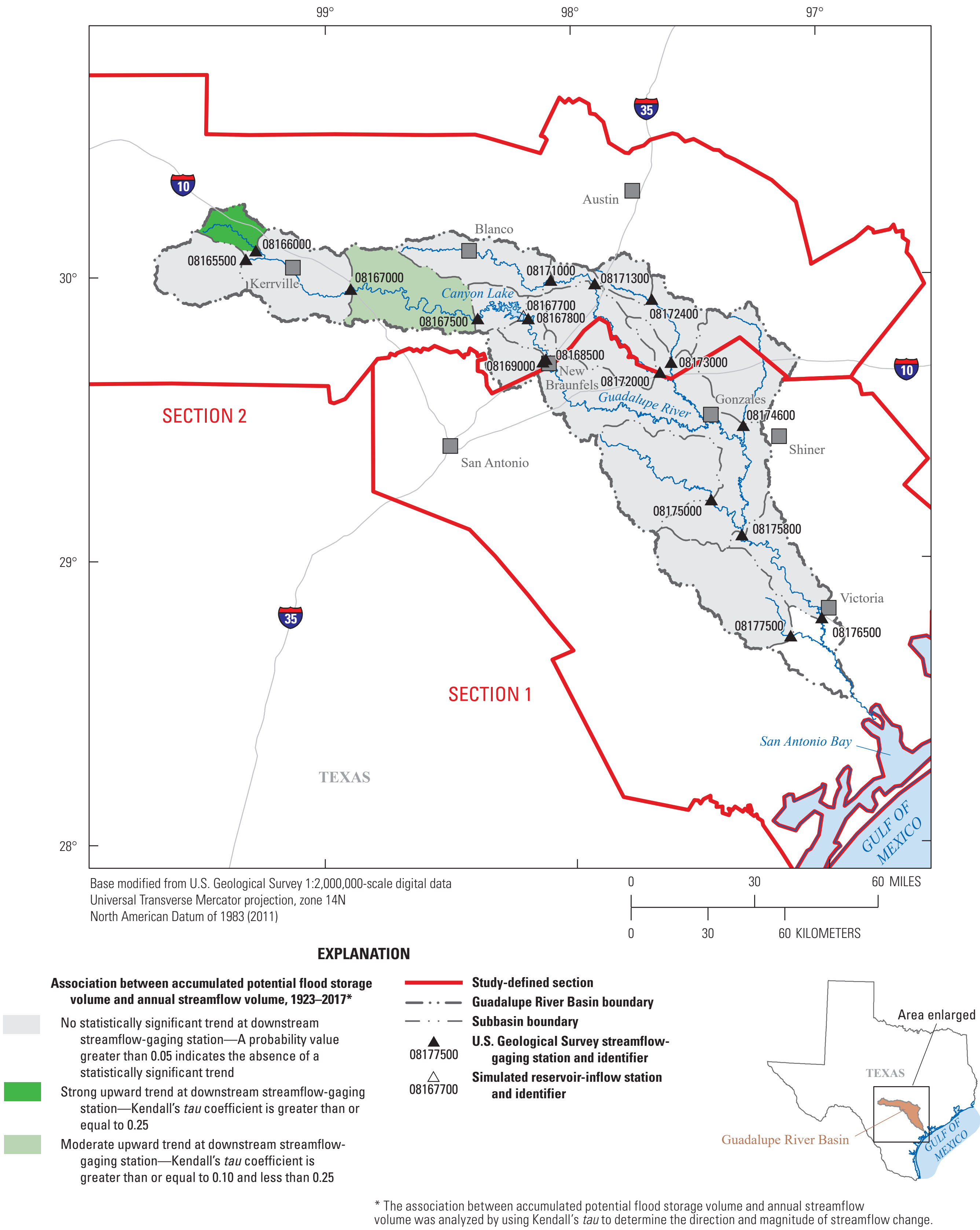

Figure 29. Association between accumulated potential flood storage volume and annual streamflow volume at 17 U.S. Geological Survey streamflow-gaging stations and 1 U.S. Army Corps of Engineers simulated reservoir-inflow station in the Guadalupe River Basin, 1923–2017.

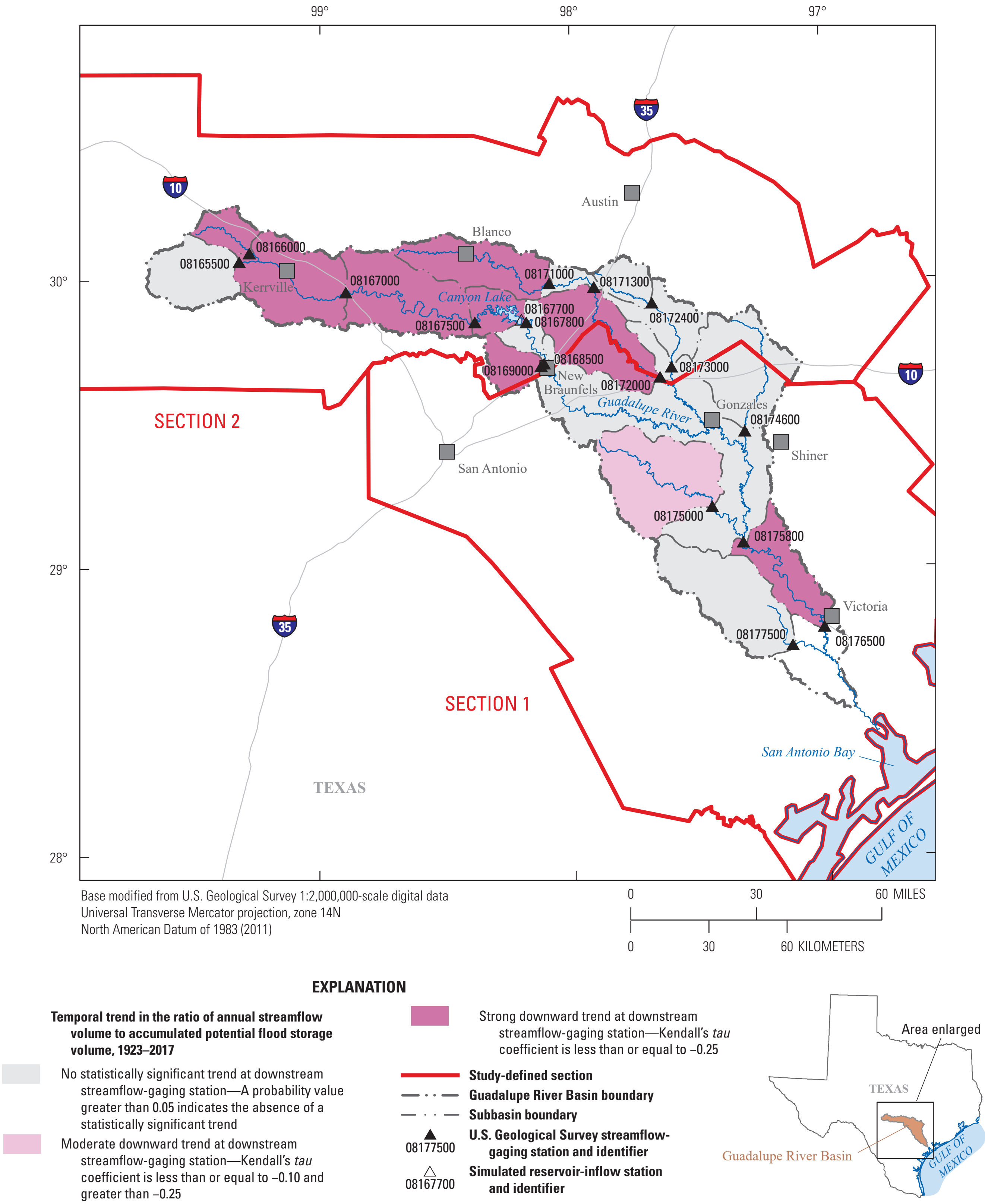

Figure 30. Temporal trends in the ratio of annual streamflow volume to accumulated potential flood storage volume at 17 U.S. Geological Survey streamflow-gaging stations and 1 U.S. Army Corps of Engineers simulated reservoir-inflow station in the Guadalupe River Basin, 1923–2017.

Neches River Basin

The Neches River Basin in east Texas covers 9,937 mi^2 and begins northwest of Tyler, Texas (fig. 31; TWDB, 2019a). Within the Neches River Basin, 17 USGS streamflow-gaging stations and 2 simulated-inflow stations were selected for streamflow trend analyses (table 17). The periods of record for these 19 stations range from 26 to 114 years, with a mean period of record of 65 years. The mean percentage of complete and continuous record was 82 percent. Six of the stations (five USGS and one simulated-inflow) are on the main stem of the Neches River. The most downstream main-stem station, USGS streamflow-gaging station 08041000 Neches River at Evadale, Texas, is about 53 mi upstream from where the river empties into Sabine Lake and has a total drainage area of 7,951 mi^2.

In the Neches River Basin, the associations between precipitation and streamflow were strong for most time steps and were all positive, indicating an increase in streamflow as precipitation increases (table 5). Of the 304 possible associations, 267 were significant.

Precipitation Trends

Results of precipitation trend analyses on an annual time step indicated upward trends in all three sections of the Neches River Basin (table 18). Data from section 1 indicated an upward trend in precipitation during dry years. Results of precipitation trend analyses on a monthly time step indicated eight monthly trends, and all were upward. If precipitation has changed over time in the Neches River Basin from 1900 through 2017, then precipitation amounts have most likely increased throughout the basin based on these results and the results of the precipitation trends within the East Texas and Upper Coast Climate Divisions (table 1).

Possible trends in the sum of precipitation on the day of the annual peak, for different numbers of days before the annual peak streamflow (365, 180, 90, 60, and 30), and for the 5 days before, the day of, and the day after annual peak streamflow for each of the 19 stations in the Neches River Basin are summarized in table 7. Of the 19 stations and 133 possible trends in peak streamflow-related precipitation, 31 were significant, consisting of 28 upward trends and 3 downward trends. Of the upward trends, all but one was in the lower sections of the basin (section 1 and 2).

Streamflow Trends

Temporal trends in streamflow volume on annual, seasonal, and monthly time steps are summarized in table 8. The trends in annual streamflow at the 19 stations within the Neches River Basin are also depicted for the areal extent of the basin (fig. 31). None of the data from streamflow-gaging stations or simulated-inflow stations analyzed in the Neches River Basin indicated annual trends in streamflow despite upward trends in annual precipitation within all three sections of the basin. Trends were indicated during seasonal and monthly time steps, particularly in section 1, and most trends were upward. Of the eight seasonal trends in the Neches River Basin, two were downward and six were upward. Of the 41 monthly trends, 14 were downward and 27 were upward. Downward trends in groundwater levels within the major aquifers with potential to discharge directly to the Neches River (Carrizo-Wilcox and Gulf Coast) did not coincide with annual streamflow trends.

The ratios of streamflow volume to precipitation volume were analyzed as part of this study (fig. 32; table 9). Temporal trends in the ratio of streamflow volume to precipitation volume indicate a change in the way the system responds to precipitation events and possibly explain downward trends in streamflow if the ratios are also downward. The analyses indicated that trends in streamflow and trends in the ratio of streamflow volume to precipitation volume were similar (figs. 31 and 32; tables 8 and 9). Neither analysis indicated any annual trends except for one trend in the ratio of streamflow volume to precipitation volume. The one station with a downward annual trend is the farthest downstream station on the main stem of the Neches River. Many of the seasonal and monthly trends for the station were downward, and they were during seasons and months accounting for most of the streamflow volume for the year (50 to 64 percent).

The Kendall's *tau* and *p*-values for trends in two extreme streamflow regimes, annual minimum and annual peak streamflow, were calculated (table 10), and any trends that were indicated for these two streamflow regimes are depicted for the areal extent of the basin (figs. 33–34). Data from 9 of the 19 stations analyzed in the Neches River Basin indicated upward trends in annual minimum streamflow. Data from one of the simulated-inflow stations indicated a downward trend in annual minimum streamflow into Sam Rayburn Reservoir. Data from two stations indicated downward trends in annual peak streamflow, and one small subbasin had an upward trend in annual peak streamflow.

Potential Flood Storage Trends

Results of the analyses of the associations between potential flood storage volume and annual streamflow volume and the trends in the ratio of annual streamflow volume to potential flood storage volume for the Neches River Basin are summarized in table 10, and the annual results are illustrated in figures 35 and 36, respectively.

Data from the two stations with negative associations between potential flood storage volume and annual streamflow volume also indicated downward trends in the ratio of annual streamflow volume to potential flood storage. However, data from neither of the stations indicated downward trends in annual streamflow. Despite the known addition of 4,839,609 acre-ft of potential flood storage between 1888 and 2008 in the subbasins analyzed (USACE, 2019a), there have not been widespread reductions in streamflow volumes in the Neches River Basin.

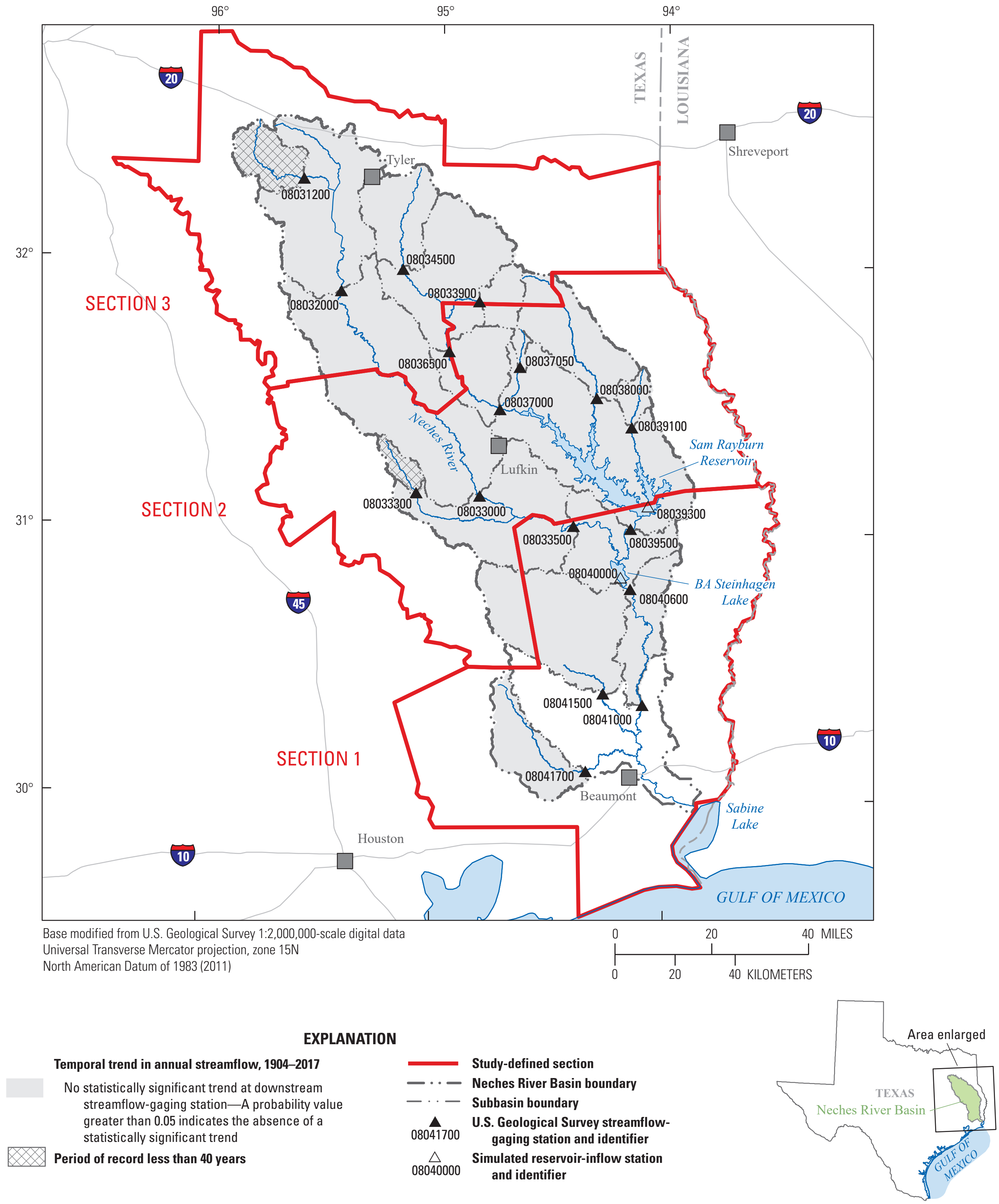

Figure 31. Temporal trends in annual streamflow at 17 U.S. Geological Survey streamflow-gaging stations and 2 U.S. Army Corps of Engineers simulated reservoir-inflow stations in the Neches River Basin, 1904–2017.

Table 17. Summary information for 17 U.S. Geological Survey streamflow-gaging stations and 2 U.S. Army Corps of Engineers simulated reservoir-inflow stations analyzed for trends in the Neches River Basin, 1903–2017.

[mi², square mile]

Section number[1]	Station number, name[2]	Total drainage area (mi²)	Contributing drainage area (mi²)	Period of record by calendar year[3]	Number of years of record	Percentage of record complete
1	08041700, Pine Island Bayou near Sour Lake, Texas	336	336	1967–2017	50	82.2
	08041500, Village Creek near Kountze, Texas	860	860	1924–2017	93	87.5
	08041000, Neches River at Evadale, Texas	7,951	7,951	1904–2017	113	82.6
	08040600, Neches River near Town Bluff, Texas	7,574	7,574	1951–2017	66	85.0
	08040000, B.A. Steinhagen Lake at Town Bluff, Texas	7,573	7,573	1951–2017	66	100
	08039500, Angelina River near Ebenezer, Texas	3,486	3,486	1928–73	45	68.1
	08039300, Sam Rayburn Reservoir near Jasper, Texas	3,449	3,449	1965–2017	52	100
	08033500, Neches River near Rockland, Texas	3,636	3,636	1903–2017	114	100
2	08039100, Ayish Bayou near San Augustine, Texas	89.0	89.0	1959–85	26	100
	08038000, Attoyac Bayou near Chireno, Texas	503	503	1924–85	61	76.1
	08037050, Bayou Lanana at Nacogdoches, Texas	31.3	31.3	1964–2017	53	55.6
	08037000, Angelina River near Lufkin, Texas	1,600	1,600	1923–79	56	91.4
	08033300, Piney Creek near Groveton, Texas	79.0	79.0	1961–89	28	100
	08033000, Neches River near Diboll, Texas	2,724	2,724	1923–2017	94	54.9
3	08036500, Angelina River near Alto, Texas	1,276	1,276	1940–2017	77	76.8
	08034500, Mud Creek near Jacksonville, Texas	376	376	1939–2017	78	72.3
	08033900, East Fork Angelina River near Cushing, Texas	158	158	1964–2017	53	51.9
	08032000, Neches River near Neches, Texas	1,145	1,145	1939–2017	78	82.3
	08031200, Kickapoo Creek near Brownsboro, Texas	232	232	1962–89	27	100

[1]Refer to figure 31 for map of sections within the Neches River Basin.

[2]Shaded cells are U.S. Geological Survey streamflow-gaging stations with measured streamflow data (U.S. Geological Survey, 2019b), and cells that are not shaded are lake and reservoir stations with simulated inflow data provided by the U.S. Army Corps of Engineers (2019b).

[3]Period of record includes the calendar year when daily mean streamflow data collection began to the end of 2017 or when data collection ended (if applicable).

Table 18. Summary of annual, seasonal, and monthly precipitation trends for the period 1900–2017 within three sections of the Neches River Basin.

[wet, years with precipitation totals above long-term mean; dry, years with precipitation totals below long-term mean; NA, not applicable; season 1, includes November, December, January, and February; season 2, includes March, April, May, and June; season 3, includes July, August, September, and October; *p*-value, probability value (considered statistically significant if less than 0.05); green shaded cells indicate statistically significant upward trends]

Time step	Neches River Basin section number[1]											
	Section 1 1900–2017				Section 2 1900–2017				Section 3 1900–2017			
	Kendall's *tau*	*p*-value	Mean precipitation (inches)	Percentage[2]	Kendall's *tau*	*p*-value	Mean precipitation (inches)	Percentage[2]	Kendall's *tau*	*p*-value	Mean precipitation (inches)	Percentage[2]
Annual	0.1945	0.0018	55.06	100	0.1312	0.0362	48.61	100	0.1279	0.0421	44.31	100
Annual (wet)	0.1247	0.1729	NA	NA	0.0066	0.9454	NA	NA	0.1360	0.1370	NA	NA
Annual (dry)	0.2690	0.0022	NA	NA	0.0234	0.8046	NA	NA	0.0894	0.3202	NA	NA
Season 1	0.1144	0.0679	17.91	32.5	0.0800	0.2017	17.28	35.5	0.0908	0.1495	15.27	34.5
Season 2	0.0656	0.2931	18.23	33.1	0.0127	0.8413	17.54	36.1	0.0482	0.4399	16.71	37.7
Season 3	0.1606	0.0100	18.92	34.4	0.1134	0.0689	13.80	28.4	0.0765	0.2203	12.33	27.8
January	0.1881	0.0026	4.32	7.8	0.0975	0.1194	4.27	8.8	0.0810	0.1959	3.61	8.1
February	0.0870	0.1628	4.17	7.6	−0.0196	0.7540	3.85	7.9	0.0764	0.2203	3.48	7.9
March	0.1393	0.0254	3.87	7.0	0.0369	0.5559	4.02	8.3	0.0628	0.3139	3.92	8.9
April	−0.0168	0.7873	4.18	7.6	−0.1164	0.0631	4.41	9.1	−0.1188	0.0565	4.33	9.8
May	0.0354	0.5704	5.10	9.3	−0.0109	0.8615	5.04	10.4	0.0278	0.6552	4.72	10.6
June	0.1347	0.0307	5.08	9.2	0.1386	0.0262	4.06	8.4	0.1478	0.0177	3.74	8.4
July	0.0281	0.6518	4.90	8.9	−0.0625	0.3161	3.54	7.3	−0.0389	0.5330	2.84	6.4
August	0.1073	0.0852	4.80	8.7	0.0602	0.3344	3.15	6.5	0.0654	0.2941	2.62	5.9
September	0.1869	0.0027	4.53	8.2	0.1718	0.0058	3.44	7.1	0.0764	0.2203	3.09	7.0
October	0.1183	0.0577	4.69	8.5	0.0677	0.2774	3.67	7.6	0.1055	0.0904	3.79	8.6
November	0.1403	0.0244	4.48	8.1	0.0745	0.2319	4.35	9.0	0.0778	0.2117	3.90	8.8
December	0.0335	0.5911	4.94	9.0	0.0065	0.9166	4.80	9.9	0.0129	0.8360	4.28	9.7

[1]Refer to figure 31 for map of sections within the Neches River Basin.

[2]Percentage of the total precipitation within the season or month for the time period specified.

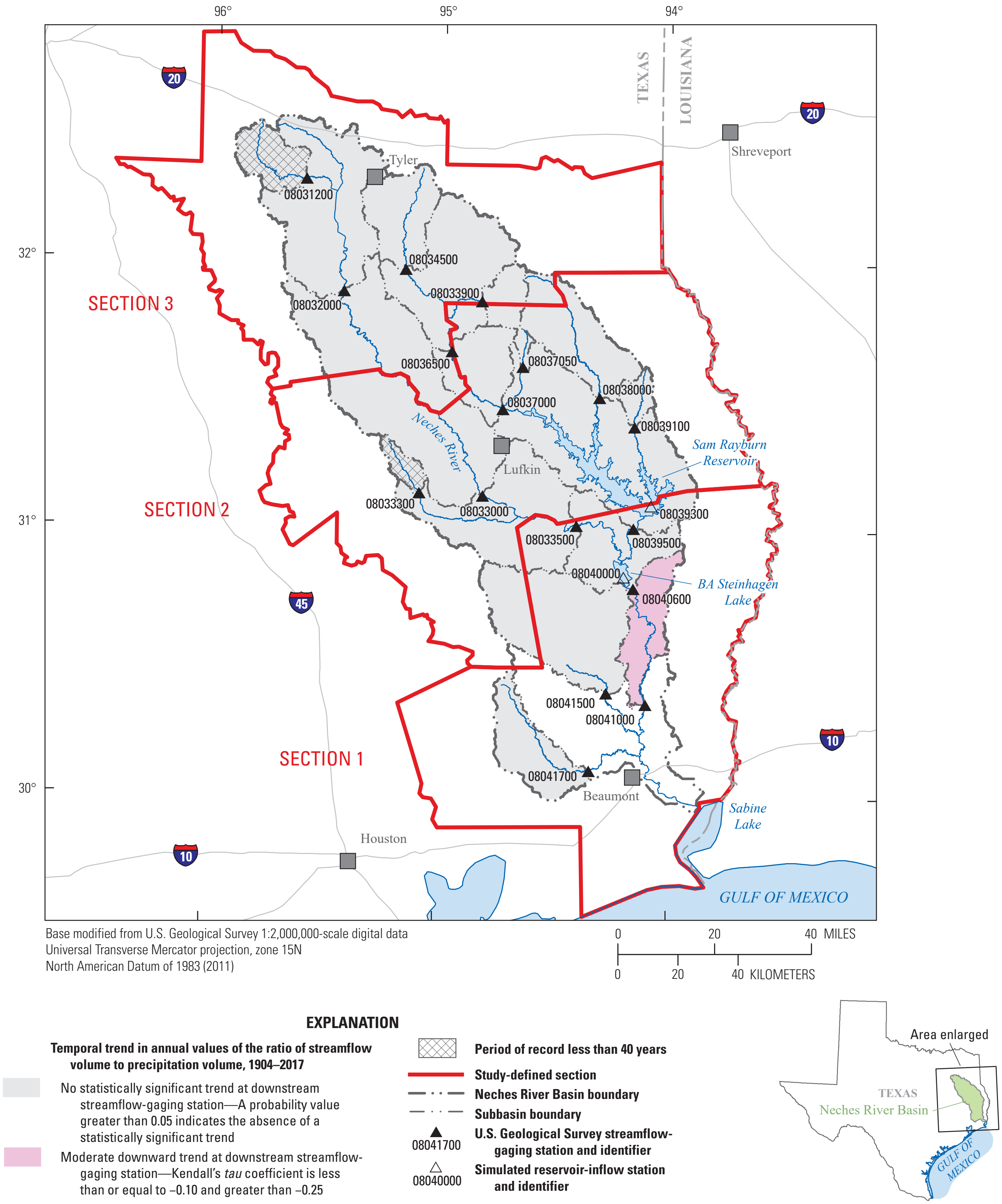

Figure 32. Temporal trends in annual values of the ratio of streamflow volume to precipitation volume at 17 U.S. Geological Survey streamflow-gaging stations and 2 U.S. Army Corps of Engineers simulated reservoir-inflow stations in the Neches River Basin, 1904–2017.

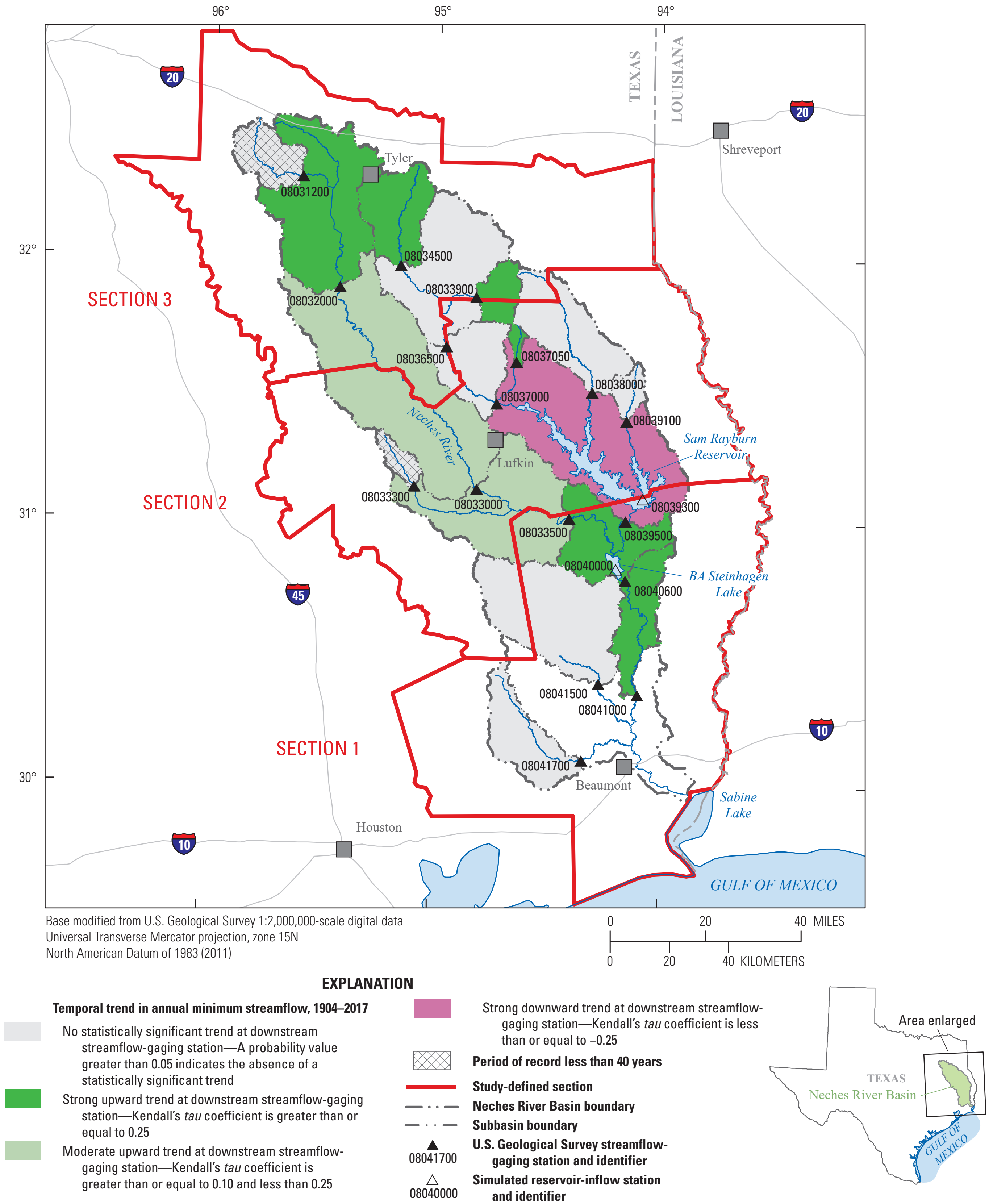

Figure 33. Temporal trends in annual minimum streamflow at 17 U.S. Geological Survey streamflow-gaging stations and 2 U.S. Army Corps of Engineers simulated reservoir-inflow stations in the Neches River Basin, 1904–2017.

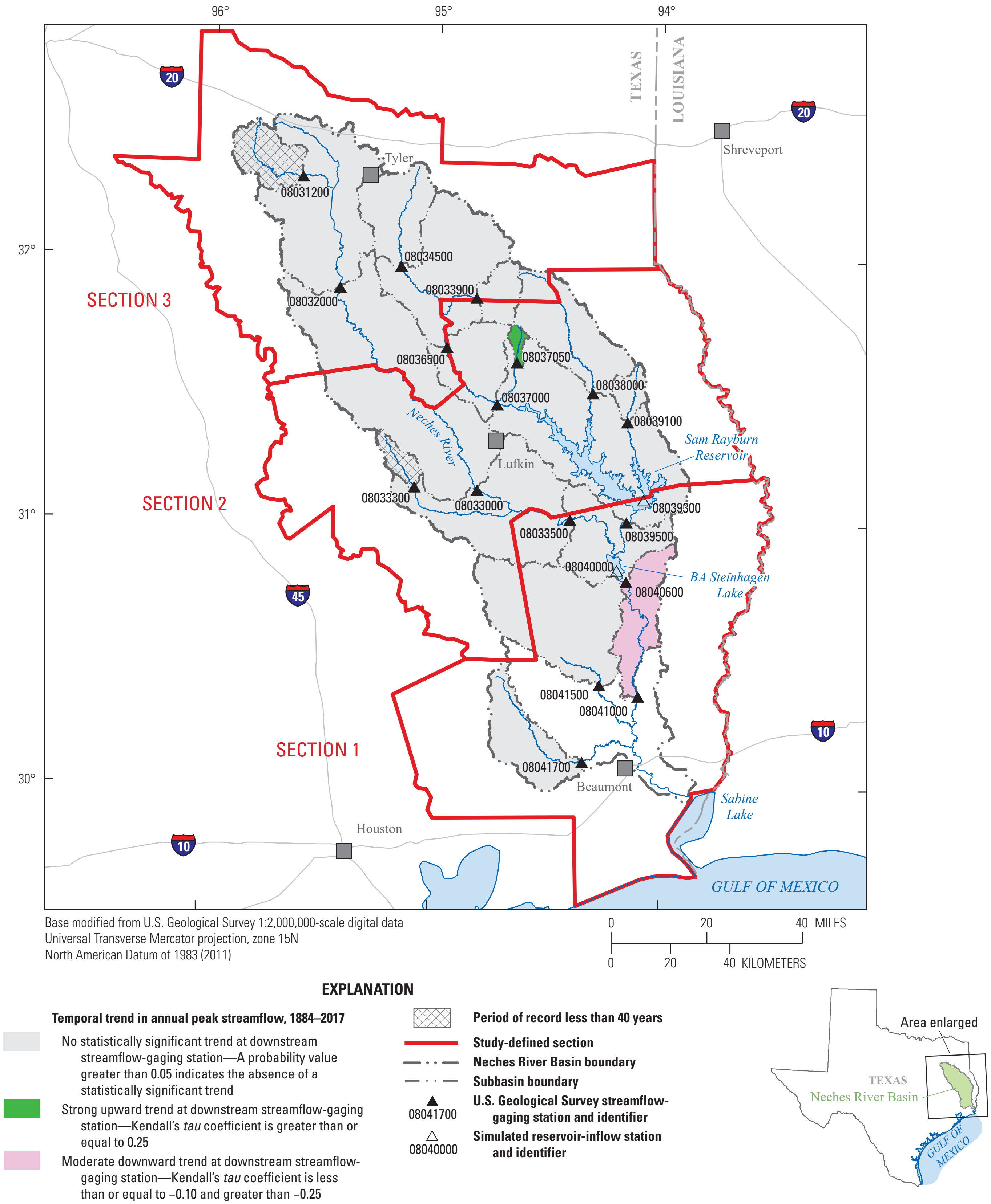

Figure 34. Temporal trends in annual peak streamflow at 17 U.S. Geological Survey streamflow-gaging stations and 2 U.S. Army Corps of Engineers simulated reservoir-inflow stations in the Neches River Basin, 1884–2017.

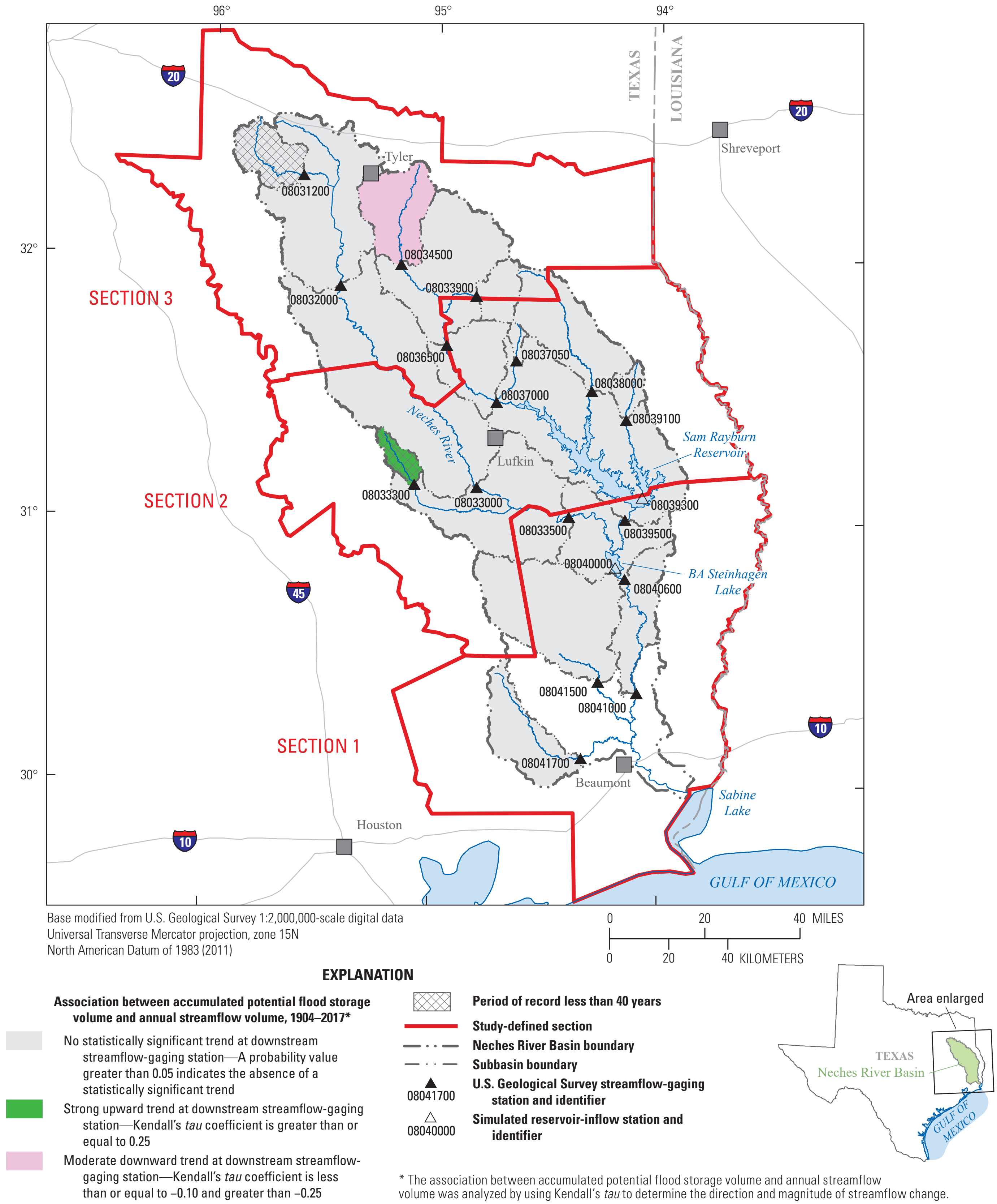

Figure 35. Association between accumulated potential flood storage volume and annual streamflow volume at 17 U.S. Geological Survey streamflow-gaging stations and 2 U.S. Army Corps of Engineers simulated reservoir-inflow stations in the Neches River Basin, 1904–2017.

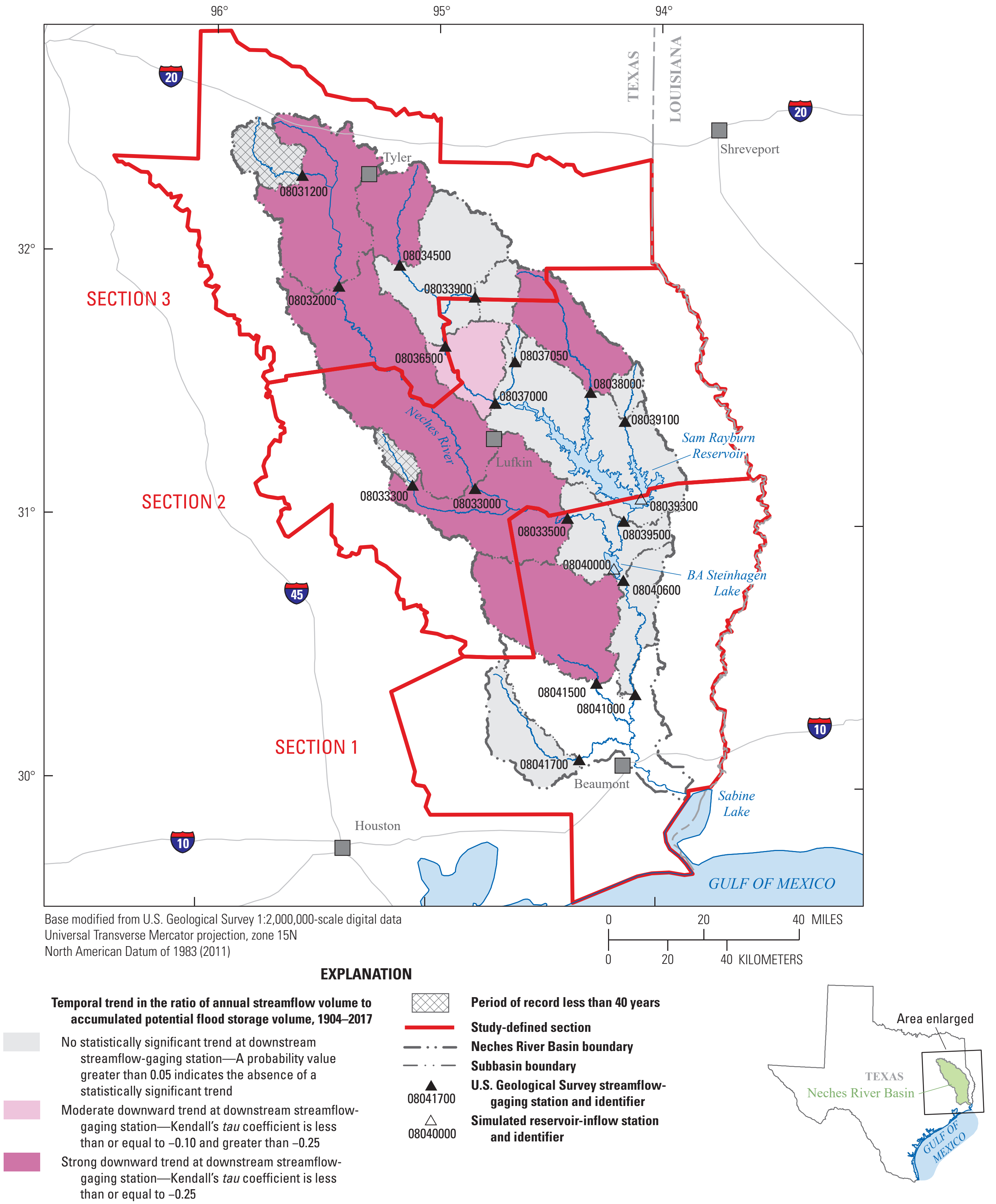

Figure 36. Temporal trends in the ratio of annual streamflow volume to accumulated potential flood storage volume at 17 U.S. Geological Survey streamflow-gaging stations and 2 U.S. Army Corps of Engineers simulated reservoir-inflow stations in the Neches River Basin, 1904–2017.

Sulphur River Basin

The Sulphur River Basin covers 3,767 mi^2 in northeast Texas and the southwest corner of Arkansas (fig. 37; TWDB, 2019a). Within the Sulphur River Basin, four USGS streamflow-gaging stations and two simulated-inflow stations were selected for streamflow trend analyses (table 19). The periods of record for these six stations range from 26 to 75 years, with a mean period of record of 60 years. The percentage of complete and continuous record was 100 percent for all stations. Two of the stations (one USGS and one simulated-inflow) are on the main stem of the Sulphur River downstream from where the North Sulphur River and the South Sulphur River join, northwest of Mount Vernon, Texas. The most downstream station, USGS streamflow-gaging station 07344200 Wright Patman Lake near Texarkana, Texas, is on the main stem of the Sulphur River about 38 mi upstream from its confluence with the Red River and has a total drainage area of 3,443 mi^2.

In the Sulphur River Basin, the associations between precipitation and streamflow were strong for all time steps and were all positive, indicating an increase in streamflow as precipitation increases (table 5).

Precipitation Trends

Results of precipitation trend analyses on an annual time step indicated a moderate upward trend in the Sulphur River Basin (table 20). Data from one season with a mean of about 31 percent of the total precipitation for the basin indicated a moderate upward trend. None of the data from individual months indicated trends.

Possible trends in the sum of precipitation on the day of the annual peak, for different numbers of days before the annual peak streamflow (365, 180, 90, 60, and 30), and for the 5 days before, the day of, and the day after annual peak streamflow for each of the six stations in the Sulphur River Basin are summarized in table 7. Of the 6 stations and 42 possible trends in peak streamflow-related precipitation, 8 trends were significant, consisting of 6 upward trends and 2 downward trends.

Streamflow Trends

Temporal trends in streamflow volume on annual, seasonal, and monthly time steps are summarized in table 8. The trends in annual streamflow at the six stations within the Sulphur River Basin are also depicted for the areal extent of the basin (fig. 37). Of the six possible annual trends, only the simulated inflow data to Jim Chapman Lake indicated a trend, which was downward (table 8). The two seasonal trends were both downward. Of the seven monthly trends, one was upward and six were downward. Downward trends in groundwater levels within the major aquifer with potential to discharge directly to the Sulphur River (Carrizo-Wilcox) did not coincide with annual streamflow trends.

The ratios of streamflow volume to precipitation volume were analyzed as part of this study (fig. 38; table 9). Temporal trends in the ratio of streamflow volume to precipitation volume indicate a change in the way the system responds to precipitation events and possibly explain downward trends in streamflow if the ratios are also downward. Data from two of the six stations indicated downward trends on an annual time step in the ratio of streamflow volume to precipitation volume, and these stations accounted for most of the seasonal and monthly trends: one each for the seasonal time steps and four each for the monthly time steps. Annually and seasonally, they accounted for 100 percent of the trends, and monthly, they accounted for 67 percent of the trends.

The Kendall's *tau* and *p*-values for trends in two extreme streamflow regimes, annual minimum and annual peak streamflow, were calculated (table 10), and any trends that were indicated for these two streamflow regimes are depicted for the areal extent of the basin (figs. 39–40). Data from three of the six stations in the Sulphur River Basin indicated upward trends in annual minimum streamflow, and data from one of the six stations indicated a downward trend in annual peak streamflow. One station with a downward trend in annual peak streamflow also had an upward trend in annual minimum streamflow, is on the South Sulphur River, and monitors the releases from Jim Chapman Lake. The downward trend in annual peak streamflow and the upward trend in annual minimum streamflow from the station monitoring the releases from Jim Chapman Lake are not depicted on figures 39 and 40 because in cases where a USGS streamflow-gaging station is immediately downstream from a simulated-inflow station, the simulated-inflow station takes precedence in visualization of any trends.

Potential Flood Storage Trends

Results of the analyses of the associations between potential flood storage volume and annual streamflow volume and the trends in the ratio of annual streamflow volume to potential flood storage volume for the Sulphur River Basin are summarized in table 10, and the annual results are illustrated in figures 41 and 42, respectively.

There were no associations between potential flood storage volume and streamflow volume. Data from five of the six stations in the basin indicated downward trends in the ratio of streamflow volume to potential flood storage volume; however, without negative associations between potential flood storage volume and streamflow volume or decreasing streamflow volumes over time, this result is not meaningful. Despite the known addition of 6,933,361 acre-ft of potential flood storage between 1904 and 2006 in the subbasins analyzed (USACE, 2019a), streamflow volumes have not decreased in the Sulphur River Basin.

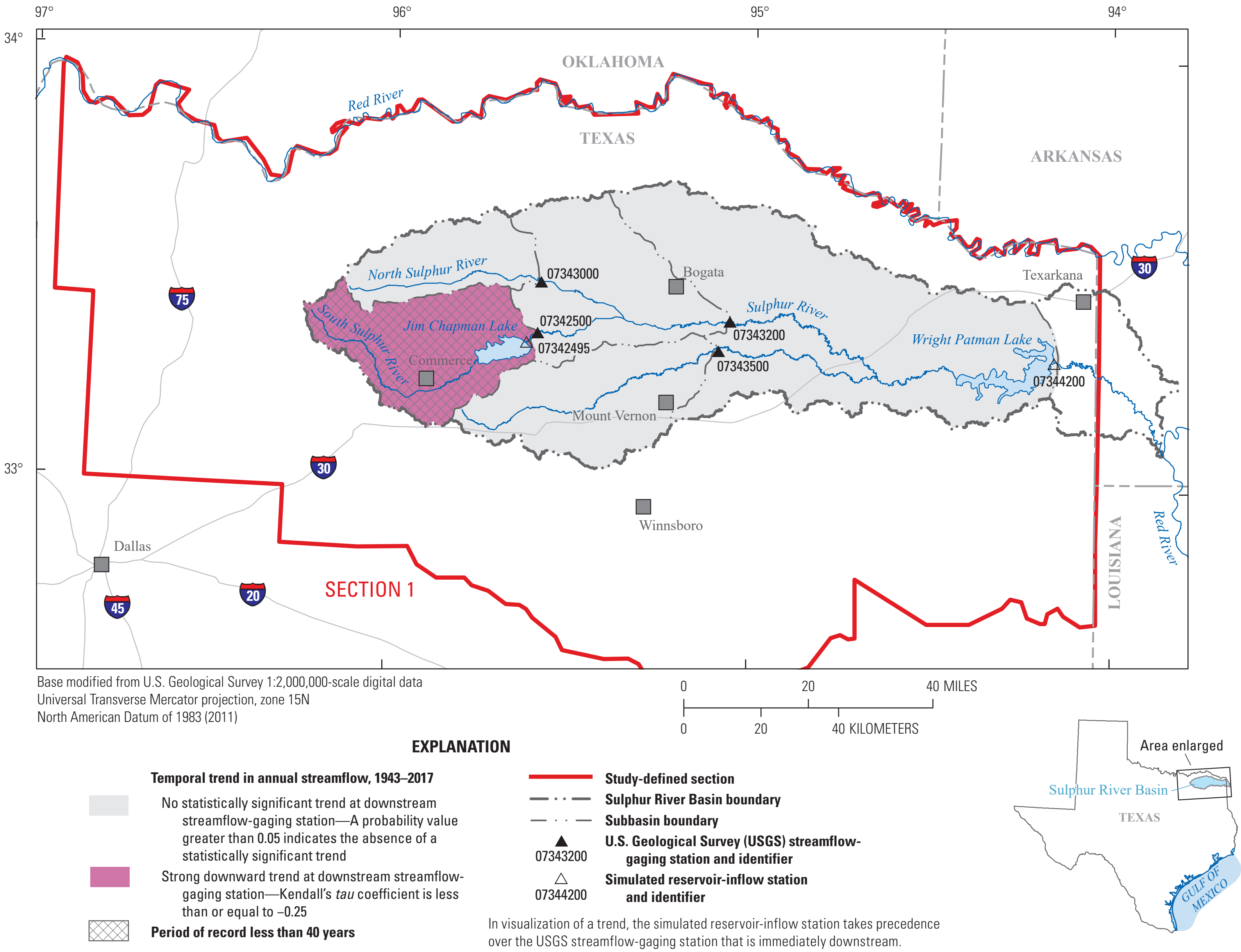

Figure 37. Temporal trends in annual streamflow at four U.S. Geological Survey streamflow-gaging stations and two U.S. Army Corps of Engineers simulated reservoir-inflow stations in the Sulphur River Basin, 1943–2017.

Table 19. Summary information for four U.S. Geological Survey streamflow-gaging stations and two U.S. Army Corps of Engineers simulated reservoir-inflow stations analyzed for trends in the Sulphur River Basin, 1942–2017.

[mi^2, square mile]

Section number[1]	Station number, name[2]	Total drainage area (mi^2)	Contributing drainage area (mi^2)	Period of record by calendar year[3]	Number of years of record	Percentage of record complete
1	07344200, Wright Patman Lake near Texarkana, Texas	3,443	3,443	1956–2017	61	100
	07343500, White Oak Creek near Talco, Texas	494	494	1949–2017	68	100
	07343200, Sulphur River near Talco, Texas	1,365	1,365	1956–2017	61	100
	07343000, North Sulphur River near Cooper, Texas	276	276	1949–2017	68	100
	07342500, South Sulphur River near Cooper, Texas	527	527	1942–2017	75	100
	07342495, Jim L. Chapman Lake near Cooper, Texas	479	479	1991–2017	26	100

[1]Refer to figure 37 for map of the Sulphur River Basin.

[2]Shaded cells are U.S. Geological Survey streamflow-gaging stations with measured streamflow data (U.S. Geological Survey, 2019b), and cells that are not shaded are lake and reservoir stations with simulated inflow data provided by the U.S. Army Corps of Engineers (2019b).

[3]Period of record includes the calendar year when daily mean streamflow data collection began to the end of 2017.

Table 20. Summary of annual, seasonal, and monthly precipitation trends for the period 1900–2017 within the Sulphur River Basin.

[wet, years with precipitation totals above long-term mean; dry, years with precipitation totals below long-term mean; NA, not applicable; season 1, includes November, December, January, and February; season 2, includes March, April, May, and June; season 3, includes July, August, September, and October; *p*-value, probability value (considered statistically significant if less than 0.05); green shaded cells indicate statistically significant upward trends]

Time step	Sulphur River Basin[1]			
	Kendall's *tau*	*p*-value	Mean precipitation (inches)	Percentage[2]
Annual	0.1439	0.0210	43.31	100
Annual (wet)	0.0415	0.6407	NA	NA
Annual (dry)	0.0063	0.9506	NA	NA
Season 1	0.1551	0.0133	13.26	30.6
Season 2	0.0814	0.1919	17.19	39.7
Season 3	0.0497	0.4263	12.86	29.7
January	0.1058	0.0899	2.95	6.8
February	0.1071	0.0861	3.15	7.3
March	0.0981	0.1159	3.83	8.8
April	−0.0823	0.1872	4.53	10.5
May	0.0426	0.4956	5.08	11.7
June	0.0893	0.1526	3.75	8.7
July	−0.0672	0.2825	3.18	7.3
August	−0.0531	0.3959	2.61	6.0
September	0.1021	0.1015	3.29	7.6
October	0.1047	0.0935	3.78	8.7
November	0.1213	0.0518	3.52	8.1
December	0.0902	0.1486	3.64	8.4

[1]Refer to figure 37 for map of the Sulphur River Basin.

[2]Percentage of the total precipitation within the season or month for the time period specified.

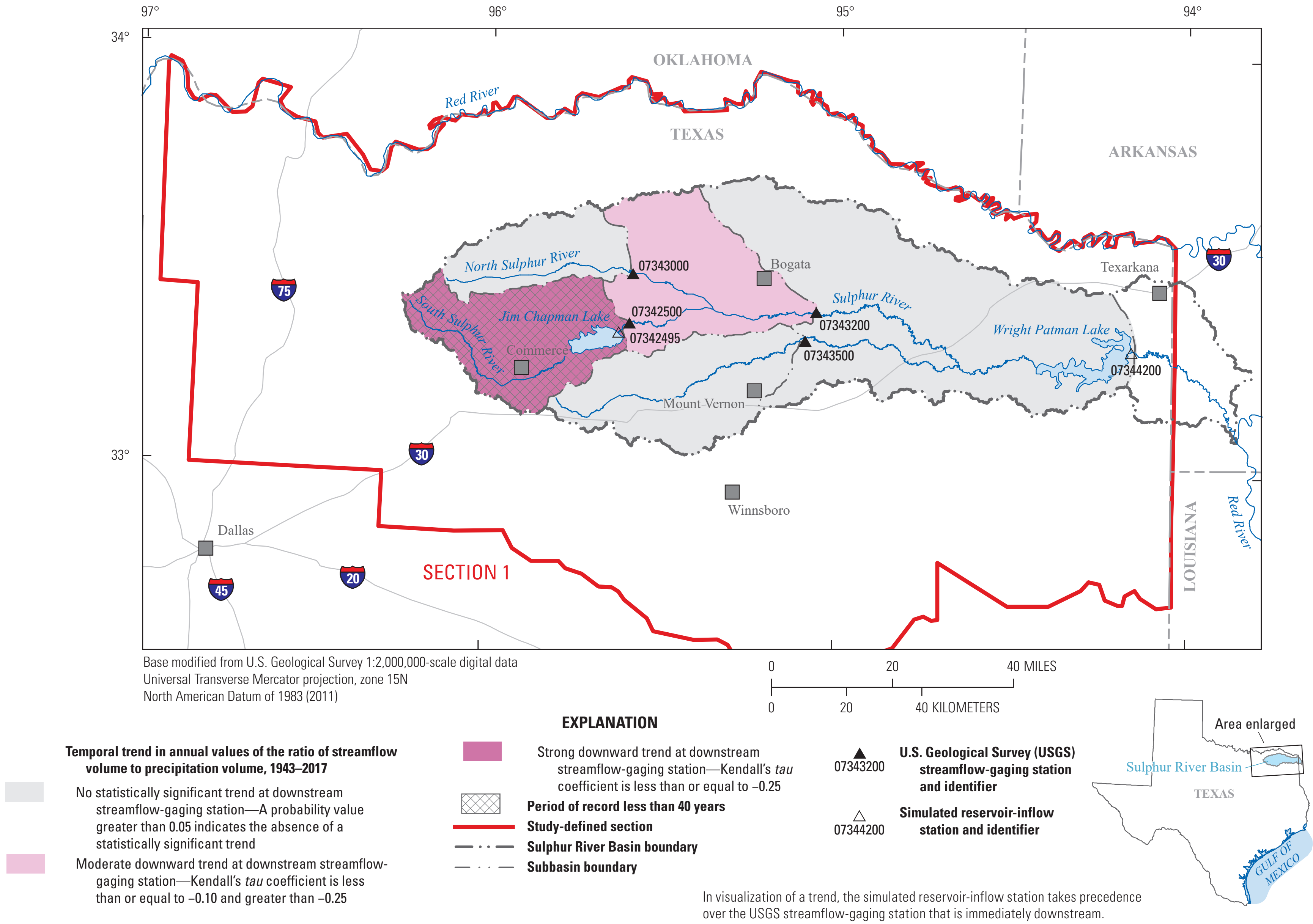

Figure 38. Temporal trends in annual values of the ratio of streamflow volume to precipitation volume at four U.S. Geological Survey streamflow-gaging stations and two U.S. Army Corps of Engineers simulated reservoir-inflow stations in the Sulphur River Basin, 1943–2017.

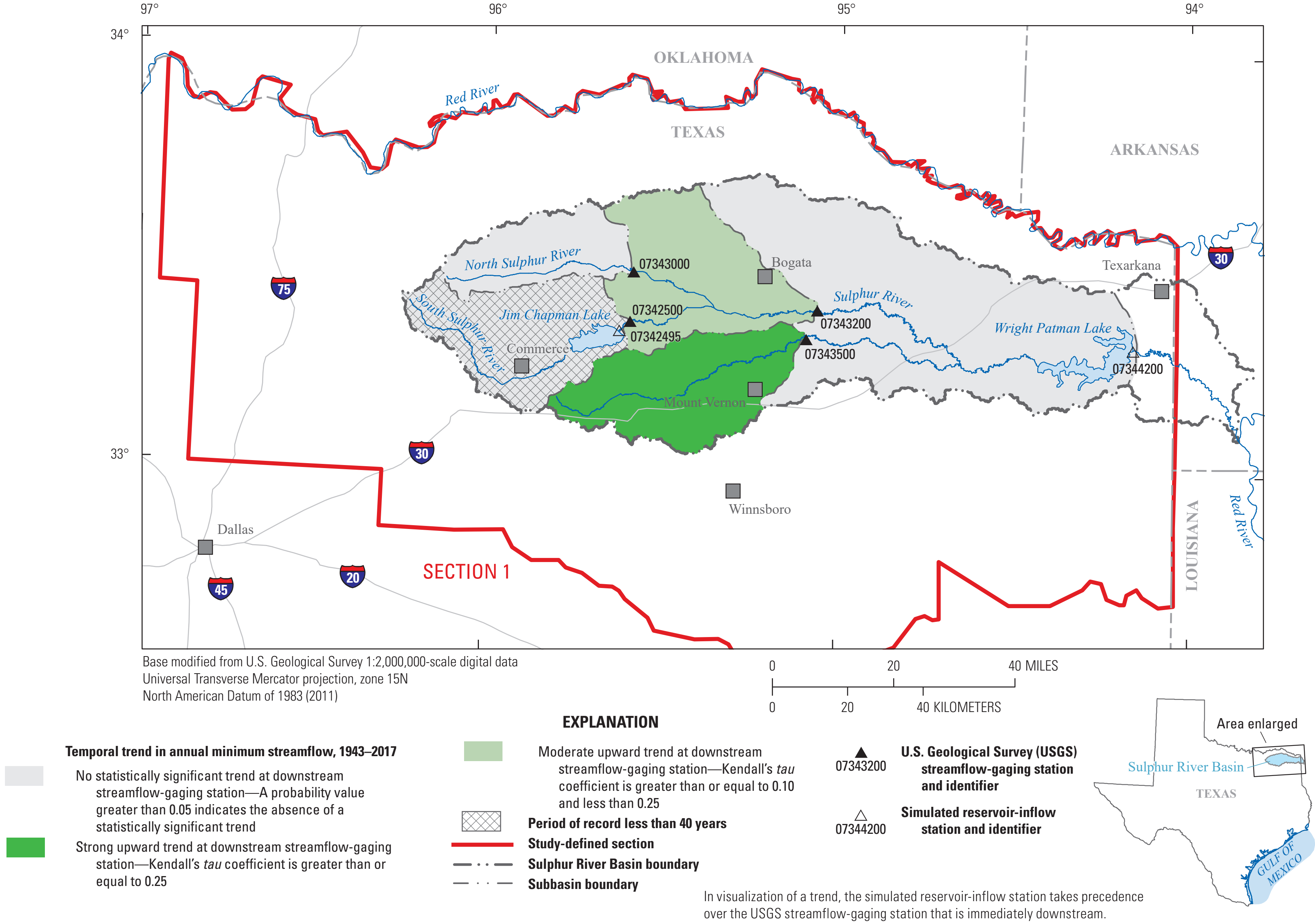

Figure 39. Temporal trends in annual minimum streamflow at four U.S. Geological Survey streamflow-gaging stations and two U.S. Army Corps of Engineers simulated reservoir-inflow stations in the Sulphur River Basin, 1943–2017.

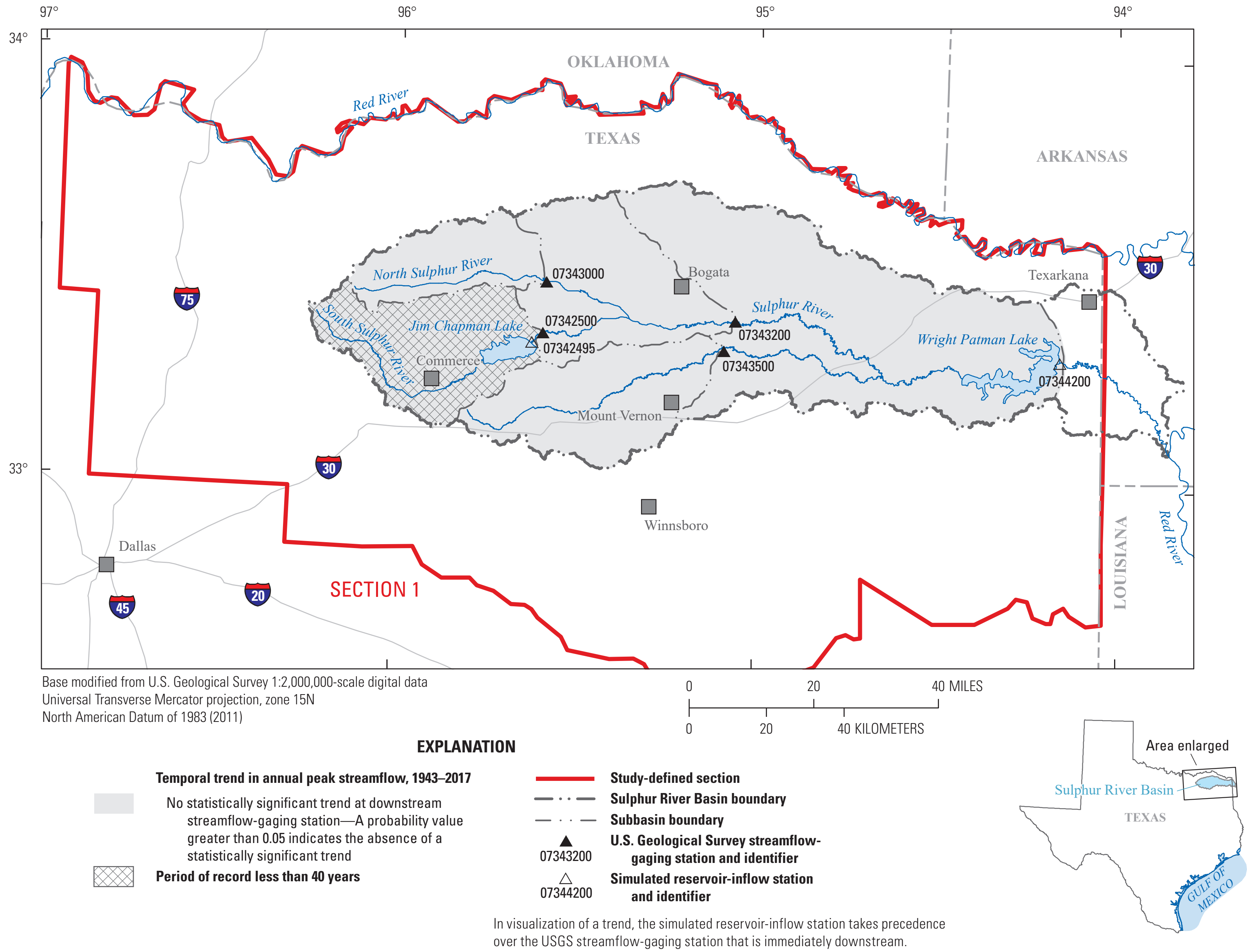

Figure 40. Temporal trends in annual peak streamflow at four U.S. Geological Survey streamflow-gaging stations and two U.S. Army Corps of Engineers simulated reservoir-inflow stations in the Sulphur River Basin, 1943–2017.

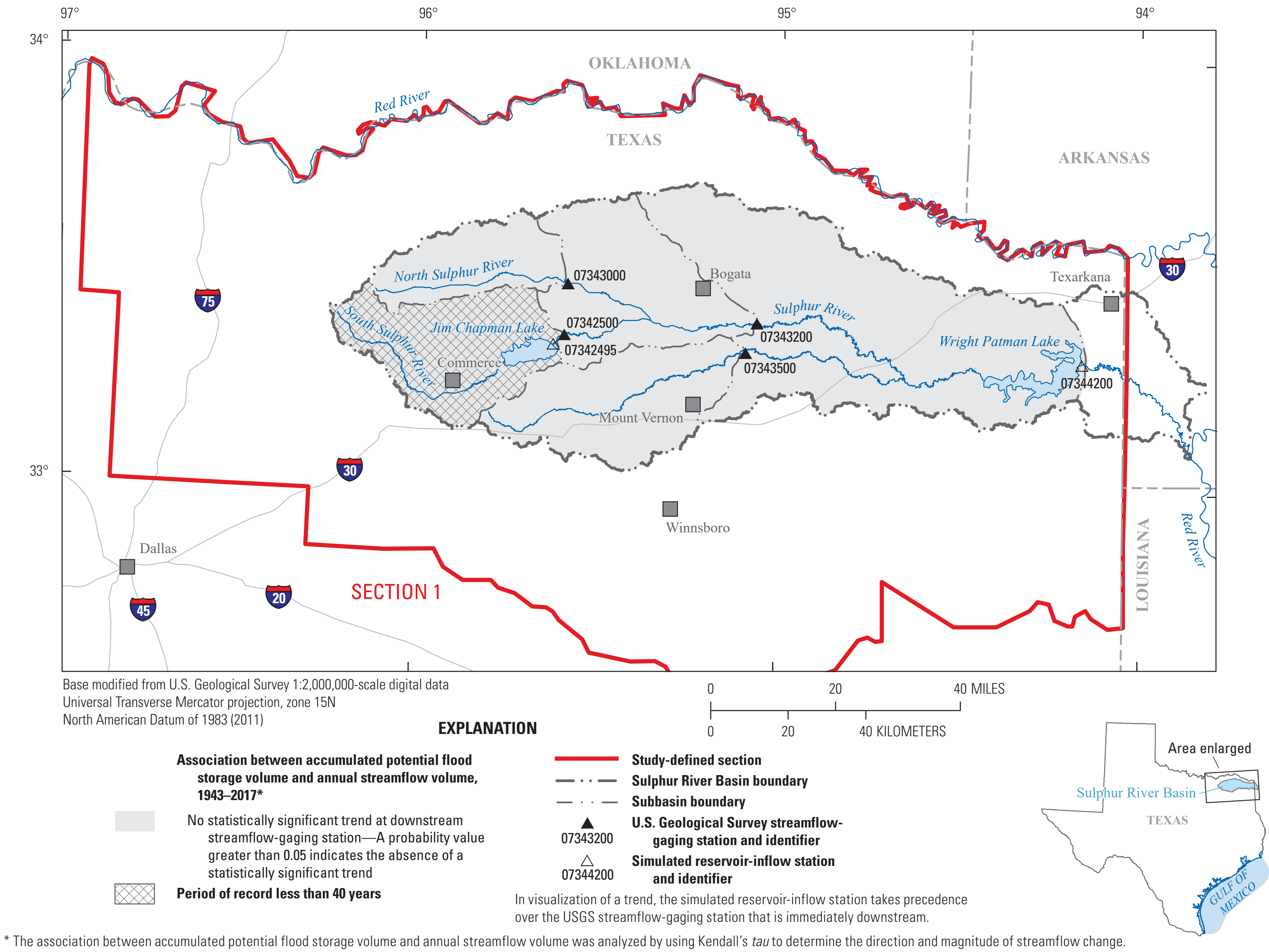

Figure 41. Association between accumulated potential flood storage volume and annual streamflow volume at four U.S. Geological Survey streamflow-gaging stations and two U.S. Army Corps of Engineers simulated reservoir-inflow stations in the Sulphur River Basin, 1943–2017.

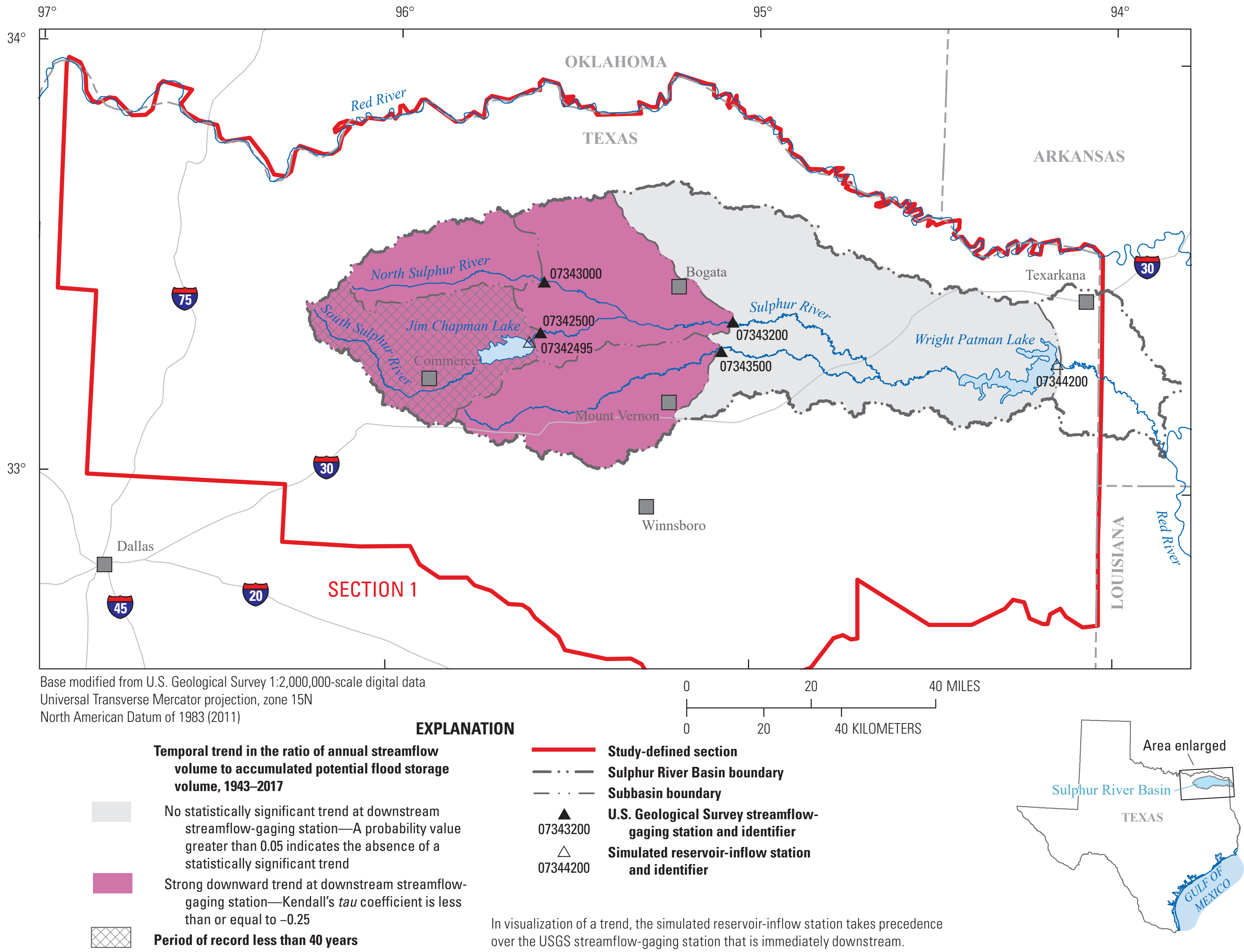

Figure 42. Temporal trends in the ratio of annual streamflow volume to accumulated potential flood storage volume at four U.S. Geological Survey streamflow-gaging stations and two U.S. Army Corps of Engineers simulated reservoir-inflow stations in the Sulphur River Basin, 1943–2017.

Trinity River Basin

The Trinity River Basin covers 17,913 mi^2 and begins in north-central Texas west of the Dallas-Fort Worth metroplex (fig. 43; TWDB, 2019a). Within the Trinity River Basin, 24 USGS streamflow-gaging stations and 14 simulated-inflow stations were selected for streamflow trend analyses (table 21). Two of the 38 stations (08067000 and 08045850; table 21) were only analyzed for trends in annual peak streamflow and precipitation associated with annual peak streamflow because of the low percentage of complete daily streamflow records (30 and 44 percent complete). The periods of record for the 38 stations within the Trinity River Basin range from 22 to 114 years, with a mean period of record of 60 years. The mean percentage of complete and continuous record was 95 percent. Ten of the stations (all USGS) are on the main stem of the Trinity River downstream from where the West Fork Trinity River and the Elm Fork Trinity River join west of Dallas, Texas. The most downstream station, USGS streamflow-gaging station 08067000 Trinity River at Liberty, Texas, is on the main stem of the Trinity River about 38 mi upstream from where it empties into Trinity Bay and has a total drainage area of 17,468 mi^2.

In the Trinity River Basin, the associations between precipitation and streamflow were strong for most time steps and were all positive, indicating an increase in streamflow as precipitation increases (table 5). Of the 576 possible associations, 519 were significant.

Precipitation Trends

Results of precipitation trend analyses on an annual time step indicated upward trends in three of the five sections (sections 1, 3, and 5) of the Trinity River Basin (table 22). Data from sections 4 and 5 indicated upward trends in precipitation during wet and dry years, respectively. Within the 5 sections, data from 5 of the 15 seasons indicated upward trends in precipitation. Results of precipitation trend analyses on a monthly time step indicated 13 monthly trends with 12 upward and 1 downward.

Possible trends in the sum of precipitation on the day of the annual peak, for different numbers of days before the annual peak streamflow (365, 180, 90, 60, and 30), and for the 5 days before, the day of, and the day after annual peak streamflow for each of the 38 stations in the Trinity River Basin are summarized in table 7. Of the 38 stations and 266 possible trends in peak streamflow-related precipitation, 30 trends were significant, consisting of 21 upward trends and 9 downward trends. Of the 21 upward trends, 12 were in the lower section of the basin (section 1).

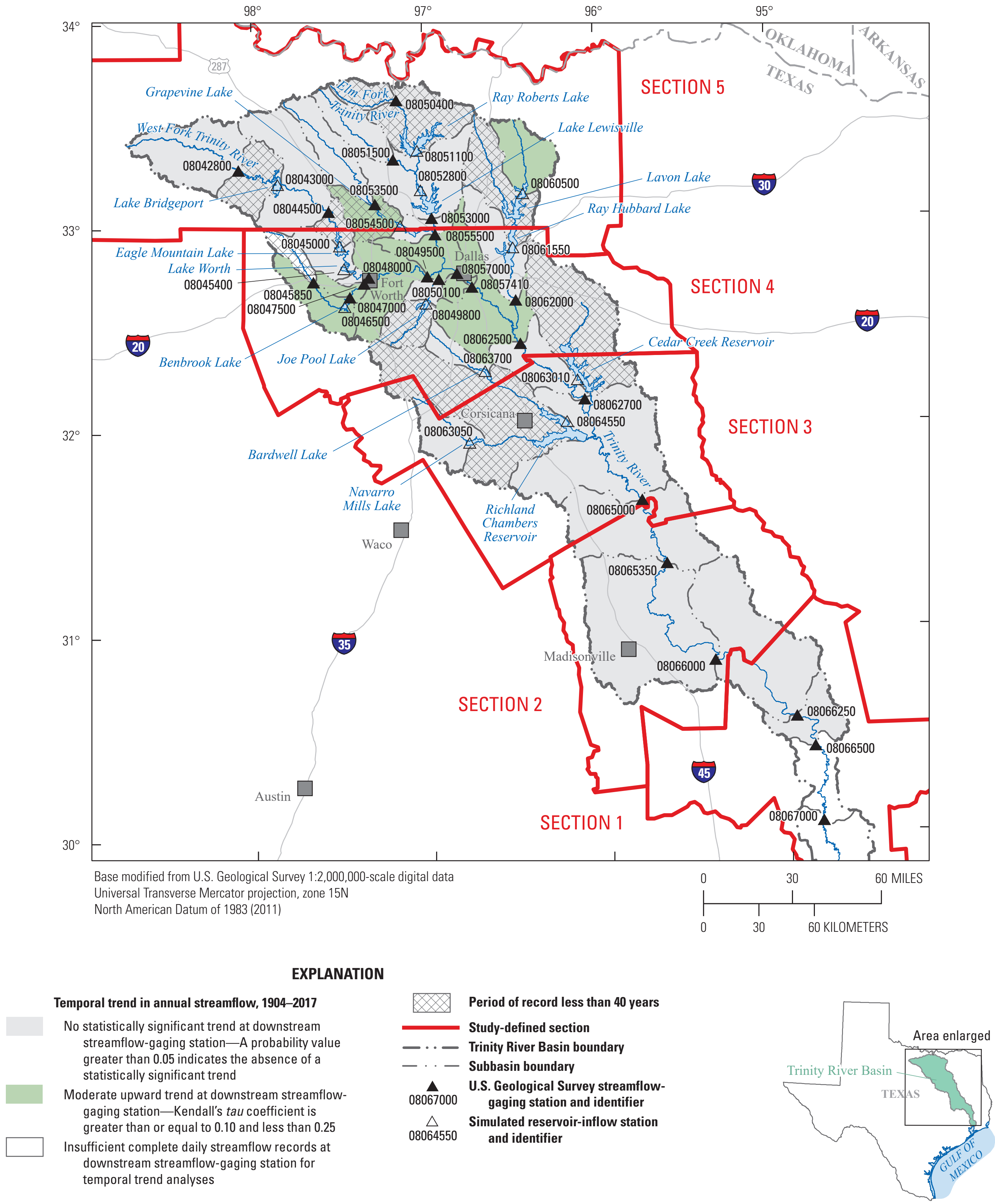

Figure 43. Temporal trends in annual streamflow at 22 U.S. Geological Survey streamflow-gaging stations and 14 simulated reservoir-inflow stations in the Trinity River Basin, 1904–2017.

Table 21. Summary information for 24 U.S. Geological Survey streamflow-gaging stations and 14 simulated reservoir-inflow stations analyzed for trends in the Trinity River Basin, 1903–2017.

[mi², square mile]

Section number[1]	Station number, name[2]	Total drainage area (mi²)	Contributing drainage area (mi²)	Period of record by calendar year[3]	Number of years of record	Percentage of record complete
1	08067000, Trinity River at Liberty, Texas[4]	17,468	17,468	1938–2017	79	30.1
	08066500, Trinity River at Romayor, Texas	17,186	17,186	1924–2017	93	100
	08066250, Trinity River near Goodrich, Texas	16,844	16,844	1965–2017	52	80.8
2	08066000, Trinity River at Riverside, Texas	15,589	15,589	1923–68	45	100
	08065350, Trinity River near Crockett, Texas	13,911	13,911	1964–2017	53	75.9
3	08065000, Trinity River near Oakwood, Texas	12,833	12,833	1923–2017	94	100
	08064550, Richland-Chambers Reservoir near Kerens, Texas	1,957	1,957	1993–2017	24	99.0
	08063050, Navarro Mills Lake near Dawson, Texas	320	320	1962–2017	55	100
	08063010, Cedar Creek Reservoir near Trinidad, Texas	1,007	1,007	1995–2017	22	98.9
	08062700, Trinity River at Trinidad, Texas	8,538	8,538	1964–2017	53	100
4	08063700, Bardwell Lake near Ennis, Texas	178	178	1965–2017	52	100
	08062500, Trinity River near Rosser, Texas	8,147	8,147	1924–2017	93	84.9
	08062000, East Fork Trinity River near Crandall, Texas	1,256	1,256	1949–2017	68	100
	08061550, Lake Ray Hubbard near Forney, Texas	1,071	1,071	1995–2017	22	99.5
	08057410, Trinity River below Dallas, Texas	6,278	6,278	1956–2017	61	95.1
	08057000, Trinity River at Dallas, Texas	6,106	6,106	1903–2017	114	100
	08055500, Elm Fork Trinity River near Carrollton, Texas	2,459	2,459	1907–2017	110	100
	08050100, Mountain Creek at Grand Prairie, Texas	298	298	1960–2017	57	96.5
	08049800, Joe Pool Lake near Duncanville, Texas	232	232	1984–2017	33	100
	08049500, West Fork Trinity River at Grand Prairie, Texas	3,065	3,065	1925–2017	92	100
	08048000, West Fork Trinity River at Fort Worth, Texas	2,615	2,615	1920–2017	97	100
	08047500, Clear Fork Trinity River at Fort Worth, Texas	518	518	1924–2017	93	100
	08047000, Clear Fork Trinity River near Benbrook, Texas	431	431	1947–2017	70	100
	08046500, Benbrook Lake near Benbrook, Texas	429	429	1952–2017	65	100
	08045850, Clear Fork Trinity River near Weatherford, Texas[4]	121	121	1980–2017	37	44.0
	08045400, Lake Worth above Fort Worth, Texas	2,052	2,052	1994–2017	23	99.7
	08045000, Eagle Mountain Reservoir above Fort Worth, Texas	1,970	1,970	1995–2017	22	98.9
5	08060500, Lavon Lake near Lavon, Texas	770	770	1953–2017	64	100
	08054500, Grapevine Lake near Grapevine, Texas	695	695	1952–2017	65	100
	08053500, Denton Creek near Justin, Texas	400	400	1949–2017	68	100
	08053000, Elm Fork Trinity River near Lewisville, Texas	1,673	1,673	1949–2017	68	98.5
	08052800, Lewisville Lake near Lewisville, Texas	1,660	1,660	1954–2017	63	100
	08051500, Clear Creek near Sanger, Texas	295	295	1949–2017	68	100
	08051100, Ray Roberts Lake near Pilot Point, Texas	692	692	1987–2017	30	100
	08050400, Elm Fork Trinity River at Gainesville, Texas	174	174	1985–2017	32	100
	08044500, West Fork Trinity River near Boyd, Texas	1,725	1,725	1947–2017	70	100
	08043000, Bridgeport Reservoir above Bridgeport, Texas	1,111	1,111	1995–2017	22	98.9
	08042800, West Fork Trinity River near Jacksboro, Texas	683	683	1956–2017	61	100

[1]Refer to figure 43 for map of sections within the Trinity River Basin.

[2]Shaded cells are U.S. Geological Survey streamflow-gaging stations with measured streamflow data (U.S. Geological Survey, 2019b), and cells that are not shaded are lake and reservoir stations with simulated reservoir-inflow data provided by the U.S. Army Corps of Engineers (2019b), the Tarrant Regional Water District, or the City of Dallas.

[3]Period of record includes the calendar year when daily mean streamflow data collection began to the end of 2017 or when data collection ended (if applicable).

[4]Due to low percentage of complete daily streamflow data, only analyzed for annual peak streamflow trends and precipitation associated with annual peak streamflow.

Table 22. Summary of annual, seasonal, and monthly precipitation trends for the period 1900–2017 within five sections of the Trinity River Basin.

[wet, years with precipitation totals above long-term mean; dry, years with precipitation totals below long-term mean; NA, not applicable; season 1, includes November, December, January, and February; season 2, includes March, April, May, and June; season 3, includes July, August, September, and October; *p*-value, probability value (considered statistically significant if less than 0.05); green shaded cells indicate statistically significant upward trends; red shaded cells indicate statistically significant downward trends]

Time step	Trinity River Basin section number[1]											
	Section 1				Section 2				Section 3			
	[2]1905–2017				1900–2017				1900–2017			
	Kendall's *tau*	*p*-value	Mean precipitation (inches)	Percentage[3]	Kendall's *tau*	*p*-value	Mean precipitation (inches)	Percentage[3]	Kendall's *tau*	*p*-value	Mean precipitation (inches)	Percentage[3]
Annual	0.1435	0.0244	51.28	100	0.0816	0.1951	44.87	100	0.1309	0.0375	38.55	100
Annual (wet)	0.0754	0.4347	NA	NA	−0.0094	0.9232	NA	NA	0.0914	0.3376	NA	NA
Annual (dry)	0.0055	0.9553	NA	NA	−0.0678	0.4520	NA	NA	0.0758	0.3833	NA	NA
Season 1	0.0795	0.2099	17.03	33.2	0.0102	0.8711	15.23	33.9	0.1307	0.0367	12.12	31.5
Season 2	0.0578	0.3638	17.51	34.1	−0.0003	0.9962	16.59	37.0	0.0292	0.6409	15.29	39.7
Season 3	0.1343	0.0342	16.75	32.7	0.1365	0.0284	13.05	29.1	0.1267	0.0438	11.13	28.9
January	0.1042	0.1003	4.14	8.1	0.0995	0.1118	3.64	8.1	0.1551	0.0129	2.72	7.0
February	0.0106	0.8677	3.56	6.9	−0.0937	0.1347	3.39	7.6	0.0860	0.1678	2.85	7.4
March	0.0606	0.3395	3.58	7.0	0.0217	0.7291	3.50	7.8	0.1166	0.0615	3.24	8.4
April	−0.0645	0.3113	4.08	7.9	−0.1340	0.0322	4.11	9.2	−0.1118	0.0742	3.90	10.1
May	0.0488	0.4419	5.07	9.9	0.0032	0.9592	5.00	11.1	−0.0206	0.7412	4.72	12.2
June	0.1436	0.0236	4.78	9.3	0.1256	0.0437	3.98	8.9	0.1569	0.0118	3.43	8.9
July	0.0308	0.6277	4.08	8.0	−0.0521	0.4037	2.91	6.5	0.0231	0.7115	2.18	5.6
August	0.0460	0.4685	4.10	8.0	0.0763	0.2211	2.93	6.5	0.1142	0.0694	2.22	5.8
September	0.1598	0.0117	4.25	8.3	0.1505	0.0158	3.46	7.7	0.0049	0.9370	3.10	8.1
October	0.0621	0.3252	4.32	8.4	0.0735	0.2383	3.76	8.4	0.1246	0.0455	3.63	9.4
November	0.1506	0.0170	4.41	8.6	0.0657	0.2920	4.09	9.1	0.0871	0.1621	3.21	8.3
December	−0.0345	0.5849	4.91	9.6	−0.0102	0.8709	4.11	9.2	0.0315	0.6137	3.35	8.7

Table 22. Summary of annual, seasonal, and monthly precipitation trends for the period 1900–2017 within five sections of the Trinity River Basin.—Continued

[wet, years with precipitation totals above long-term mean; dry, years with precipitation totals below long-term mean; NA, not applicable; season 1, includes November, December, January, and February; season 2, includes March, April, May, and June; season 3, includes July, August, September, and October; *p*-value, probability value (considered statistically significant if less than 0.05); green shaded cells indicate statistically significant upward trends; red shaded cells indicate statistically significant downward trends]

Time step	Trinity River Basin section number[1]							
	Section 4				Section 5			
	1900–2017				1900–2017			
	Kendall's *tau*	*p*-value	Mean precipitation (inches)	Percentage[3]	Kendall's *tau*	*p*-value	Mean precipitation (inches)	Percentage[3]
Annual	0.0891	0.1533	37.38	100	0.1755	0.0049	34.53	100
Annual (wet)	0.1933	0.0296	NA	NA	0.1623	0.0757	NA	NA
Annual (dry)	0.1762	0.0517	NA	NA	0.2257	0.0104	NA	NA
Season 1	0.1150	0.0661	10.77	28.8	0.1713	0.0062	8.49	24.6
Season 2	0.0272	0.6619	15.41	41.2	0.1091	0.0799	14.58	42.2
Season 3	0.0420	0.5000	11.20	30.0	0.0720	0.2477	11.46	33.2
January	0.1087	0.0811	2.41	6.4	0.1040	0.0954	1.79	5.2
February	0.0770	0.2168	2.61	7.0	0.1223	0.0499	2.12	6.2
March	0.1305	0.0363	3.03	8.1	0.1494	0.0166	2.66	7.7
April	−0.0923	0.1384	3.99	10.7	−0.0284	0.6485	3.60	10.4
May	−0.0151	0.8089	4.88	13.0	0.0081	0.8964	4.76	13.8
June	0.0947	0.1288	3.51	9.4	0.1273	0.0411	3.55	10.3
July	−0.0431	0.4897	2.28	6.1	−0.0360	0.5640	2.49	7.2
August	0.0589	0.3450	2.25	6.0	0.0595	0.3403	2.29	6.6
September	0.0087	0.8890	3.07	8.2	0.0884	0.1559	3.22	9.3
October	0.0732	0.2401	3.60	9.6	0.0648	0.2985	3.45	10.0
November	0.0723	0.2458	2.89	7.7	0.0829	0.1834	2.40	6.9
December	0.0591	0.3426	2.86	7.6	0.1089	0.0807	2.18	6.3

[1]Refer to figure 43 for map of sections within the Trinity River Basin.

[2]Section 1 precipitation data begins in 1905 because of a lack of data in that area.

[3]Percentage of the total precipitation within the season or month for the time period specified.

Streamflow Trends

Temporal trends in streamflow volume on annual, seasonal, and monthly time steps are summarized in table 8. The trends in annual streamflow at the 36 stations within the Trinity River Basin are also depicted for the areal extent of the basin (fig. 43). Data from 8 of the 36 stations analyzed for trends in annual streamflow indicated upward trends, and all are in the upper sections of the basin (sections 4 and 5). None of the data from stations in the lower sections of the basin (sections 1, 2, and 3) indicated trends in annual streamflow. Streamflow trends in the Trinity River Basin were upwards despite downward trends in the groundwater-level elevations in the Carrizo-Wilcox aquifer and the Trinity aquifer within counties, such as Denton, Tarrant, and Johnson, along the Interstate 35 corridor. All the seasonal trends among the 36 stations were upward and were during seasons 1 and 3, which accounted for 29 and 17 percent of the annual streamflow volume, respectively. Of the 108 possible seasonal trends, 23 were upward and all but 2 were in the upper sections of the basin. Of the 432 possible monthly trends, 133 were significant, and of those, 127 were upward and 6 were downward.

The ratios of streamflow volume to precipitation volume were analyzed as part of this study (fig. 44; table 9). Temporal trends in the ratio of streamflow volume to precipitation volume indicate a change in the way the system responds to precipitation events and possibly explain downward trends in streamflow if the ratios are also downward. The analyses indicated that trends in streamflow and trends in the ratio of streamflow volume to precipitation volume are similar (figs. 43 and 44; tables 8 and 9). Data from the lower sections of the basin (sections 1, 2, and 3) indicated some seasonal and monthly trends (mostly upward) in the ratio of streamflow volume to precipitation volume without upward trends in streamflow on an annual time step. Data from all eight of the stations in the upper sections of the basin (sections 4 and 5) that indicated upward trends in annual streamflow also indicated upward trends in the ratio of streamflow volume to precipitation volume on an annual time step.

Streamflow trends in the Trinity River Basin were upwards despite downward trends in the groundwater-level elevations in the Carrizo-Wilcox aquifer and the Trinity aquifer within counties, such as Denton, Tarrant, and Johnson, along the Interstate 35 corridor.

The Kendall's *tau* and *p*-values for trends in two extreme streamflow regimes, annual minimum and annual peak streamflow, were calculated (table 10), and any trends that were indicated for these two streamflow regimes are depicted for the areal extent of the basin (figs. 45–46). Throughout all sections of the Trinity River Basin, data from 16 of the 36 stations indicated upward trends in annual minimum streamflow. Of the basins included in this study, the Trinity River Basin has the second largest amount of potential flood storage at 8,947,349 acre-ft from dams added between 1890 and 2013 (USACE, 2019a). Upward trends in annual minimum streamflow could be the result of managed reservoir releases in combination with wastewater treatment plant releases in the large Dallas-Fort Worth metroplex in the upper sections of the basin.

All the statistically significant trends in annual peak streamflow are in section 4 of the Trinity River Basin, which includes the Dallas-Fort Worth metroplex. Data from two stations, one USGS streamflow-gaging station and one simulated-inflow station, indicated upward trends in annual peak streamflow, and data from one streamflow-gaging station indicated a downward trend in annual peak streamflow.

Potential Flood Storage Trends

Results of the analyses of the associations between potential flood storage volume and annual streamflow volume and the trends in the ratio of annual streamflow volume to potential flood storage volume for the Trinity River Basin are summarized in table 10, and the annual results are illustrated in figures 47 and 48, respectively.

Eleven stations had positive associations between potential flood storage volume and annual streamflow volume, indicating that annual streamflow increases as potential flood storage increases. Data from 7 of the 11 stations also indicated upward trends in annual streamflow. Four stations had upward trends in annual streamflow, upward trends in minimum streamflow, and positive associations between potential flood storage volume and annual streamflow volume. The positive associations may be the result of increases in minimum streamflow, which could be caused by any combination of managed reservoir releases, wastewater treatment plant releases, or increased runoff from urbanized areas, particularly in the urbanized area of the Dallas-Fort Worth metroplex.

There are 17 stations that had downward trends in the ratio of annual streamflow volume to potential flood storage volume throughout the Trinity River Basin. However, data from the stations with downward trends in the ratio of annual streamflow volume to potential flood storage volume did not indicate downward trends in annual streamflow (fig. 43), and many indicated upward trends in annual streamflow. Downward trends in the ratio of annual streamflow volume to potential flood storage volume in the absence of downward trends in annual streamflow result from the denominator (potential flood storage volume) always increasing as additional dams and flood retention structures are built.

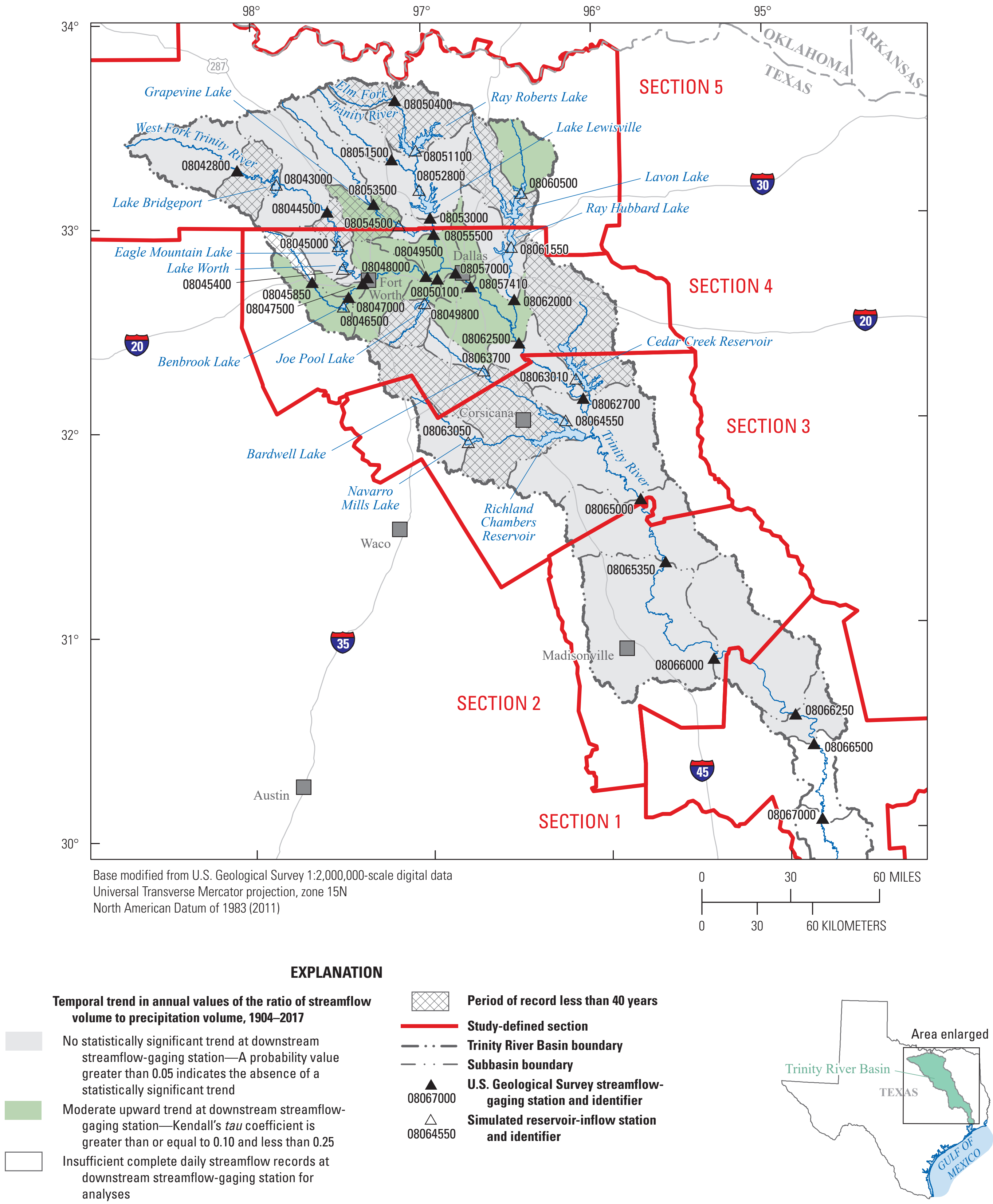

Figure 44. Temporal trends in annual values of the ratio of streamflow volume to precipitation volume at 22 U.S. Geological Survey streamflow-gaging stations and 14 simulated reservoir-inflow stations in the Trinity River Basin, 1904–2017.

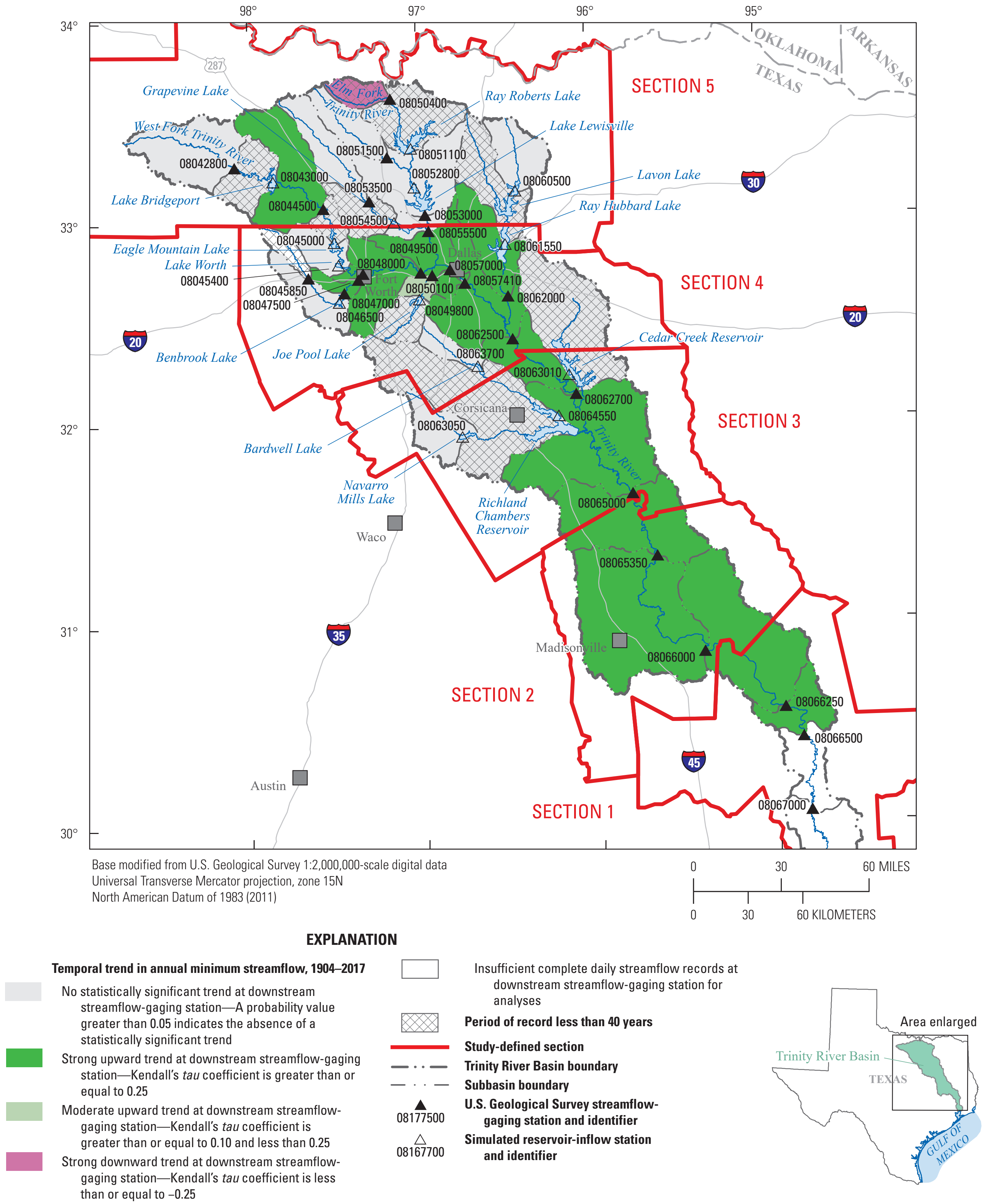

Figure 45. Temporal trends in annual minimum streamflow at 22 U.S. Geological Survey streamflow-gaging stations and 14 simulated reservoir-inflow stations in the Trinity River Basin, 1904–2017.

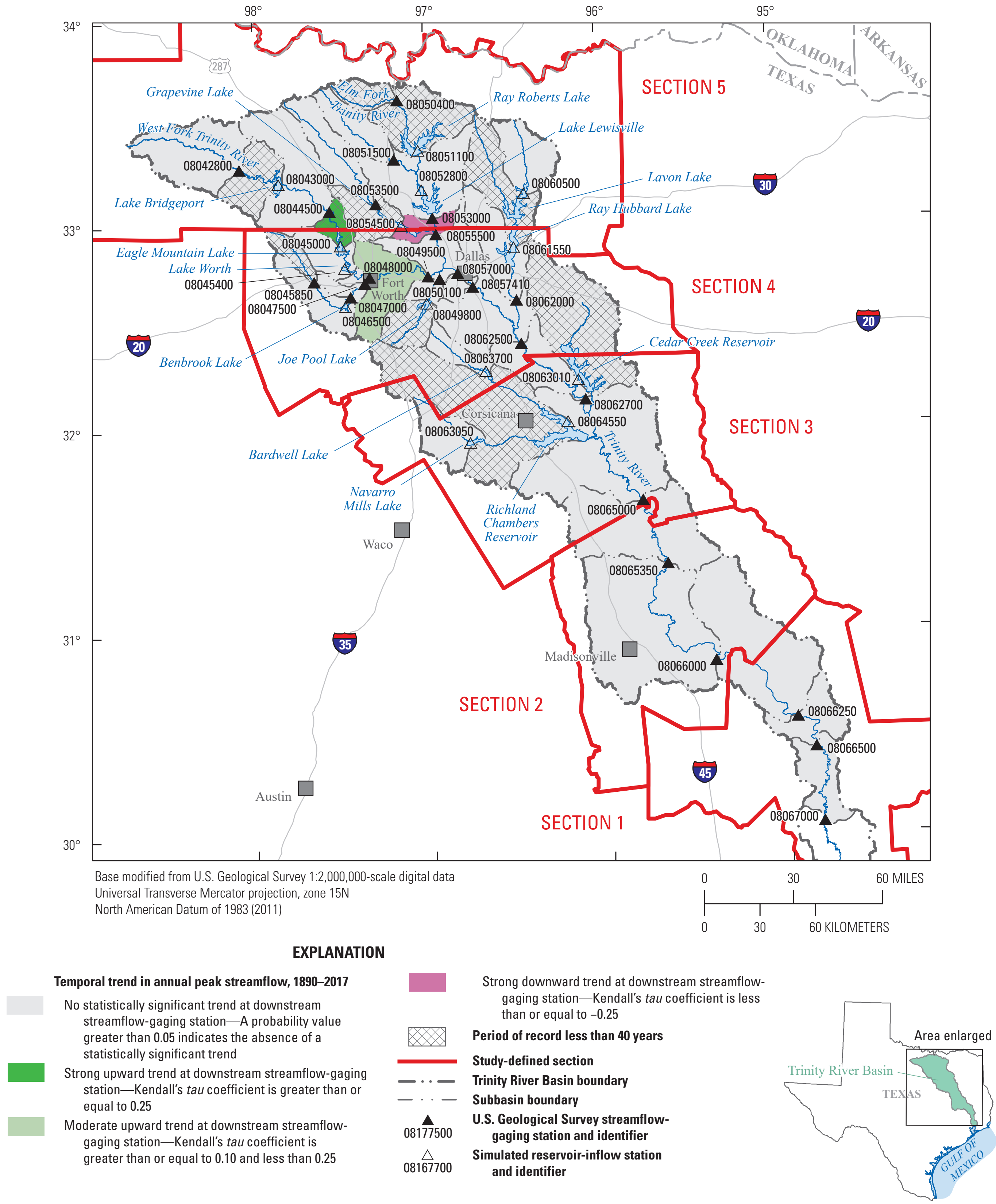

Figure 46. Temporal trends in annual peak streamflow at 24 U.S. Geological Survey streamflow-gaging stations and 14 simulated reservoir-inflow stations in the Trinity River Basin, 1890–2017.

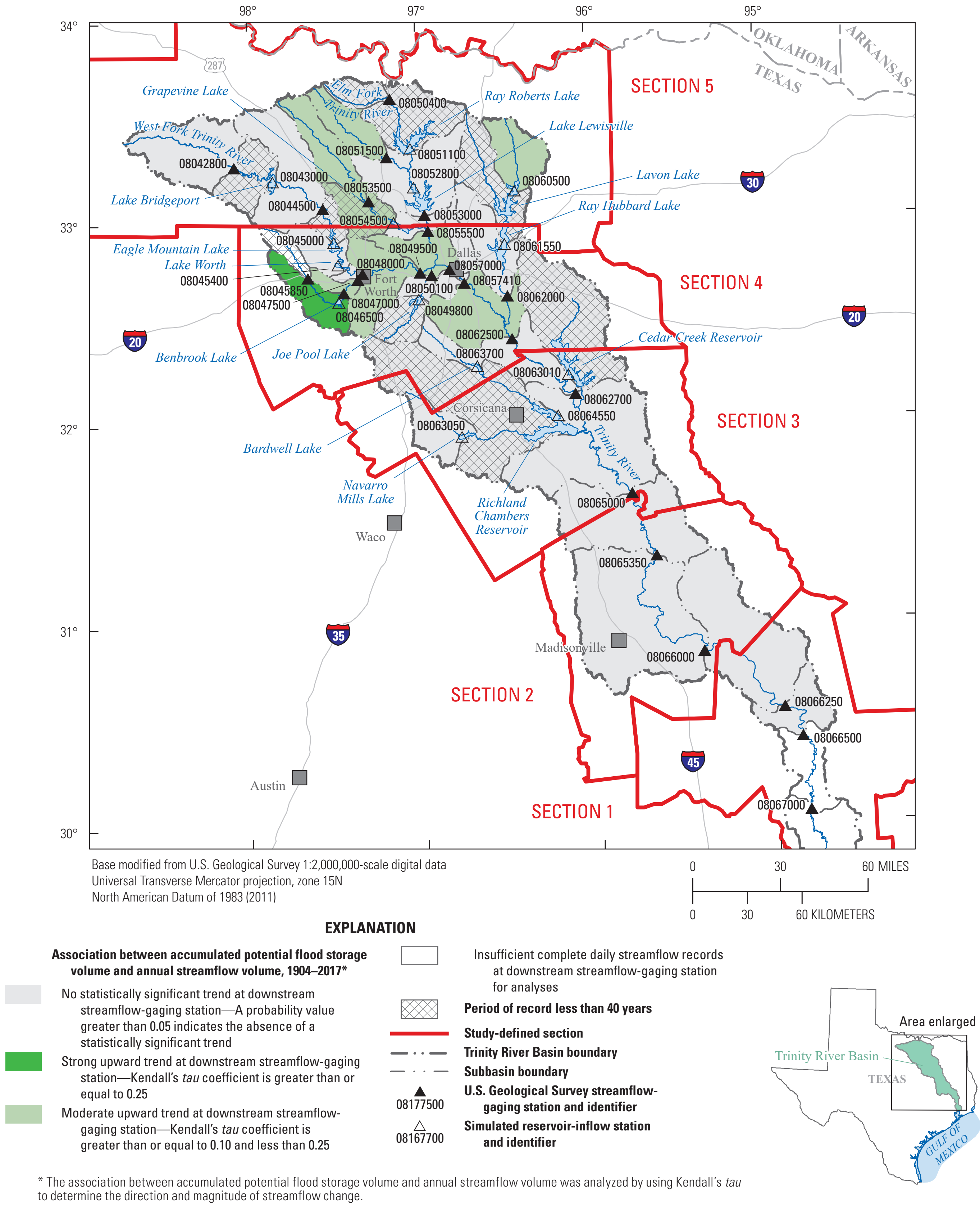

Figure 47. Association between accumulated potential flood storage volume and annual streamflow volume at 22 U.S. Geological Survey streamflow-gaging stations and 14 simulated reservoir-inflow stations in the Trinity River Basin, 1904–2017.

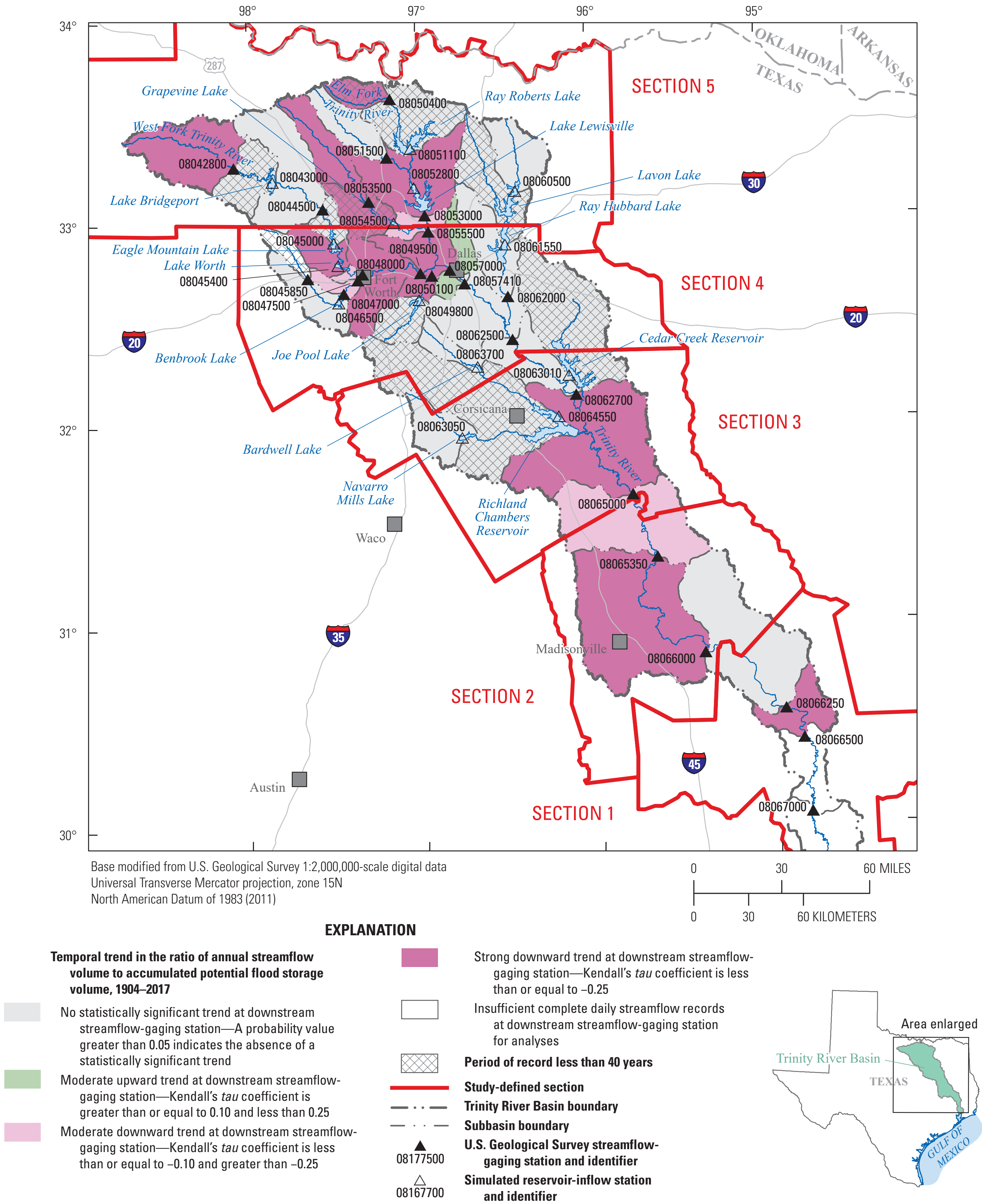

Figure 48. Temporal trends in the ratio of annual streamflow volume to accumulated potential flood storage volume at 22 U.S. Geological Survey streamflow-gaging stations and 14 simulated reservoir-inflow stations in the Trinity River Basin, 1904–2017.

Summary

The U.S. Geological Survey (USGS), in cooperation with the U.S. Army Corps of Engineers (USACE), analyzed streamflow trends and streamflow-related variables through 2017 in seven important water-supply basins to provide information that can help water managers with the USACE and river authorities make future water management decisions. The primary purpose of this report is to document trends in long-term streamflow data at 114 selected USGS streamflow-gaging stations and 36 simulated reservoir-inflow stations, in 7 river basins primarily in Texas: Brazos, Colorado, Big Cypress, Guadalupe, Neches, Sulphur, and Trinity. In this report, trends are considered statistically significant if their *p*-values are less than or equal to 0.05 (p-value ≤ 0.05). Streamflow data selected for temporal trend analyses include annual minimum streamflow, annual peak streamflow, and streamflow volume. Precipitation, air temperature, and groundwater-level elevations were analyzed for trends that may help to explain changes observed in the streamflow statistics. Basins were divided into sections along county lines for precipitation analyses. Within all the basins, the associations between precipitation and streamflow were strong for most time steps, and were all positive, indicating an increase in streamflow as precipitation increases. Streamflow volumes were analyzed for associations with potential flood storage. The potential flood storage, defined as the difference between maximum storage and normal storage, was computed for each dam from the National Inventory of Dams database and accumulated over time based on the completion date of the dam.

Precipitation and air temperature trends were analyzed for each of the eight climate divisions (High Plains, Trans-Pecos, Low Rolling Hills, Edwards Plateau, North Central Texas, South Central Texas, East Texas, and Upper Coast). Results of precipitation trend analyses indicated moderate upward trends in the Upper Coast and East Texas Climate Divisions analyzed on an annual time step from 1900 through 2017. These two climate divisions are in the eastern and southeastern parts of Texas, and they receive more mean annual precipitation (45.88 and 46.09 inches, respectively) than the other climate divisions. No trends were found in annual precipitation during drought conditions, normal conditions, or moist conditions as measured by the mean annual Palmer Drought Severity Index for all climate divisions. Multiple regression analysis with periodic functions was used to analyze for temporal trends in annual mean air temperature. The results indicated upward trends in annual mean air temperature within all climate divisions, with a mean slope of 0.02 degree Fahrenheit per year, or 1 degree every 50 years.

Within the Brazos River Basin, 19 USGS streamflow-gaging stations and 12 simulated-inflow stations were selected for streamflow trend analyses. Results of precipitation trend analyses on an annual time step indicated that precipitation amounts have most likely increased in the lower and middle sections of the basin. Downward trends in annual streamflow and in the ratio of streamflow volume to precipitation volume were indicated at 7 of the 15 stations in the upper sections of the basin. Data from the lower sections of the basin indicated mostly downward trends in annual minimum streamflow, whereas upward trends in annual minimum streamflow were indicated in the upper sections of the basin. Downward trends in annual peak streamflow were indicated at many of the stations in the upper sections of the basin. At the same seven stations in the upper sections of the basin where there were downward trends in annual streamflow, there were also downward trends in the ratio of streamflow volume to precipitation volume. Data from these same seven stations indicated negative associations between potential flood storage volume and annual streamflow volume and downward trends in the ratio of annual streamflow volume to potential flood storage volume. With the known addition of 13,006,394 acre-feet (acre-ft) of potential flood storage between 1900 and 2010 in the subbasins analyzed, streamflow volumes have decreased in the upper sections of the basin. Springs that historically flowed within the upper Brazos River Basin from the Ogallala aquifer that no longer flow could be contributing to decreased streamflows because their presence kept areas moist to very wet so that less inputs from precipitation would be required to generate meaningful downstream flow. Similarly, decreasing groundwater-level elevations in many of the Seymour aquifer wells within Baylor, Haskell, and Knox Counties and the continued increase in pumping for irrigation and municipal supply could cause further declines in groundwater-level elevations and contribute to decreasing streamflow.

Within the Colorado River Basin, 26 USGS streamflow-gaging stations and 4 simulated-inflow stations were selected for streamflow trend analyses. Results of precipitation trend analyses on an annual time step indicated no trends in the basin. Downward trends in annual streamflow were indicated at 16 stations in the upper sections of the basin, whereas no trends in annual streamflow were indicated in the lower section of this basin. Despite downward trends in the Carrizo-Wilcox and Gulf Coast aquifers, streamflow volumes downstream from the outcrop areas in the basin were not decreasing. Downward groundwater-level trends in the Trinity aquifer near Austin, Texas, coincided with some downward streamflow trends in the Colorado River Basin. In the lower section of the basin, data from one station operated as a continuous streamflow-gaging station through 2017 indicated a downward trend in annual minimum streamflow, and data from another station (operated through 2007) indicated an upward trend in annual minimum streamflow. In the upper sections of the basin, data from seven stations indicated upward trends in annual minimum streamflow, and data from six stations indicated downward trends. Data from 18 stations in the upper sections of the basin indicated a downward trend in annual peak streamflow. Data from 13 of the 16 stations in the upper sections of the basin indicated downward trends in annual streamflow and indicated downward trends in the ratio of streamflow volume to precipitation volume. Data from the same 13 stations indicated negative associations between

potential flood storage volume and annual streamflow volume and downward trends in the ratio of annual streamflow volume to potential flood storage volume. With the known addition of 7,193,147 acre-ft of potential flood storage between 1891 and 2014 in the subbasins analyzed, streamflow volumes have decreased in the upper sections of the basin.

Within the Big Cypress Basin, seven USGS streamflow-gaging stations and one simulated-inflow station were selected for streamflow trend analyses. Results of precipitation trend analyses on annual, seasonal, and monthly time steps indicated almost no trends in the basin as defined in this report. However, the annual precipitation *p*-value only slightly exceeded the *p*-value threshold for a statistically significant trend. Given the upward trend in precipitation in the East Texas Climate Division, which includes the Big Cypress Basin, and the low *p*-value for annual precipitation within the basin, precipitation in the basin may be increasing over time. Two annual streamflow trends, one upward and one downward, were at stations in the upper parts of the basin. Data from USGS streamflow-gaging station 07346000 Big Cypress Bayou near Jefferson, Texas, indicated an upward trend in annual minimum streamflow and a downward trend in annual peak streamflow. The station is immediately downstream from Lake O' the Pines; presumably, minimums have increased because of regulated releases, and annual peaks have decreased because of storage from the lake for flood control. Despite the known addition of 2,737,154 acre-ft of potential flood storage between 1898 and 2011 in the subbasins analyzed, there have not been widespread reductions in streamflow volumes in the Big Cypress Basin, except for within the drainage for the farthest upstream station on the main stem downstream from Mount Pleasant, Texas. The upstream parts of the basin, particularly the area contributing to the station on the main stem downstream from Mount Pleasant, could be affected by the downward groundwater-level trends in the Carrizo-Wilcox aquifer.

Within the Guadalupe River Basin, 17 USGS streamflow-gaging stations and 1 simulated-inflow station were selected for streamflow trend analyses. Results of precipitation trend analyses on an annual time step indicated an upward trend in the lower section of the basin, but no trends in annual streamflow were indicated in the lower section of the basin. In the upper section of the basin, data from 1 of the 13 stations in the northwest part of the basin indicated an upward trend in annual streamflow. Data from 6 of the 13 stations in the upper section of the basin indicated a trend in annual minimum streamflow, with 4 upward and 2 downward trends. Data from 2 of the 13 stations in the upper section of the basin indicated downward trends in annual peak streamflow. Despite the known addition of 2,016,534 acre-ft of potential flood storage between 1849 and 2013 in the subbasins analyzed, streamflow volumes have not decreased in the Guadalupe River Basin. Downward trends in groundwater levels within the major aquifers with potential to discharge directly to the Guadalupe River (Carrizo-Wilcox and Gulf Coast) did not coincide with annual streamflow trends.

Within the Neches River Basin, 17 USGS streamflow-gaging stations and 2 simulated-inflow stations were selected for streamflow trend analyses. Results of precipitation trend analyses on an annual time step indicated upward trends in the basin. None of the data from stations analyzed in the Neches River Basin indicated annual trends in streamflow despite upward trends in annual precipitation within the basin. Data from 9 of the 19 stations analyzed in the basin indicated upward trends in annual minimum streamflow. Data from one of the simulated-inflow stations indicated a downward trend in annual minimum streamflow into Sam Rayburn Reservoir. Data from two stations indicated downward trends in annual peak streamflow, and data from one small subbasin indicated an upward trend in annual peak streamflow. Despite the known addition of 4,839,609 acre-ft of potential flood storage between 1888 and 2008 in the subbasins analyzed, there have not been widespread reductions in streamflow volumes in the Neches River Basin. Downward trends in groundwater levels within the major aquifers with potential to discharge directly to the Neches River (Carrizo-Wilcox and Gulf Coast) did not coincide with annual streamflow trends.

Within the Sulphur River Basin, four USGS streamflow-gaging stations and two simulated-inflow stations were selected for streamflow trend analyses. Results of precipitation trend analyses on an annual time step indicated a moderate upward trend within the basin. Data from only one of the stations, the simulated inflow to Jim Chapman Lake, indicated an annual upward trend in streamflow despite an upward trend in annual precipitation throughout the basin. Data from three of the six stations in the Sulphur River Basin indicated upward trends in annual minimum streamflow, and data from one of the six stations indicated a downward trend in annual peak streamflow. Despite the known addition of 6,933,361 acre-ft of potential flood storage between 1904 and 2006 in the subbasins analyzed, streamflow volumes have not decreased in the Sulphur River Basin. Downward trends in groundwater levels within the major aquifer with potential to discharge directly to the Sulphur River (Carrizo-Wilcox) did not coincide with annual streamflow trends.

Within the Trinity River Basin, 24 USGS streamflow-gaging stations and 14 simulated-inflow stations were selected for streamflow trend analyses. Results of precipitation trend analyses on an annual time step indicated upward trends in most of the basin. Data from 8 of the 36 stations analyzed for trends in annual streamflow indicated upward trends, and all 8 stations are in the upper sections of the basin. None of the data from the stations in the lower sections of the basin indicated trends in annual streamflow. Streamflow trends in the Trinity River Basin were upwards despite downward trends in the groundwater-level elevations in the Carrizo-Wilcox aquifer and the Trinity aquifer within counties along the Interstate 35 corridor. Data from 16 of the 36 stations indicated upward trends in annual minimum streamflow. Upward trends in annual minimum streamflow could be the result of managed reservoir releases in combination with wastewater treatment plant releases in the large Dallas-Fort Worth metroplex in the upper sections of the basin. All the trends in annual peak streamflow were in the sections of the basin that include the Dallas-Fort Worth metroplex. Data from two stations, one USGS streamflow-gaging station and one simulated-inflow station, indicated upward trends in annual peak streamflow, and data from one streamflow-gaging station indicated a downward trend in annual peak streamflow. Of the basins included in this study, the Trinity River Basin has the second largest amount of potential flood storage at 8,947,349 acre-ft from dams added between 1890 and 2013. Eleven stations in the Trinity River Basin had positive associations between potential flood storage volume and annual streamflow volume, indicating that annual streamflow increases as potential flood storage increases. Data from 7 of the 11 stations also indicated upward trends in annual streamflow. The positive associations may be the result of increases in minimum streamflow, which could be caused by any combination of managed reservoir releases, wastewater treatment plant releases, or increased runoff from urbanized areas, particularly in the urbanized area of the Dallas-Fort Worth metroplex.

References Cited

Anaya, Roberto, and Jones, Ian, 2009, Groundwater availability model for the Edwards-Trinity (Plateau) and Pecos Valley aquifers of Texas: Texas Water Development Board Report 373, 115 p. [Also available at http://www.twdb.texas.gov/groundwater/models/gam/eddt_p/ET-Plateau_Full.pdf?d=9651.799999875948.]

Asquith, W.H., 2001, Effects of regulation on L-moments of annual peak streamflow in Texas: U.S. Geological Survey Water-Resources Investigations Report 01–4243, 66 p.

Asquith, W.H., Vrabel, Joseph, and Roussel, M.C., 2007a, Summary of percentages of zero daily mean streamflow for 712 U.S. Geological Survey streamflow-gaging stations in Texas through 2003: U.S. Geological Survey Data Series 247, 721 p. [Also available at http://pubs.usgs.gov/ds/2007/247/.]

Asquith, W.H., Vrabel, Joseph, and Roussel, M.C., 2007b, Summary of annual mean, maximum, minimum, and L-scale statistics of daily mean streamflow for 712 U.S. Geological Survey streamflow-gaging stations in Texas through 2003: U.S. Geological Survey Data Series 248, 721 p. [Also available at http://pubs.usgs.gov/ds/2007/248/.]

Asquith, W.H., and Heitmuller, F.T., 2008, Summary of annual mean and annual harmonic mean statistics of daily mean streamflow for 620 U.S. Geological Survey streamflow-gaging stations in Texas through water year 2007: U.S. Geological Survey Data Series 372, 1259 p. [Also available at https://pubs.usgs.gov/ds/372/.]

Barlow, P.M., and Leake, S.A., 2012, Streamflow depletion by wells—Understanding and managing the effects of groundwater pumping on streamflow: U.S. Geological Survey Circular 1376, 84 p. [Also available at https://doi.org/10.3133/cir1376.]

Benson, M.A., 1964, Factors influencing the occurrence of floods in the southwest: U.S. Geological Survey Water-Supply Paper 1580-D.

Brune, Gunnar, 2002, Springs of Texas, volume 1: College Station, Tex., Texas A&M University Press, 566 p.

Deeds, N.E., Harding, J.J., Jones, T.L., Singh, A., Hamlin, S., and Reedy, R.C., eds., 2015, Final conceptual model report for the High Plains aquifer system groundwater availability model: Texas Water Development Board, 590 p. [Also available at https://www.twdb.texas.gov/groundwater/models/gam/hpas/HPAS_GAM_Conceptual_Report.pdf.]

Eckhardt, G., 2019, The Edwards aquifer website, accessed July 16, 2019, at https://www.edwardsaquifer.net/index.html.

George, P.G., Mace, R.E., and Petrossian, R., 2011, Aquifers of Texas: Texas Water Development Board Report 380, 172 p. [Also available at http://www.twdb.texas.gov/publications/reports/numbered_reports/doc/R380_AquifersofTexas.pdf.]

Groisman, P.Y., Knight, R.W., Karl, T.R., Easterling, D.R., Sun, B., and Lawrimore, J.H., 2004, Contemporary changes of the hydrological cycle over the contiguous United States—Trends derived from in situ observations: Journal of Hydrometeorology, v. 5, no. 1, p. 64–85. [Also available at https://doi.org/10.1175/1525-7541(2004)005<0064:CCOTHC>2.0.CO;2.]

Gutentag, E.D., Heimes, F.J., Krothe, N.C., Luckey, R.R., and Weeks, J.B., 1984, Geohydrology of the High Plains aquifer in parts of Colorado, Kansas, Nebraska, New Mexico, Oklahoma, South Dakota, Texas, and Wyoming: U.S. Geological Survey Professional Paper 1400-B.

Helsel, D.R., and Hirsch, R.M., 2002, Statistical methods in water resources: U.S. Geological Survey Techniques of Water-Resources Investigations, book 4, chap. A3, 510 p.

Jones, T.L., Ewing, J.E., Yan, T., Pickens, J.F., Scanlon, B.R., Olyphant, J., and Chastain-Howley, A., 2012, Final report—Conceptual model for the refined Seymour aquifer groundwater availability model—Haskell, Knox, and Baylor Counties: Texas Water Development Board, 274 p., accessed June 11, 2019, at https://www.twdb.texas.gov/groundwater/models/gam/symr_hkb/SYMR_HKB_Conceptual_Model_Report.pdf.

Mace, R.E., Davidson, S.C., Angle, E.S., and Mullican, W.F., III, eds., 2006, Aquifers of the Gulf Coast of Texas: Texas Water Development Board Report 365, 304 p. [Also available at https://www.twdb.texas.gov/publications/reports/numbered_reports/doc/R365/R365_Composite.pdf.]

McDowell, J.S., Garrett, B.S., and Harwell, G.R., 2020, Data used to assess precipitation, temperature, groundwater-level elevation, streamflow, and potential flood storage trends within the Brazos, Colorado, Big Cypress, Guadalupe, Neches, Sulphur, and Trinity River Basins in Texas through 2017: U.S. Geological Survey data release, https://doi.org/10.5066/P9L1F7PT.

McGuire, V.L., 2014, Water-level changes and change in water in storage in the High Plains aquifer, predevelopment to 2013 and 2011–13: U.S. Geological Survey Scientific Investigations Report 2014–5218, 14 p., accessed June 11, 2019, at http://dx.doi. org/10.3133/sir20145218.

Menne, M.J., Durre, I., Vose, R.S., Gleason, B.E., and Houston, T.G., 2012, An overview of the global historical climatology network-daily database: Journal of Atmospheric and Oceanic Technology, v. 29, no. 7, p. 897–910, accessed June 12, 2019, at https://doi.org/10.1175/JTECH-D-11-00103.1.

National Oceanic and Atmospheric Administration [NOAA], 2019a, National Climatic Data Center—National environmental satellite, data, and information service, accessed July 8, 2019, at https://www7.ncdc.noaa.gov/CDO/CDODivisionalSelect.jsp#.

National Oceanic and Atmospheric Administration [NOAA], 2019b, National Centers for Environmental Information—Climate data online search, accessed July 8, 2019, at http://www.ncdc.noaa.gov/cdo-web/search#t=secondTabLink.

National Weather Service, 2019, Advanced Hydrologic Prediction Service, accessed June 7, 2019, at https://water.weather.gov/precip/.

Palmer, W.C., 1965, Meteorological drought: U.S. Weather Bureau Research Paper 45, 58 p.

Shah, S.D., Ramage, J.K., and Braun, C.L., 2018, Status of groundwater-level altitudes and long-term groundwater-level changes in the Chicot, Evangeline, and Jasper aquifers, Houston-Galveston region, Texas, 2018: U.S. Geological Survey Scientific Investigations Report 2018–5101, 18 p., accessed October 16, 2019 at https://doi.org/10.3133/sir20185101.

Shuttleworth, W.J., 1993, Handbook of hydrology: New York, McGraw-Hill, p. 4.1–4.53.

Texas Water Development Board [TWDB], 2015, Llano Estacado (Region O) 2016 regional water plan, prepared by Llano Estacado Regional Water Planning Group for Texas Water Development Board, accessed June 6, 2019, at http://www.twdb.texas.gov/waterplanning/rwp/plans/2016/O/Region_O_2016_RWP.pdf?d=10316.004999999677.

Texas Water Development Board [TWDB], 2016, Texas aquifers study—Groundwater quantity, quality, flow, and contributions to surface water: 304 p. [Also available at http://www.twdb.texas.gov/groundwater/docs/studies/TexasAquifersStudy_2016.pdf.].

Texas Water Development Board [TWDB], 2019a, River basins, accessed July 8, 2019, at http://www.twdb.texas.gov/surfacewater/rivers/river_basins/index.asp.

Texas Water Development Board [TWDB], 2019b, Major aquifers, accessed July 8, 2019, at http://www.twdb.texas.gov/groundwater/aquifer/major.asp.

Texas Water Development Board [TWDB], 2019c, Groundwater Database reports, accessed July 8, 2019, at http://www.twdb.texas.gov/groundwater/data/gwdbrpt.asp.

Thomas, J.V., Teeple, A.P., Payne, J.D., and Ikard, Scott, 2016, Changes between early development (1930–60) and recent (2005–15) groundwater-level altitudes and dissolved-solids and nitrate concentrations in and near Gaines, Terry, and Yoakum Counties, Texas: U.S. Geological Survey Scientific Investigations Map 3355, 2 sheets, pamphlet, accessed October 16, 2019, at http://dx.doi.org/10.3133/sim3355.

U.S. Army Corps of Engineers [USACE], 2019a, National inventory of dams, accessed April 2, 2019, at https://nid-test.sec.usace.army.mil/ords/f?p=105:1.

U.S. Army Corps of Engineers [USACE], 2019b, Fort Worth district water management information, accessed July 12, 2019, at http://www.swf-wc.usace.army.mil/cgi-bin/rcshtml.pl?page=Hydrologic.

U.S. Department of Agriculture, 2019, Texas Climate Divisions map, accessed March 11, 2019, at https://www.nass.usda.gov/Statistics_by_State/Texas/Publications/Charts_&_Maps/cwmap.php.

U.S. Geological Survey [USGS], 2019a, How wet is your State—The water area of each State, accessed April 2, 2019, at https://water.usgs.gov/edu/wetstates.html.

U.S. Geological Survey [USGS], 2019b, USGS water data for the Nation: U.S. Geological Survey National Water Information System database, accessed October 17, 2019, at https://doi.org/10.5066/F7P55KJN.

Winters, K.E., 2013, A historical perspective on precipitation, drought severity, and streamflow in Texas during 1951–56 and 2011: U.S. Geological Survey Scientific Investigations Report 2013–5113, 24 p., accessed October 16, 2019, at https://doi.org/10.3133/sir20135113.

For more information about this publication, contact
Director, Oklahoma-Texas Water Science Center
U.S. Geological Survey
1505 Ferguson Lane
Austin, TX 78754–4501

For additional information, visit
https://www.usgs.gov/centers/tx-water/

Publishing support provided by
Lafayette Publishing Service Center

Harwell and others—**Precipitation, Temperature, Groundwater-Level Elevation, Streamflow, and Potential Flood Storage Trends**—SIR 2019–5137, ver. 1.1

ISSN 2328-0328 (online)
https://doi.org/10.3133/sir20195137